NSF/CEE-84002

PB84-192939

CONCRETE MECHANICS

COOPERATIVE RESEARCH BETWEEN INSTITUTIONS IN THE NETHERLANDS AND THE USA

Summaries of papers and discussions
presented at the third meeting at
Delft University of Technology
June 22-24, 1983

and

Summaries of Meetings 1 and 2

Editors: P. Gergely and R.N. White
Cornell University

J.W. Frénay and H.W. Reinhardt
Delft University of Technology

March 1984

INFORMATION RESOURCES
NATIONAL SCIENCE FOUNDATION

50272-101

REPORT DOCUMENTATION PAGE | 1. REPORT NO. NSF/CEE-84002 | 2. | 3. PB84 192939

4. Title and Subtitle: Cooperative Research Between Institutions in the Netherlands and the USA

5. Report Date: March 1984

6.

7. Author(s): P. Gergely, R.N. White, J.W. Frenay, H.W. Reinhardt

8. Performing Organization Rept. No.

9. Performing Organization Name and Address:
Cornell University
Department of Civil Engineering
Ithaca, NY 14850

10. Project/Task/Work Unit No.

11. Contract(C) or Grant(G) No.
(C)
(G) CEE8023479

12. Sponsoring Organization Name and Address:
Directorate for Engineering (ENG)
National Science Foundation
1800 G Street, N.W.
Washington, DC 20550

13. Type of Report & Period Covered

14.

15. Supplementary Notes

16. Abstract (Limit: 200 words)

Summaries are provided of papers and discussions presented at the third of three meetings held at the Delft University of Technology. Research related to the analytical modeling of reinforced concrete is addressed, with emphasis on the following topics: fatigue of concrete in tension; long-term tensile strength; creep of concrete in seawater; post-peak cyclic behavior of plain concrete in tension; the bond between concrete and reinforcement; the fracture mechanics of concrete; round-slip relationships for reinforced concrete; and crack shear in concrete. A program of the meeting and list of participants is included. Summaries of the first two meetings are supplied.

17. Document Analysis a. Descriptors

Earthquakes
Reinforced concrete
Earthquake resistant structures
Fracture (materials)
Dynamic structural analysis
Creep properties
Tensile strength
Fracture properties
Concretes
Meetings
Tension
Shear properties

b. Identifiers/Open-Ended Terms
P. Gergely, /PI

c. COSATI Field/Group

18. Availability Statement: NTIS

19. Security Class (This Report)

21. No. of Pages 166

20. Security Class (This Page)

22. Price

See ANSI-Z39.18 | See Instructions on Reverse | OPTIONAL FORM 272 (4-77) (Formerly NTIS-35) Department of Commerce

CONTENTS

I. INTRODUCTION

A cooperative research effort was started in 1981 between Cornell University, other research laboratories in the U.S., and institutions in the Netherlands: The Delft University of Technology, TNO-IBBC, and the Rijkswaterstaat. The main objective of this program has been the coordination of research related to the analytical modeling of reinforced concrete. The second goal has been the frequent and immediate exchange of research ideas and results.

Three meetings were held: in June, 1981 in Delft, in January, 1982 in Atlanta, Georgia, and in June, 1983 in Delft. The first two meetings concentrated on basic problems with analytical modeling: constitutive relationships, effects of cyclic loading, long-term effects, representation of cracking, bond, and interface shear transfer across cracks.

Several benchmark problems were selected during 1982 and these were analyzed independently by participants prior to the meeting in 1983. The approaches and results were discussed at the meeting. This report contains summaries of the presentations at the meeting, including some results of benchmark analyses.

Financial support for the participation by U.S. researchers was provided by the National Science Foundation.

FATIGUE OF CONCRETE IN TENSION

dr.ir. H.A.W. Cornelissen.
Delft University of Technology

In a co-operative research program the fatigue behaviour of concrete is studied. Our contribution consists of an investigation of the fatigue properties of concrete in pure tension. Different loading types have been applied (see fig. 1).
The research program was started with the determination of S-N lines for various combinations of upper and lower limits of the cyclic stress. Apart from repeated tensile stresses, also stress reversals have been applied. The result of the constant amplitude tests (6 Hz) have been combined in a modified Goodman-diagram. (see fig. 2) From this diagram it could be concluded that at a given upper limit of the cyclic tensile stress, a decrease of the lower limit (increase of amplitude) resulted in shorter lives, especially if the lower limit was a compressive stress (stress reversals).

During the tests also the longitudinal strain was measured. The strains at the upper limit of the stresses followed a cyclic creep curve (see fig. 3). The slope of the secondary part of this curve proved to be strongly related to the number of cycles to failure (see fig. 4). This relation could be used to estimate the stress-strength levels of the specimens, since the real strength varied because of scatter.

In order to check Miners rule the research program had been continued with program loadings with two and more blocks, having the same lower stress limit, but different upper limits. The results showed that Miners rule provided a practical prediction of life. In general the failure criterion M=1 proved to be safe.

In order to simulate service load conditions, variable amplitude tests have been conducted this year.
In all tests the development of the longitudinal strain has been recorded to indicate internal damage of concrete.

In an additional program the damaging effect of stress reversals is studied more in detail as well as crack propagation during fatigue in general.
In this program strain controlled tests with post peak cycles are performed.

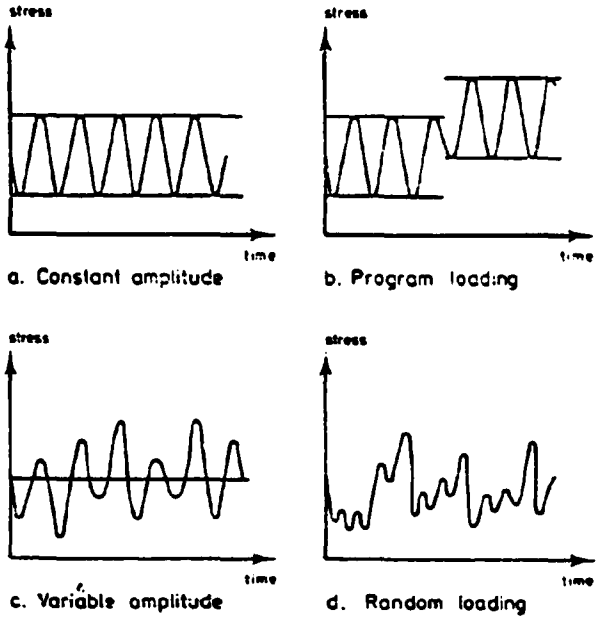

Fig. 1 Different loading types for fatigue tests

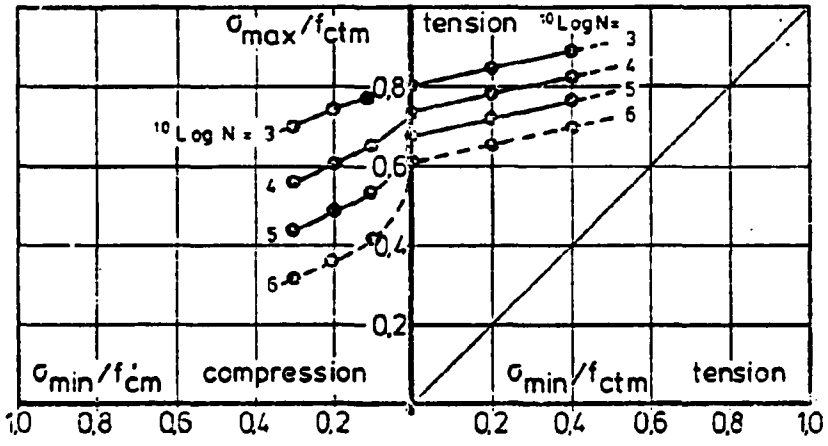

Fig. 2 Modified Goodman-diagram for uniaxial repeated tension and tension-compression

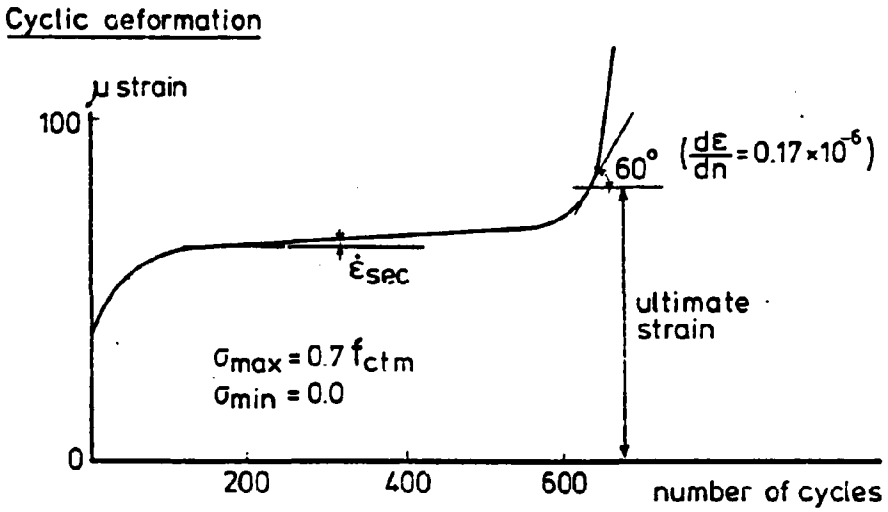

Fig. 3 Cyclic creep curve for concrete under repeated tensile loading

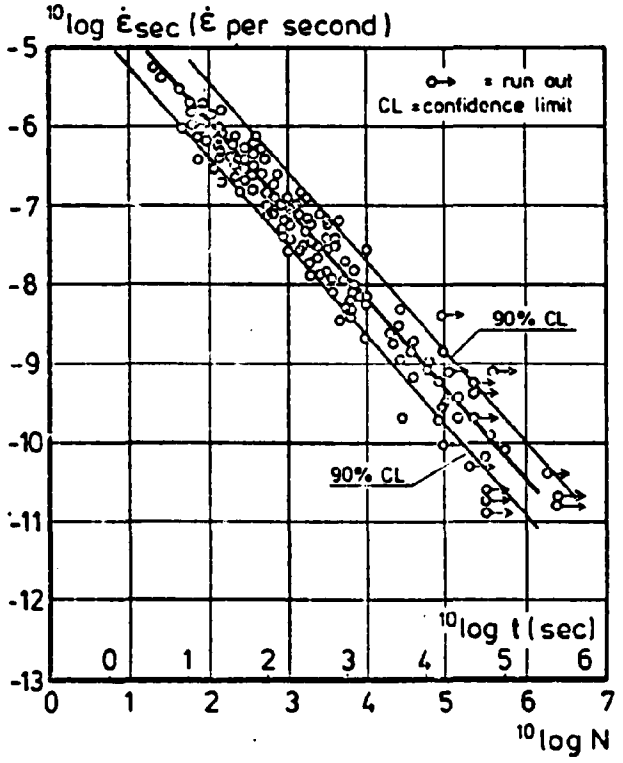

Fig. 4 Relation between secondary creep rate and life

LONG-TERM TENSILE STRENGTH

dr.ir. H.A.W. Cornelissen
Delft University of Technology

To quantify shear behaviour of concrete, information on the tensile properties is necessary, too. Mainly as a completion of the concrete mechanics projects on shear transfer in cracks, a testing program was set up to study deformation and life of concrete under sustained tensile loadings.
The variables were chosen in accordance with off-shore structures such as gravity platforms. Therefore creep tests were performed at $4^{\circ}C$ (temperature of seawater) and at $21^{\circ}C$ (reference temperature); tests at $40^{\circ}C$ (temperature of crude oil) are in preparation.
Four different concrete compositions were tested. The specimens were loaded in pure tension at stress levels in the range of 60 to 85 percent of the static strength. Time to failure as well as longitudinal creep deformations were recorded.
Because of the similarities with the running program "fatigue of concrete in tension", the same specimen dimensions and curing conditions were chosen.

Up till now about 100 creep tests have been executed. The results have been presented in "stress-life" diagrams. An example is shown in fig. 1.
Also the relation between secondary creep velocity and life has been evaluated. This relation could be used to adjust the data in the "stress-life diagrams". A result is shown in fig. 2. As can be observed the scatter could be reduced resulting in a more reliable relation.

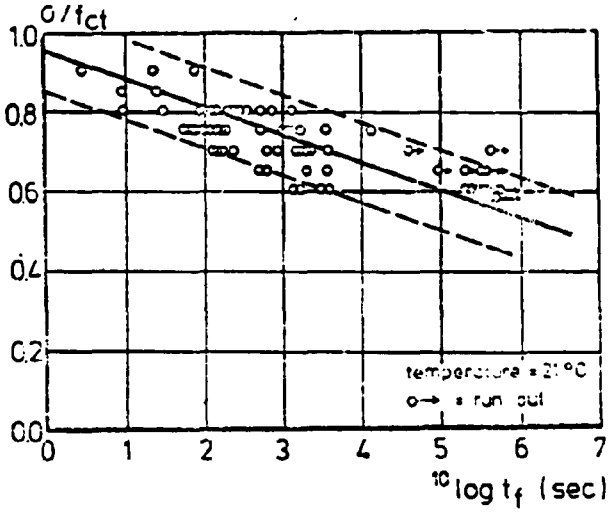

Fig. 1 Stress-life diagram for concrete under sustained pure tension

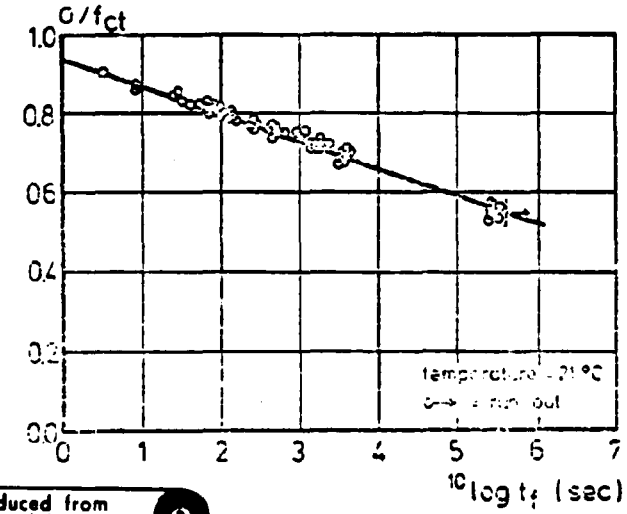

Fig. 2 Stress-life diagram with corrected stress-strength levels

Theoretical and experimental research on shear transfer across cracks in concrete under sustained loading.

J.W.I.J. Frénay
J.C. Walraven

Delft University of Technology

1. Introduction

For numerical computer programs experimental information is needed about the behaviour of cracked concrete under shear and normal loading. A practical example is the substructure of a concrete offshore platform in which shear forces play an important role. The first part of the research project "Concrete Mechanics" dealt with short time tests on specimens with a single preformed crack. The stiffness normal to the crack-plane was obtained either by embedded reinforcement or by external bars. Crack width and shear displacement were measured as a function of the shear loading. The experimental results are well described by the "aggregate interlock" model of Walraven [1] .

The second part of the research program concerns cracked concrete under constant shear loading.

2. Theoretical model for short term loading

The "aggregate interlock" model has been developed for short term loading. Concrete is modelled as a two-phase material consisting of stiff spherical aggregate particles embedded in a cement matrix. The matrix material includes air voids, fine sand (< 0,1 mm) kept together by partially hydrated cement. As far as normal strength concrete is concerned the preformed crack will run into the matrix along the surface of the aggregate particles because the bond zone between both materials is the weakest link of the system.

After the application of an external shear force F_x on the cracked concrete specimen, the crack opening increases and the stiff spheres of one crack face are pushed into the matrix material of the opposite crack face. The required normal force F_y is obtained by external or internal reinforcement. Figure 1 shows the two-phase system for one particle.

Taking into account all particles the equilibrium conditions can be formulated as;

$$\tau = \sigma_{pu} (\Sigma a_y + \mu \Sigma a_x) \tag{1}$$

$$\sigma = \sigma_{pu} (\Sigma a_x - \mu \Sigma a_y) \tag{2}$$

with: $\tau = \frac{\Sigma F_x}{A_c}$ and $\sigma = \frac{\Sigma F_y}{A_s}$

A_c and A_s are the areas of the cross section of the cracked concrete face and of the reinforcement across the crack; σ_{pu} is the matrix strength; Σa_x, Σa_y are the total projected contact areas both being a function of parallel and normal displacements Δ and w and of the concrete characteristics. If F_x is increased the contact areas are about to slide, so that (fig.1);

$$\tau_{pu} = \mu . \sigma_{pu} \tag{3}$$

The matrix material is assumed to be rigid-plastic. As a result of pore volume reduction the plastic deformations are expected to dominate the elastic deformations. This phenomenon is even strengthened by the multiaxial state of stress on the contact area between matrix and particle. From the experiments it was found that;

$$\sigma = 6.39 \, f_c'^{\,0.56} \tag{4}$$

$$\mu = 0.40 \tag{5}$$

The model given by the equations (1) - (5) gives a realistic description of the physical short-term behaviour of cracked plain concrete. It should be noted that σ_{pu} exceeds uniaxial concrete strength f_c';

- f_c' - not σ_{pu} - is reduced by cracks in the bond zone. The matrix has a more homogeneous structure
- σ_{pu} includes multiaxial material strength

3. Theoretical description of long-term strength

a. Cracks in plain concrete

In order to adjust the theoretical model to the behaviour under sustained loading it is proposed to reduce matrix strength as a function of the time of load-application. Hence it is not necessary to know explicitly the time-dependent deformation of the matrix. The first attempt is to pay attention to long-term strength of concrete as this material is described mostly in literature. Moreover as shown in (4) concrete and cement-matrix resemble considerably:

- both are cement-based, so that crack-development is influenced by the hydration-process.
- both materials have "crack-arresters", i.e. aggregate particles in concrete and air voids in the matrix.

Figure 2 shows experimental results schematically. The so-called creep-curves include the opposing processes in concrete under high sustained loading;

- crack-initiation and -extension causing the failure of the material after a certain time of load-application
- crack-arrestment governed both by relaxation near the crack-tips (caused by creep) and by the cement-hydration. In micro-cracks free water may move, potentially leading to micro-structural self repair [2] .

It is essential to determine the place of the minimum (t_f^*, $\sigma_{cr}^*/f_c(t_o)$) of the curves drawn in figure 2. For concrete loaded at an early age the minimum is clearly present because hydration is still important. The dotted lines represent no physical reality but indicate that crack-arrestment dominates for $t_f > t_f^*$. The hydration-process is described by the change of uniaxial concrete strength $f_c(t_o)$;

$$f_c(t_o) = \frac{f'_c . t_o}{a + b . t_o} \qquad (6)$$

in which $f'_c = f_c$ (t_o = 28 days). The constants a and b make it possible to characterize the velocity of hydration (or: the type of mix and the environmental conditions). See figure 3. These phenomenons are valid for tensile as well as compressive strength.

Creep tests carried out by Sčerbakov et.al. [3] indicate that the critical stress level is determined by t_o and f'_c. The following approximation has been derived;

$$\frac{\sigma^*_{cr}}{f_c(t_o)} = \frac{\log t_o}{A + B.\log t_o} \qquad (7)$$

with: $A = -1.1530 + 0.0364\, f'_c - 0.0003\, (f'_c)^2$

$B = 2.5314 - 0.0376\, f'_c + 0.0003\, (f'_c)^2$

For young concrete (t_o = 7 days) the concrete strength has hardly any influence on $\sigma^*_{cr}/f_c(t_o)$ whereas for $t_o > 14$ days the critical stress-level grows with increasing concrete quality.

An extensive research project started by Fouré [4] shows that there is a linear relation bewteen ln t_f and $\sigma_{cr}/f_c(t_o + t_f)$ with only small scatter of creep test results. The additional advantage of his approach is that specimens loaded at different ages t_o can be presented in one plot. Now the equation for curves in figure 2 becomes;

$$\frac{\sigma_{cr}}{f_c(t_o)} = \left\{ \frac{\sigma_{cr}}{f_c(t_o + t_f)} \right\} \left\{ \frac{f_c(t_o + t_f)}{f_c(t_o)} \right\} \qquad (8)$$

$$= \{C - D.\ln t_f\} \quad \left\{ \frac{f_c(t_o + t_f)}{f_c(t_o)} \right\}$$

in which C en D are constants.
The analysis of a wide variety of test results gives D = 0.010-0.050 which is in good agreement with a theoretical derivation (D = 0.013-0.025). After combining (6) and (8) the minimum of the curves can be computed;

$$\frac{d}{dt_f} \left(\frac{\sigma_{cr}}{f_c(t_o)} \right) = 0 \rightarrow \alpha \left(\frac{t_o}{t_f^*} \right)^2 + \left(2\alpha - \frac{\sigma^*_{cr}}{f_c(t_o)} \cdot \frac{1}{D} \right) \left(\frac{t_o}{t_f^*} \right) + \alpha = 0 \qquad (9)$$

for: $\alpha = 1 + \frac{b}{a}.t_o$ and $\frac{\sigma^*_{cr}}{f_c(t_o)} \geq 4.\alpha.D$

Now the complete curve is known for $t_f \leq t_f^*$. The examples given in figure 4 show that if t_o, D and the critical stress-level are kept constant, the time to failure increases for low values of $f_c(t_o \rightarrow \infty)/f'_c$.

In that case the amount of cement is relatively big (rapid initial hydration) so that crack-arrestment is stimulated hence prolonging the life-time of the specimen. Moreover the critical time to failure increases for decreasing critical stress-level. Concrete loaded at an old age has nearly no extra hydration, yet according to (9) a minimum is found.
The equations (4) - (9) are able to formulate time-dependent matrix strength σ_{pu}. The results will be implemented into the theoretical model.

Another problem is that the amount of friction depends on the fact whether cracks are formed through the aggregate particles or not. As no information is available about time-dependency of coefficient of friction, μ is kept constant. In 4. series of tests are proposed to solve this problem.

b. Cracks in reinforced concrete

The shear transfer mechanism differs if embedded steel bars cross the crack plane:

- compared with "aggregate interlock", dowel action can be neglected for small crack widths ($w < 0.25$ mm)
- the stiffness of the reinforcement is governed by time dependent bond, the reinforcement ratio, the bar diameter and the transverse pressure
- contrary to plain concrete the crack opening path remains nearly unaffected by the amount of steel and the concrete strength. The probable reason is that secondary cracking around the bars locally influences crack width and hence the shear transfer mechanism.

4. Experiments

To verify the extended theoretical model tests are being carried out on a similar type of specimen as used by Walraven [1] . The main variables of the experiments are;

- concrete strength : $f'_c = 55$ or 70 N/mm^2, maximum particle size 16 mm. The high concrete quality is necessary to meet the structural demands of offshore industry. For the high strength concrete it is expected that cracks will run through the aggregate instead of following the bond-zone.

- shear stress level :: $\tau = 5 - 11$ N/mm^2
  i.e. 50-85% of static shear strength
- initial crack width : $w = 0.01-0.10$ mm
- restraint stiffness : external or embedded bars ($\rho = 1,12-2,24\%$)

The concrete specimens are stored under humid environmental conditions (95% RH) during 22 days. Tests start at a constant concrete age of 28 days (20°C; 50% RH) and last approx. 90 days. During the experiments the shear stress is kept constant; crack width and shear displacements are measured by a microcomputer.
For each combination of variables several tests are conducted in order to pay attention to the scatter of test results.

5. Literature

[1] Walraven, J.C., Reinhardt, H.W.:
"Theory and experiments on the mechanical behaviour of cracks in plain concrete and reinforced concrete subjected to shear loading".
Heron, Vol.26, no.1a, 1981, p.68

[2] Garrett, G.G., et.al.:
"The fatigue hardening behaviour of cement-based materials",
Journal of the materials science, 14, 1979, p.296-306.

[3] Ščerbakov, E.N., Zaitsev, J.:
"Voraussage der Verformungs- und Festigkeitseigenschaften von Beton unter Dauerlast"
Cement and concrete research, Vol.6, no.4, 1976, p.515-528

[4] Fouré, B.
"Résistance du béton sous contrainte soutenue",
Essais et measures, 191, no.405, June 1982, p.110-121.

6. Notations

a_x, a_y - projected contact areas parallel and normal to the crack

f'_c - concrete strength at 28 days age

t_f - time to failure

t_o - concrete age

w - crack width

μ - coefficient of friction (particle-matrix)

ρ - reinforcement ratio

σ - stress normal to crack plane

σ_{cr} - constant stress on creep-specimen

σ_{pu} - matrix yielding stress

τ - shear stress

τ_{pu} - shear stress on particle

Δ - shear displacement

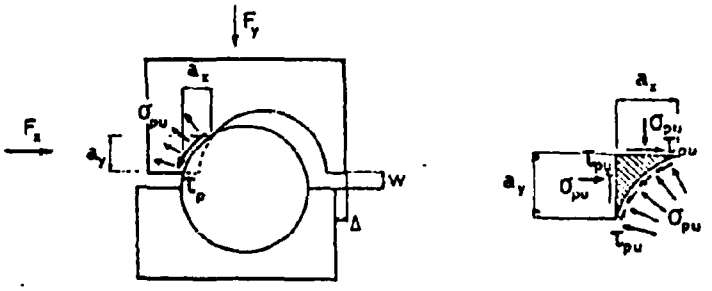

Figure 1. Formation of a contact area and equilibrium of forces [1].

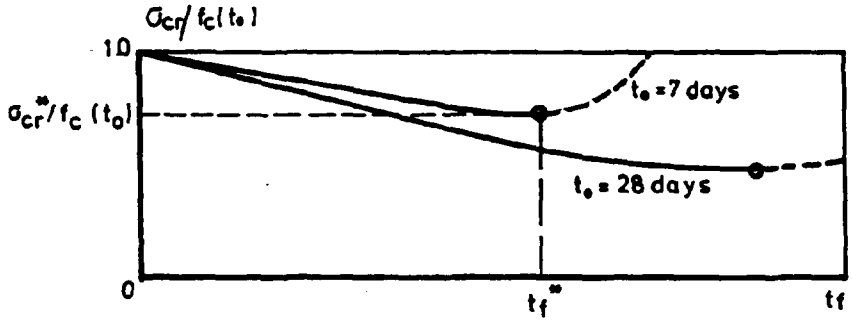

Figure 2. Concrete strength under constant stress level, depending on age t_o. Time to failure t_f.

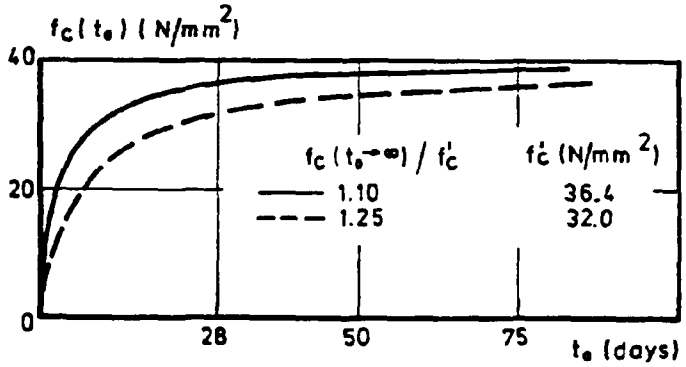

Figure 3. Development of short time concrete strength for two types of concrete; $f_c\ (t_o \to \infty) = 40.0\ N/mm^2$

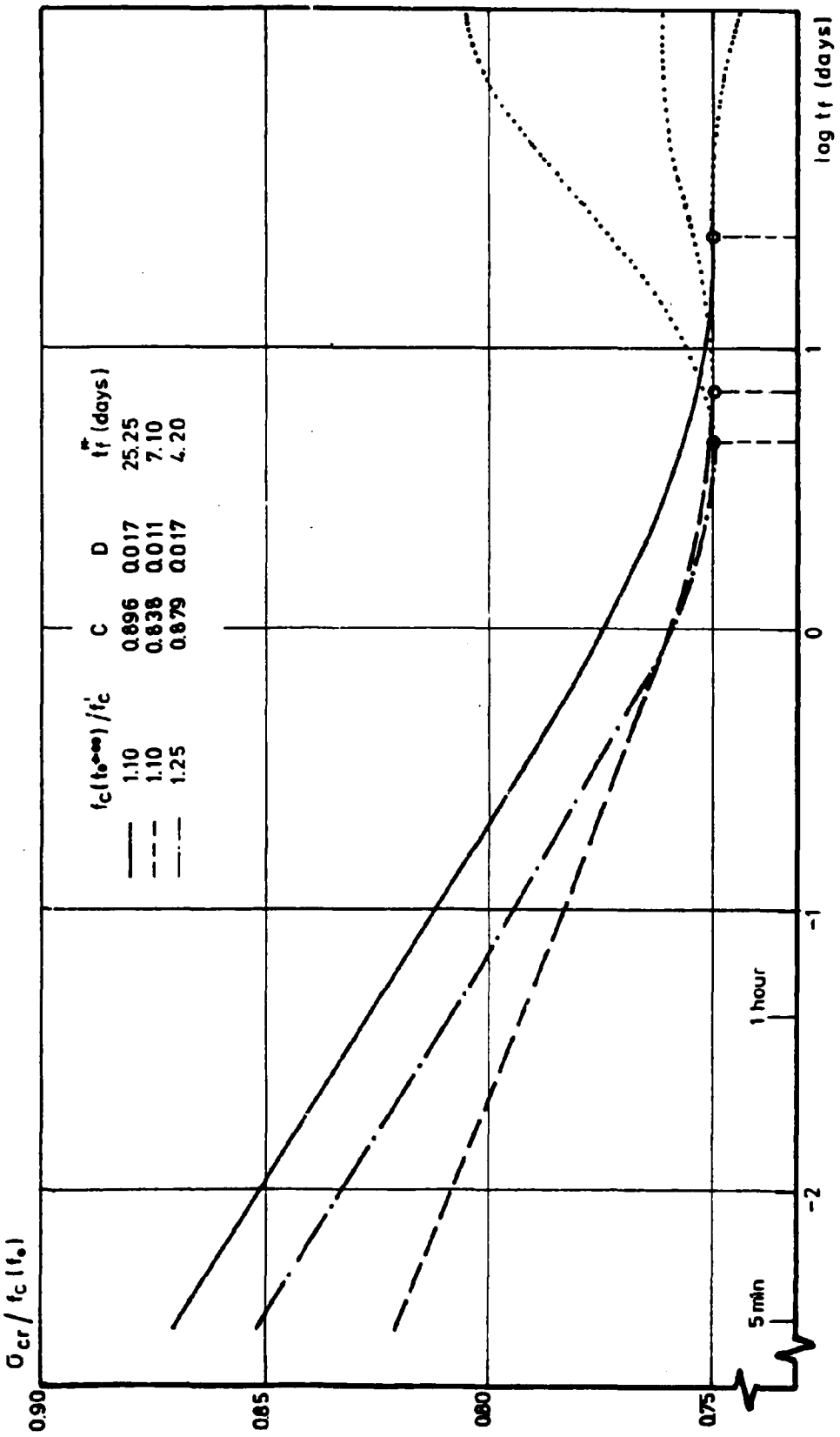

Figure 4. Curves according to (8) with $\sigma_{cr}^* / f_c(t_o)$ = 0.75; t_o = 28 days and f_c' = 50.2 Nmm^{-2}.
For $t_f > t_f^*$ the dotted curves (....) are fictitious.

CREEP OF CONCRETE IN SEAWATER

ir.J. Mijnsbergen
Delft University of Technology

Summary.

Due to the penetration of seawater, the long term behaviour of concrete may be affected by some micro structural processes that take place within the concrete. Creep experiments are being carried out in which specimens are loaded in uniaxial compression as well as in bending. The parameters are the concrete composition, the presence of seawater and the hydrostatic pressure (up to 15 Nmm^{-2}).
The observed creep behaviour is described by a method based on the rate theory. Starting point of the method used is the equation which describes the strain rate: $\dot{\varepsilon} = \alpha \cdot \exp(-Q/kT)\sinh(V\sigma/kT)$. Although the experimental program is far from being completed it is clear that seawater penetration affects the creep behaviour and increases the creep deformations.

1. Introduction.

The long term behaviour of concrete strongly depends on the environment, e.g. moisture, temperature and the influence of liquids and gasses. When concrete is placed in a marine environment, seawater and the dissolved salts will penetrate into the concrete. Seawater penetration due to diffusion and hydrostatic pressure has often been investigated and may be described by Fick's law and Valenta's equation. The effects of penetration on both concrete and hardened cement paste in (synthetic) seawater or salt solutions is well known, e.g. the formation of ettringite and Friedel's salt, bond of chlorides and sometimes a change of the porosity and the pore size distribution. The influence of seawater penetration on the creep behaviour however is unknown.

2. Scope of the research program.

It is the aim of the research program to investigate and to describe the creep behaviour of concrete in seawater and also to look for an explanation of the observed phenomena.
Creep experiments are being performed which give clearness with regard to the seawater penetration. Two aspects of the marine environment will be investigated. At first the presence and influence of seawater and second a high hydrostatic pressure (up to 1500 m sea depth), both separated and together. To determine the influence of the seawater penetration and the hydrostatic pressure, also creep experiments will be performed in lime water ($Ca(OH)_2$) and with sealed specimens.

With regard to the concrete composition 3 kinds of cement are used and 2 different values of the water cement ratio. Portland cement, Portland blast furnace cement and a new developed cement: Portland flyash cement. The water cement ratios are equal to 0.40 and 0.60.

3. Theoretical description of the creep deformations.

Starting point of the method used are the deformation kinetics. This method is based on the principle that the time dependent deformations are the result of a thermal activated process which can be described by the rate theory. From the fundamental deformation kinetics, an equation with regard to the strain rate of the creep deformations can be derived (equation 1).

$$\dot{\varepsilon} = \alpha \cdot \exp\left(\frac{-Q}{kT}\right) \sinh\left(\frac{VW}{kT}\right) \qquad (1)$$

which can be rewritten to equation 2

$$\dot{\varepsilon} = \dot{\varepsilon}_0 \cdot \exp\left(\frac{-(Q-Q_0)}{kT}\right) \qquad (2)$$

Normally in literature, the activation energy (Q) and the work per volume (W) are kept constant. The derivation however which is used considers Q as well as W time dependent. The relation between Q and time t is given in equation 3.

$$\frac{\delta Q}{\delta t} = \frac{m \cdot kT}{t+d} \qquad (3)$$

The solution for ε_{cr} is given in equation 4 which contains only time t and 3 constants: a, d and n (n=1-m).

$$\varepsilon_{cr} = \dot{\varepsilon}_0 \cdot \frac{d}{n} \cdot \left(\left(\frac{t+d}{d}\right)^n - 1\right) = a\left(\left(\frac{t+d}{d}\right)^n - 1\right) \qquad (4)$$

$$a = \dot{\varepsilon}_0 \cdot \frac{d}{n}$$

With help of equation 4 creep data are fitted.

4. Creep experiments.

In the experimental part of the research program to types of experiments are to be distinguished, namely creep experiments in which specimens are loaded in bending and specimens loaded in uniaxial compression. The bending experiments are ment to collect relative creep data with regard to the several parameter combinations primarily the hydrostatic pressure. Two specimens loaded in bending and a pressure vessel are shown in the figures 1 and 2. Due to small specimen dimensions and a hydrostatic pressure of 15 Nmm^{-2} the seawater will penetrate very fast.

The creep experiments in uniaxial compression are of a more conservative type, and lead to absolute creep data. In figure 3 a specimen is shown. The specimen is placed in a seawater vessel, containing seawater which is refreshed continuously during the 90 days lasting creep test and following 30 days creep recovery period. The seawater which is used conforms to ASTM-D 1142.

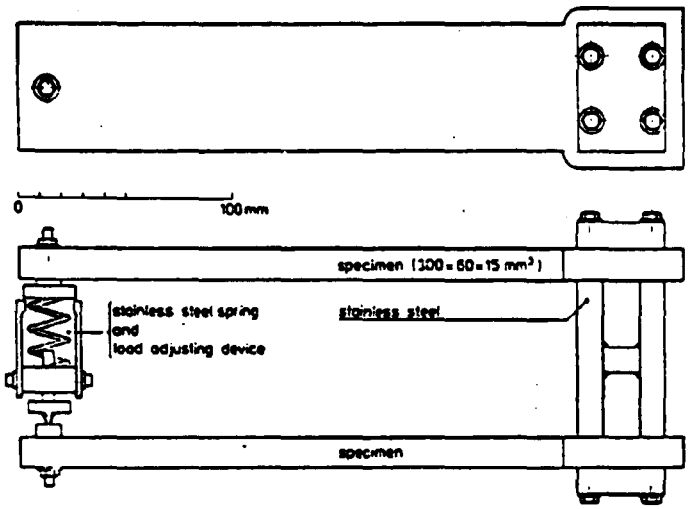

fig.1. 2 specimens loaded in bending.

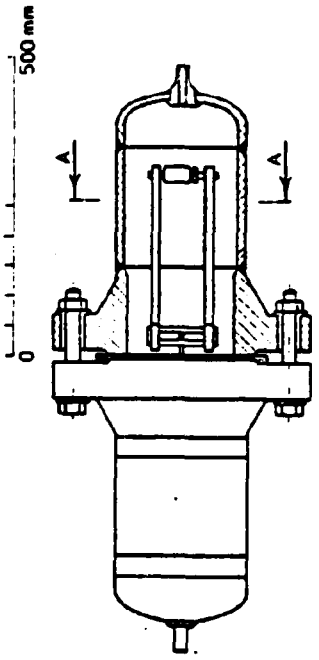

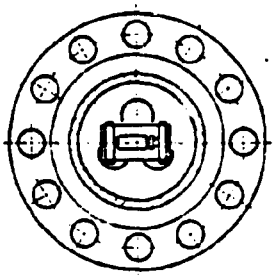

cross section A-A

fig.2. Pressure vessel containing 4 specimens loaded in bending.

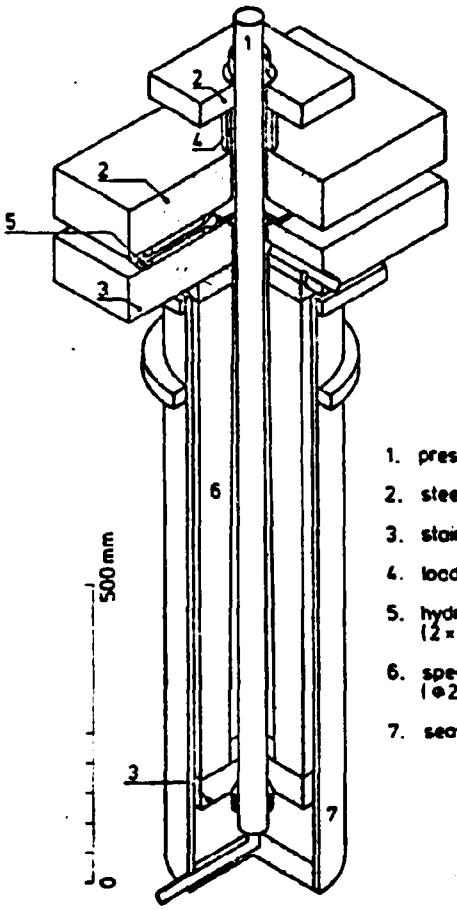

1. prestressing bar
2. steel plate
3. stainless steel plate
4. load cell
5. hydraulic jack (2 × 400 kN)
6. specimen (⌀ 200 × 750 mm³)
7. seawater vessel

fig.3. Concrete specimen loaded in uniaxial compression.

5. Experimental results and preliminary conclusion.

Although the experimental program is far from being completed, several creep tests with regard to the specimens loaded in uniaxial compression have been performed untill now. In figure 4 the specific creep (ε_{crsp}) is plotted as a function of time t. It should be mentioned that the creep tests start at an age of 28 days and that the specimens were placed in seawater resp. limewater at an age of 2 days. All 3 creep curves consist of 3 specimens. The specific creep data have been fitted by means of equation 5.

$$\varepsilon_{crsp} = a \cdot \left(\left(\frac{t+d}{d}\right)^n - 1\right) \quad (10^{-6}\ mm^2N^{-1}) \qquad (5)$$

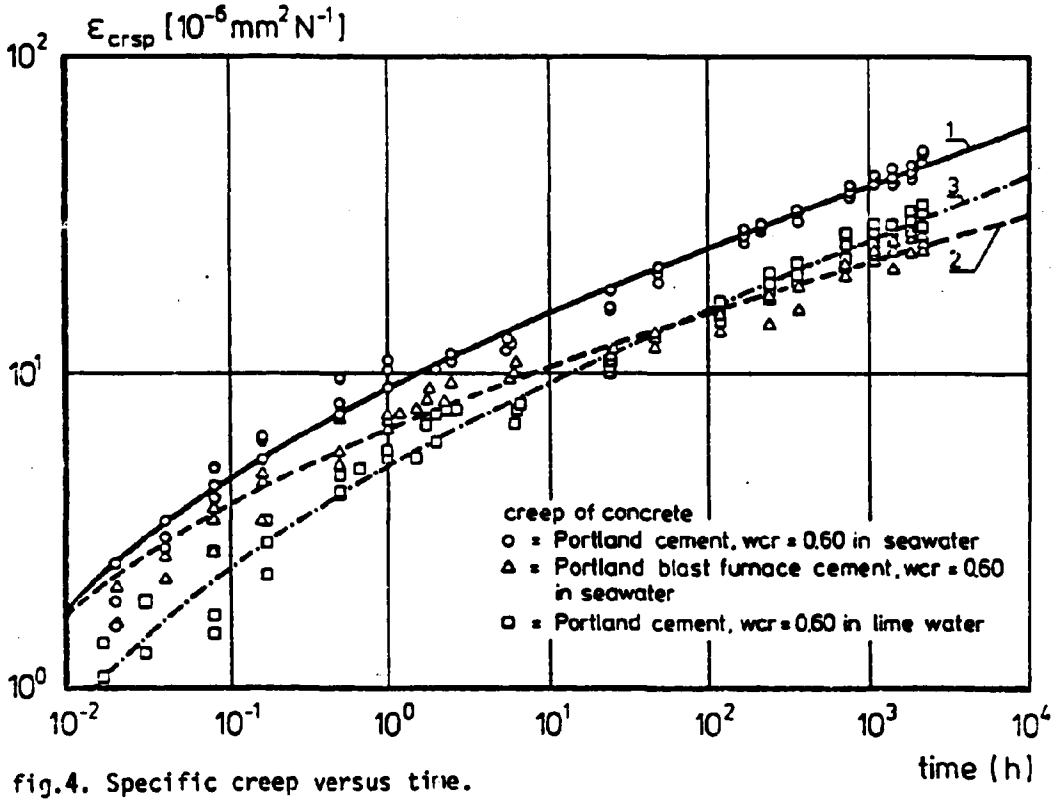

fig.4. Specific creep versus time.

The average of the calculated regression coefficients stands at 0.995 which gives some qualitative information about the fitting.
Two conclusions may be derived. In seawater (curves 1 and 2) a big difference can be seen with regard to Portland cement and Portland blast furnace cement. At time t=0 the creep deformations are almost equal but at 90 days Portland cement creeps almost twice as much as blast furnace cement. It is known that the creep deformations of blast furnace cement are a bit smaller, but such a big difference is somewhat surprising.

During the whole creep test seawater leads to bigger creep deformations (curves 1 and 3) than limewater, up to 40% at 90 days. So it can be concluded that seawater penetration increases the creep deformations. With regard to some mechanical properties such as Young's modulus and compressive strength (cubes and cylinders) no significant differences between seawater and limewater have been found.

The first creep tests on bending show that the creep deformations in seawater under high hydrostatic pressure (15 Nmm^{-2}) are much bigger in relation to a hydrostatic pressure equal to 0.1 Nmm^{-2}.

6. Notations.

a	constant (mm^2N^{-1})
d	constant (h)
k	Boltzmann constant (NmK^{-1})
m	constant
n	constant
t	time (h)
wcr	water cement ratio
Q	activation energy (Nm)
T	temperature (K)
V	activation volume (m^3)
W	work per volume (Nm^{-2}) $W = \int \sigma \delta \varepsilon$
α	constant
ε_{cr}	creep
ε_{crsp}	specific creep (mm^2N^{-1})

Theoretical and experimental research on the behaviour of cracks in concrete subjects to shear and normal forces.

A.F. Pruijssers
J.C. Walraven
Delft University of Technology

In an earlier stage of the investigation a theoretical model was developed which was subsequently compared with experimental results, obtained on cracks which were subjected to static loading.
The theory was based on the assumption that concrete can be conceived as a "two-phase" material which is composed of a collection of aggregate particles with high strength and stiffness (phase I), and a matrix material consisting of hardened cement paste with fine sand (< 0.25 mm or 0.002 in.) with lower strength and stiffness (phase II).
A crack in this composite material generally intersects the matrix, but not the aggregate particles, because the contact layer between particles and matrix is of relatively low quality. The transmission of forces during shear displacement of the crack faces is effected via local contact areas between the particles protruding from one of the crack faces and the matrix in the opposite crack face. The interdependence between forces and displacements of the crack faces is closely related to the deformation of the matrix material. The aggregate particles were simplified to spheres, whereas the behaviour of the matrix was assumed to be rigid plastic. The coefficient of friction between particles and matrix at overriding, and the stress at which plastic deformation of the matrix occurs, were used as "adjusting parameters" in the model. For the coefficient of friction between matrix and particles a value of 0.4 was found: the matrix strength was found to be a simple function of the cube compressive strength.
Excellent agreement with the experimental values was obtained:
the influence of concrete strength and other mix properties, like maximum particle diameter and grading curve were adequately described by the model.
The model can be extended to cyclic loading. In this case the influence of load history has to be involved.
The principle of the model is demonstrated for one particle section, the restraining stiffness normal to the crack being represented by a couple of springs. Fig. 1.a represents the neutral position at the beginning of the first cycle of loading (Point A, Fig. 2). During shear loading (Fig. 1.b) a contact area between matrix and particle is formed, between which shear and normal stresses are transmitted, providing equilibrium with the external forces.

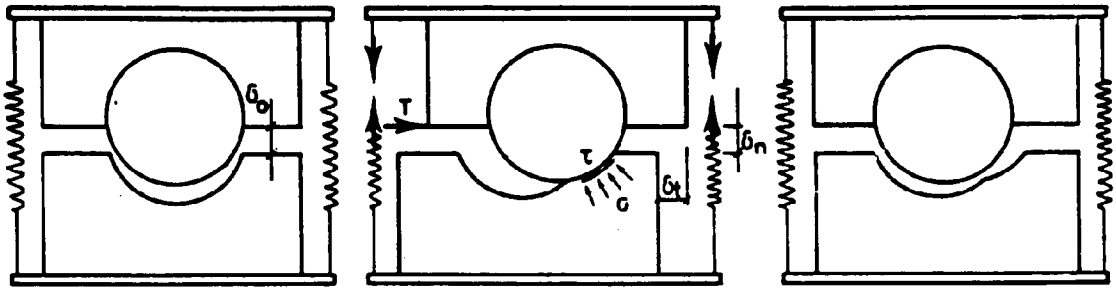

Fig. 1a 1b 1c

The need for equilibrium at increasing values of the shear force T results in increasing values of the crack width δ_n and the shear displacement δ_t (branche OA in Fig.2).

If the shear load, after having reached a certain value, is released, the shear displacement will first remain constant: the shear stress at the contact area will change sign and sliding back to the neutral position will only occur after surpassing the frictional resistance in the inverse direction (branche AB, Fig.2); then only a small shear force is necessary to bring the specimen halves back to the neutral position. (Fig. 1.c and BDO in Fig.2). A similar behaviour can be expected for the other direction of loading (OA'B', Fig.2). The second cycle will be basically different from the first one: the specimen halves have to travel a larger distance to get in touch and will then reach full bearing in a short interval of δ_t, which results in a pronounced hardening character (OA', Fig.2). Each subsequent cycle will cause some further excavation of the matrix, so that an ongoing increase of maximum shear displacement can be expected.

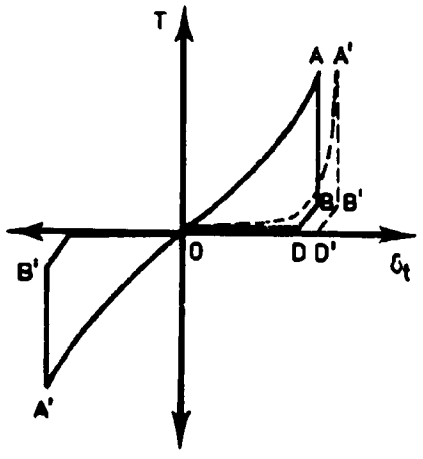

Fig. 2. Theoretical response

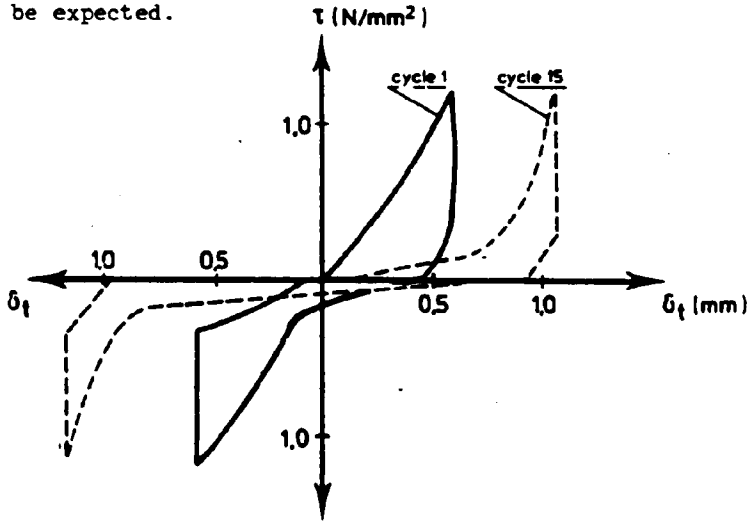

Fig. 3. Test, carried out by Laible

The model takes into account that a particle can be intersected by the crack at arbitrary levels and that, in a mix, particles of various sizes are found, depending on the grading curve.
The resistance of the crack plane, for arbitrary values of δ_n and δ_t after any arbitrary load history can be calculated with a relatively simple numerical calculation program, integrating all particle contributions. For this program two versions have been developed: one version divides the range of particle diameters into a number of classes for which the average most probable contact areas are calculated and added: this approach enables an analysis of the role of the grading curve.
The other version considers only one general particle diameter, from which the general crack resistance is calculated using a conversion factor which couples the individual particle response to the response of a complete mix with a Fuller particle gradation.
Using the characteristics for the friction between particles and matrix and the plastic strength of the matrix obtained in the previous, static, investigation, the calculated behaviour of cracks subjected to cyclic loading is in fairly good agreement with results obtained from other investigators (Fig.3).
In both versions of the numerical calculation program the normal restraint stiffness should be known.
A prediction based on bond stress-slip relations under repeated loading gives satisfactory results.
In addition to the theoretical analysis of the problem series of experiments are carried out. The parameters are so chosen that the results will yield information which is complementary to the information gained in the experiments at Cornell and Washington.
This is shown in the following survey.

Cornell/Washington	Delft
- Intermediate concrete quality $16 < f'_c < 25$ N/mm^2, or $2250 < f'_c < 3600$ psi	- High concrete quality $30 < f'_c < 65$ N/mm^2 ($4000 < f'_c < 9000$ psi)
- Crack widths > 0.25 mm (0.01 in.)	- Crack widths < 0.25 mm (0.01 in.)
- Low cycle high intensity	- High cycle low intensity

Until now only tests on reinforced specimens are carried out. The average crack opening path obtained in these tests is in good agreement with the crack opening path obtained in the previous static tests (Concrete Mechanics I, Walraven 1980). This supports the assumption that the theoretical model of Walraven can be used for dynamic tests.
Further tests are needed for a good implementation of the normal restraint stiffness into this model.

Post-peak cyclic behaviour of plain concrete in tension

H.W. Reinhardt, Delft University of Technology

Fatigue of concrete is a phenomenon which is usually treated by empirical relations such as S-N- curves and Goodman diagrams and the mechanism of which is not yet well understood. It is believed that crack propagation is an essential feature of fatigue and that a rational approach should start from cracking behaviour of concrete.

A physical model for cracks in concrete may depart from the Barenblatt - Dugdale idea of cohesive cracks. It is assumed that a certain zone exists in front of a visible crack where stresses act holding the crack faces together. The distribution of these stresses depends on two quantities: the shape of the crack and the stress-strain curve of the concrete. Fig. 1 (insert) shows the situation of a crack in an infinitely large panel with a central crack.

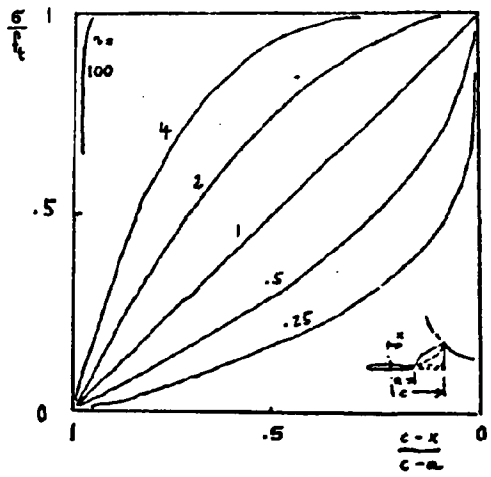

Fig. 1. Stress distribution in softening zone

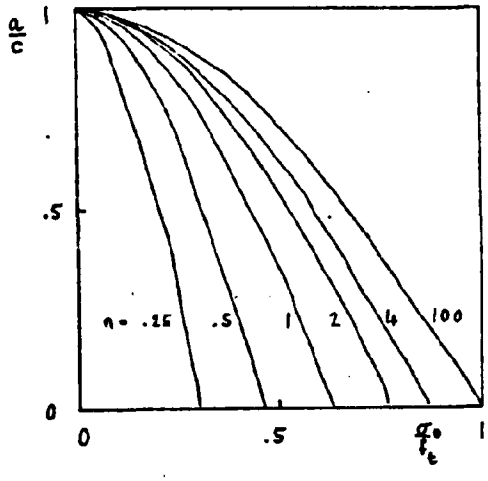

Fig. 2. Size of softening zone as function of relative stress

First an analysis has been done in regard of the influence of the stress-distribution in the softening zone. The stresses have been described by

$$\sigma/f_t = 1 - \left(\frac{c-x}{c-a}\right)^n \qquad (1)$$

$n = 1$ is a linear distribution, $n \to \infty$ is the Dugdale case and $n = 0$ would

mean a visible crack of length 2 c. Fig. 1 is an illustration of eq.(1). The length of the softening zone (c-a) is determined by the requirement, that, at x = c, the stress is equal to the tensile strength and that the stress singularity vanishes. The condition can be fulfilled by equating the stress intensity factors due to the stresses in the softening zone, K_s, and due to the remote stress σ acting on a panel with crack length 2c, K_σ. This condition reads as

$$K_s = 2\sqrt{\frac{c}{\pi}} \int_0^c \frac{\sigma(x)dx}{\sqrt{c^2 - x^2}} \qquad (2)$$

$$K_\sigma = \sigma_0 \sqrt{\pi c} \qquad (3)$$

Combination of eq. (1) and (2) and equating (2) and (3) leads to an expression for $^a/_c$. The results of numerical integration are plotted in fig. 2. They show how the softening zone spreads with increasing stress-strength ratio indicating clearly the strong influence of the power n on the results.

Regarding a/c =o a failure criterion (independent on real length of the crack and dimension of the panel) it is obvious that failure occurs at a low stress-strength ratio for small n and that high failure stress (σ/f_t=1) is present at complete yielding (n=100). In a material such as concrete one may state that the tensile strength f_t is an apparent strength which is smaller than the real material strength. The smaller n the greater the difference between these two strength values.

A first step to use the model in concrete is to establish a complete stress-strain curve in uniaxial tension. For this reason tests on 120 mm thick cylinders have been carried out in three loading types:

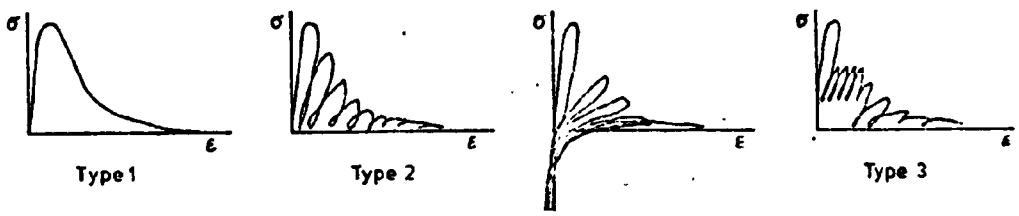

Fig. 3. Types of deformation controlled loading

1, deformation controlled until failure; 2, cyclic loading towards the envelope curve; 3, after passing the peak cyclic loading between fixed upper and lower stress, fig. 3.

The results two examples of which are given in fig.4 and 5, show no significant difference in the envelope curve. Independent on type of loading

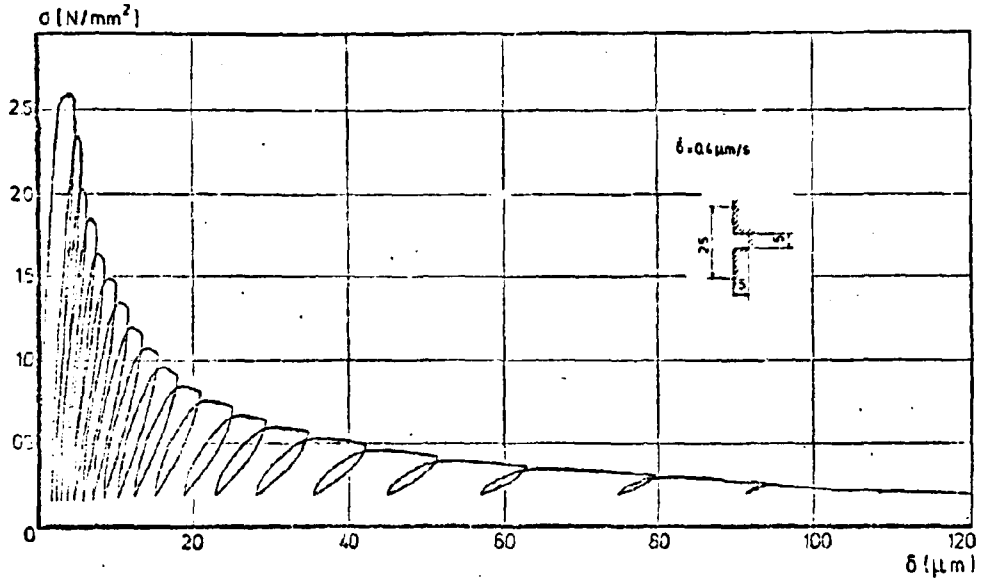

Fig. 4. Cyclic loading to the envelope curve

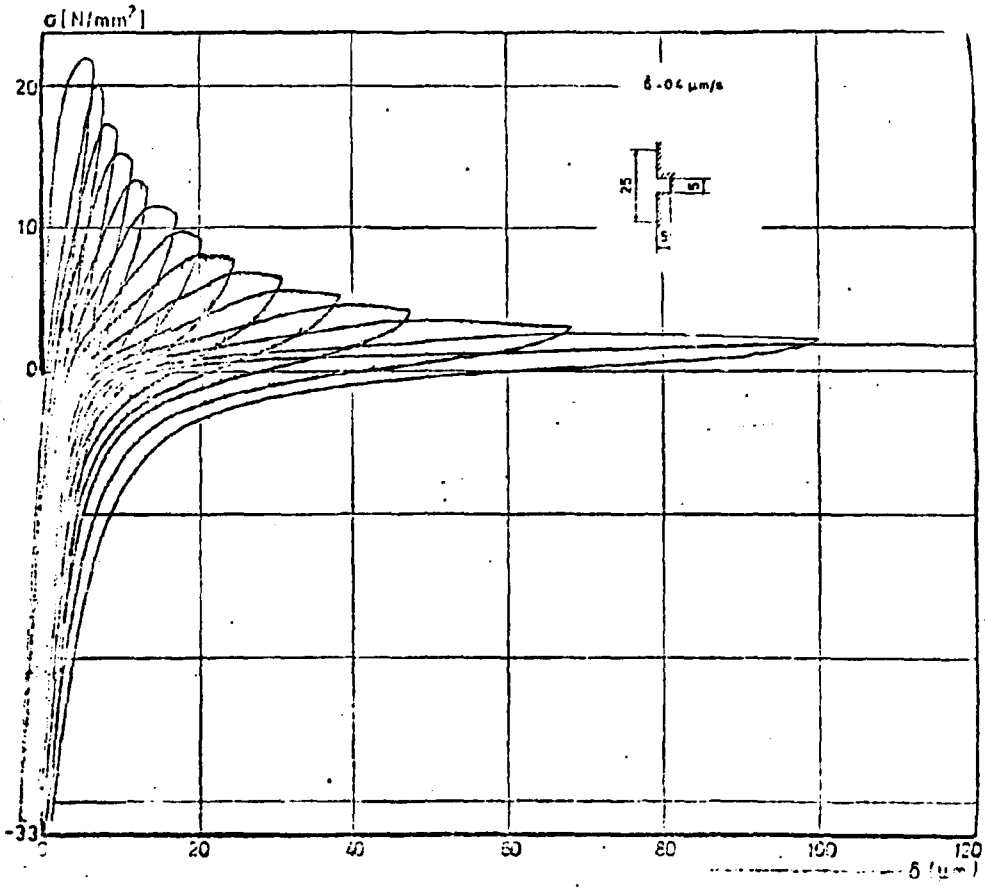

Fig. 5. Alternating loading

and on lower stress during cycling the curve remains the same as has been found earlier in case of compressive loading. Fig. 6 gives the relation between crack opening (which is defined as total deformation minus elastic strain measured over 25 mm) and relative strength σ/f_t. The concrete used

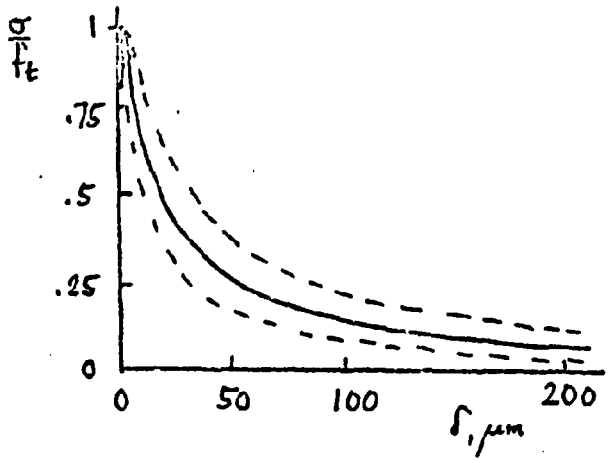

Fig. 6. Average envelope curce in tension

was a gravel concrete with max.aggregate size of 16 mm, cube compressive strength f_c = 45 N/mm^2.
A second conclusion from the experiment is that the strength decrease per cycle seems greater for a compressive lower stress than for a tensile one. More data should be evaluated to support this finding.

A second series of experiments is started to establish the shape of the crack during cycling. Stress-strain curve and crack shape together will provide the information necessary to evaluate the model for concrete.

Van Mier, Jan, G.M. "Complete stress-strain behaviour of concrete under multiaxial-conditions",
presented at the workshop on "Concrete-mechanics", Delft University of technology, June 22-24, 1983 / extended summary

COMPLETE STRESS-STRAIN BEHAVIOUR OF CONCRETE UNDER MULTIAXIAL CONDITIONS

Jan G.M. van Mier *

1. Introduction

In the last decade, computer models based on finite-element-methods are used very frequently for studying the highly non-linear behaviour of concrete structures under various loading conditions.
A major input parameter in these models is the stress-strain behaviour of concrete under multiaxial conditions. Consequently very much attention has been paid on gathering multiaxial-test results, and much energy has been stored in the development of general constitutive equations, describing the complete stress-strain behaviour of concrete, including softening behaviour and unloading/reloading characteristics. /1/

Some of these models can describe last mentioned effects, however tuning the models only was possible, using uniaxial compressive and tensile test results. Very scarce experimental data are available regarding the softening behaviour and the unloading/reloading characteristics of concrete under multiaxial conditions.

It is in the scope of this research to learn more about the overall behaviour of plain concrete under multiaxial loading, in order to develop usefull constitutive equations.
In 1981 the construction of a triaxial testing machine for cubical specimens was completed at Eindhoven University of Technology. The major difference to other existing triaxial testing machines, is the ability of deformation controlled testing, using servo-hydraulic loading equipment.

2. Experimental details

The experimental machine is composed of three very stiff identical loading-frames. The three frames are hung in a fourth overall frame by means of steel-cables. Movement of the loading-axes with regard to each other is possible in the horizontal plane and is fixed in the vertical direction. Each loading axis is completed with a 2000 kN compression / 1400 kN tension servo hydraulic actuator. All jacks are connected to a high pressure oil-system through accumulators. It should be mentioned that the tensile capacity is not necessary for the concrete-tests.
Loading is applied to the cubical specimens (dimensions d = 100 mm) by means of brush bearing platen. In case of tensile loading, the specimen is glued between the brushes.

* research assistent, Eindhoven University of Technology, The Netherlands

Forces are measured with callibrated dynamometers, strains are recorded using LVDT's, measuring the relative displacement between two opposite loading platen.
In each direction two LVDT's are installed in a diagonal position with regard to the cube (see fig. 1).
Test-control is - in case of deformation controlled tests - through these LVDT's.

It was shown in the international multiaxial testing program /2/, that unconstrained boundary conditions are necessary in order to avoid an over-estimation of the concrete-strength. Also important is the fact that scatter in strain-results decrease by using friction-poor boundary conditions. The results by Gerstle et.al. showed that very great deviations are observed by using different strain-measuring systems.
In our case, a number of uniaxial pre-tests was carried out, in order to compare surface strains (measured with 60 mm long strain-gauges) and the overall strains, which were measured between the loading platen. A linear relationship between brush-deformation and loading level was derived (in cases of pre-peak strains). The same relationship is used for post-peak strains.
The relationship derived was in close resemblance with results obtained with an aluminium cube.

Also a number of pre-tests was carried out, in order to investigate the influence of manufacturing-methods of the specimens on strength and strain results. (six cubes were sawn from a prism ⌀ 135 x 700 mm, after sawing the cubes were ground flat and plan-parallel with a diamond grinding-disk)

The concrete used was a medium strength gravel mix (cyl. strength ~ 45 N/mm^2) with a maximum aggregate size $d_a = 16$ mm.
The grading curve of the aggregate was according to curve B16 of the dutch-codes VB74. The water-cement ratio was chosen 0.5, the cement used being an ordinary portland cement (type A, 320 kg/m^3).

3. Multiaxial test-results

Until now several bi- and triaxial tests have been carried out. Variables in the triaxial series were: the loading path (constant strain-ratio E1/E2, or constant stress-ratio S1/S2) on four levels in the tension-compression-compression region and in the triaxial compression region; the lateral stress-level (S3 = 0.05 S1 or S3 = 0.10 S1); the direction of casting with regard to the major and minor compressive direction, and monotonic loading or cyclic loading to the envelope.
Loading speed (strain-rate) was held constant in all tests: E1 $\sim$?.10^{-5}/sec. in the major compressive direction. The experimental design was constructed using statistical methods.

Strength results are plotted in fig. 2. Also plotted are the results of the biaxial series, which show excellent agreement with Kupfer's results /3/. Each point in the stress-plane S1-S2 of figure 2 represents one test-result.

Examples of monotonic and cyclic stress-strain curves are shown in fig. 3 (specimen 8B2-4, S1/S2/S3 = -1.0/-0.33/-0.05, cyclic, parallel to the direction of casting and specimen 8A1-3, S1/S2/S3 = -1.0/-0.33/-0.05, monotonous, perpendicular to the direction of casting).

By using the servo-hydraulic loading equipment, we managed to get a stable test - also in the descending branch of the stress-strain curve.
At this stage only preliminary conclusions can be drawn: not yet all tests have been plotted, and the statistical analysis is not yet finished.
Some first observations will be summarized.

When we confine ourselves to the triaxial-compression region, in general two types of stress- or strain induced anisotropy can be distinguished. The first type is called CTI, cylindrical transverse isotropy, when all load-induced cracks run parallel to the major compressive direction. This type of failure-mode is characterised by:

$$\varepsilon_1 < 0 < \varepsilon_2 \leq \varepsilon_3$$

The second type is PTI, planar transverse isotropy. All cracks run parallel to a plane. The deformational responseis:

$$\varepsilon_1 \leq \varepsilon_2 < 0 < \varepsilon_3$$

$\varepsilon_i (i=1,2,3)$ represent the three principal strains.

From the tests, it was observed that post-peak behaviour is strongly influenced by the kind of failure mode. In the PTI-case a very fast degradation of material strength is found. Energy release is concentrated in one direction. In the CTI-case the descending branch showed to be more gradual.

Also in close relation to this anisotropic behaviour, is the direction of the initial damage field with regard to the major and minor compressive direction. The initial damage is the result from creep, shrinkage and bleeding during the hardening process of the concrete. Weaker spots develop under the bigger aggregate particles.

The influence of this factor is shown in figure 3. In the cyclic-case the major compressive load is applied parallel to the direction of casting. (specimen 8B2-4). In the second test (8A1-3) monotonic loading is applied perpendicular to the direction of casting. In general, an increase of energy-requirement was observed when loading was parallel rather than perpendicular. In the case shown (fig. 3) also some of the extra energy-requirement is due to load-cycling.
The cyclic loading path did not influence the peak stress-level. However, we did observe some influence of load-cycling on the peak-strain-level.

The effect of initial-anisotropy on the descending branch, was already observed in uniaxial pre-tests. However, in the uniaxial case only a difference of energy-requirement of about 10 % was measured.

4. Conclusions

At this stage only very preliminary conclusions can be drawn:

- In the triaxial compression-region, two major types of failure-modes can be distinguished. Both types (PTI and CTI) have a typical post-peak behaviour.

- The alignment of the initial damage field with regard to the current stress-state, very much affects the energy-requirement for fracturing the specimen.
- Cyclic-loading to the envelope, does not seem to affect the peak-stress-level.

5. References

-1- Chen, W.F. - Saleeb, A.T.
"Constitutive equations for engineering materials",
vol. 1., Elasticity and modelling, John Wiley & Sons, 1982.

-2- Gerstle, K.H. - Aschl, H. - et.al.
"Behaviour of concrete under multiaxial stress-states",
Journal of the Engineering Mechanics Division, proc. ASCE,
vol. 106, no. EM 6., dec. 1980, pp. 1383-1403.

-3- Kupfer, H.B. - Gerstle, K.H.
"Behaviour of concrete under biaxial stresses",
Journal of the Engineering Mechanics Division, proc. ASCE,
vol. 99, no. EM 4, August 1973, pp. 853-866.

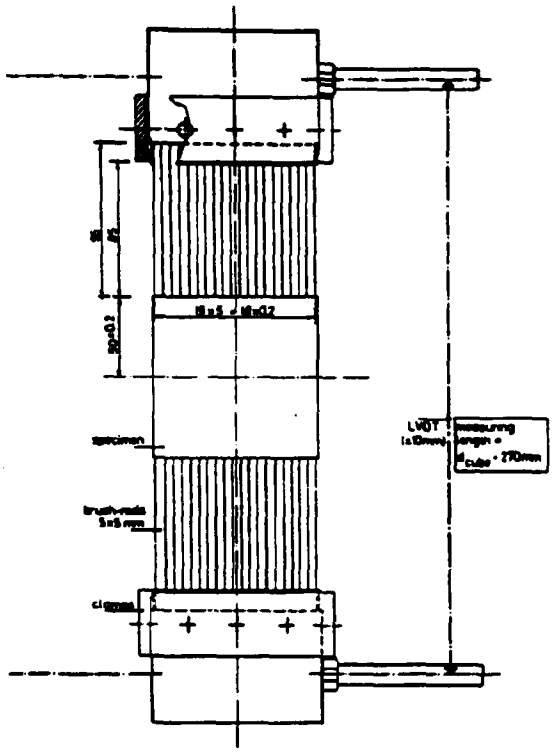

fig.1. strain measuring system

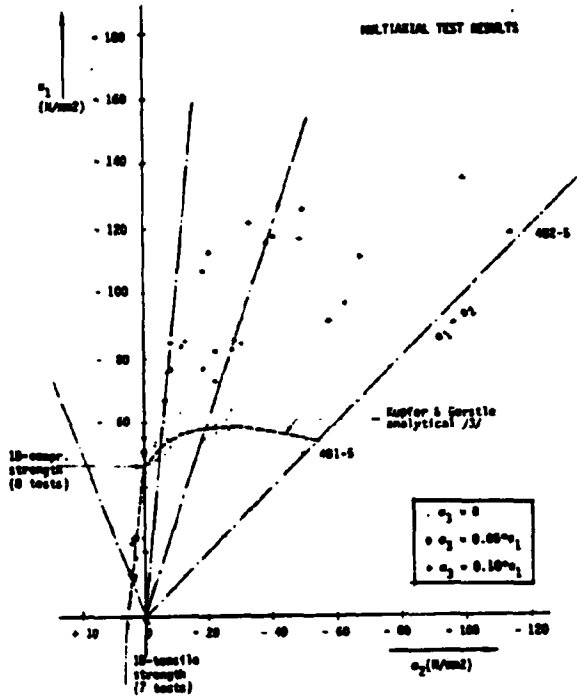

fig.2. strength results

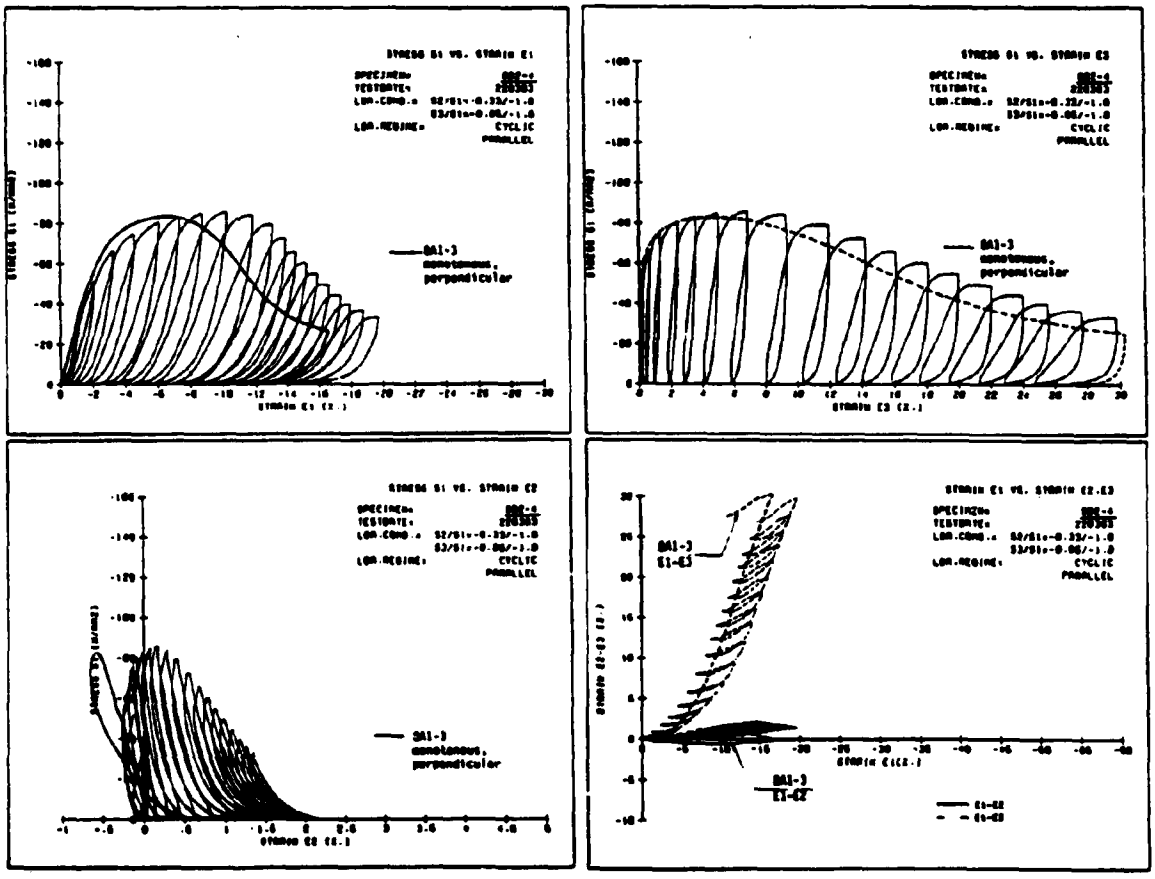

fig. 3. examples of stress-strain curves

NUMERICAL MODELLING OF CONCRETE: SOME NEW DEVELOPMENTS IN DIANA

Summary of lecture presented at Delft University of Technology

R. de Borst
Institute TNO for Building Materials and Building Structures
Software Engineering Department / Section DIANA

Rijswijk, August 1983.

NUMERICAL MODELLING OF CONCRETE: SOME NEW DEVELOPMENTS IN DIANA.

R. de Borst
Institute TNO for Building Materials and Building Structures
Software Engineering Department / Section DIANA.

Rijswijk, August 1983.

Summary of lecture presented at Delft University of Technology, Delft,
June 1983.

1 INTRODUCTION

The main theme of the lecture is the numerical modelling of concrete under multiaxial compressive loading, both with respect to the constitutive modelling and with respect to the numerical treatment of the derived constitutive law. The lecture concludes with a brief survey of new methods for solving nonlinear equations, which have recently been implemented in the DIANA finite element package.

2 PLAIN CONCRETE UNDER MULTIAXIAL COMPRESSIVE LOADING

The mechanical behaviour of concrete in compression is among other phenomena characterized by friction, by inelastic volume changes, and by an increasing ductility at higher stress levels. Presently, three different types of models exist for describing the nonlinear response of solids under short-time loading. These are nonlinear elastic models, plasticity models and fracturing models. Nonlinear elastic models cannot adequately represent the phenomena just mentioned. Further, a number of theoretical objections exist against such models, especially when they are employed in a three-dimensional situation.

Fracturing models have only recently been developed (Doughill, 1976) and promise to be versatile for describing concrete behaviour, especially when they are combined with a plasticity model to account for the more ductile behaviour of concrete at higher stress levels. Therefore, implementation in DIANA of such a model is currently in progress (de Borst, 1983).

Classical plasticity theory as originally developed for metals can also not represent the phenomena as described above. From geomechanics it is known however, that plasticity theories can be developed such that the frictional character and the inelastic volume changes can be described quite well (Vermeer, 1978). To this end, failure criteria which also involve the first stress invariant are employed and Drucker's postulate is abandoned so that a non-associated plasticity model is obtained. In contrast to failure criteria which also involve the first stress invariant, non-associated flow rules are not yet frequently employed in

concrete mechanics. Nevertheless, their influence upon the load-deformation behaviour of a structure can be significantly. For certain structures, even the collapse load can be affected, as is shown by the example of a dome (see figure 1). The results of the calculations are shown in figure 2, one being performed with a Mohr-Coulomb yield criterion with a classical associated flow rule, and one with a simple non-associated flow rule (see figure 3). The results reveal a clear influence of the adopted flow rule on the collapse behaviour.

Another property of concrete which cannot be described within classical plasticity theory is the increased ductility at higher stress levels. In the hardening regime, this phenomenon can however be accommodated for by a hardening law in which the friction angle rather than the cohesion depends upon the strain history (see figure 4). The difference in response of a concrete specimen at increasing confining pressure is illustrated in figure 5 for both types of hardening. It is clear that this improved description in DIANA for the hardening regime has to be augmented by a suitable model for the softening regime. This has not yet been done.

3 NUMERICAL TREATMENT OF RATE LAWS

Owing to their computational simplicity, rate laws are mostly integrated by an explicit scheme in order to arrive at a relation between finite increments. In the past, some researchers have pointed out that such schemes have rather poor convergence properties and that implicit strategies should be preferred (for instance Willam, 1978). Even more so than for metals this statement holds for materials as concrete, rocks, and soils due to their frictional character (Vermeer, 1979).

Detailed treatment of the implicit scheme which is currently employed within DIANA is beyond the scope of this extended summary. The interested reader is referred to Vermeer (1979), and to de Borst (1982). To demonstrate the differences which may result from using different integration schemes, the dome of figure 1 has been analyzed using the explicit scheme as previously employed in DIANA and by the implicit scheme. Especially at higher load levels, significant differences occur. From figure 6 it can be observed that at impending failure, the explicit scheme predicts a much too stiff structural response.

4 SOLUTION OF NONLINEAR FINITE ELEMENT EQUATIONS

The last part of the lecture is devoted to solution procedures of nonlinear finite element equations. Currently, much attention is paid to implementing and testing new solution algorithms like arc-length control procedures (Riks, 1979) for overcoming limit and bifurcation points, modified initial stress procedures, and Quasi-Newton or Secant methods (Crisfield, 1979) for improving the convergence within a loading step. An example of a large displacement analysis of a shallow circular arch, computed by displacement control as well as by an arc-length constraining

method is included (figure 7).

5 CONCLUDING REMARKS

A brief survey has been given of new development which currently take place in DIANA. Although not all these developments are original, bringing them together in one programme seems to be rather unique. The options which are now available, and the ones which will become available shortly, make DIANA to be one of the more powerful packages in the field of concrete mechanics.

REFERENCES

Borst, R. de (1982), Numerical prediction of the ultimate bearing capacity of soil masses. Rep. No. 220, Geotechnical Laboratory, Delft University of Technology.

Borst, R. de (1983), Plastic-fracturing theory for concrete: an assessment and implementation aspects. To be published as TNO-IBBC report.

Crisfield, M.A. (1979), A faster modified Newton-Raphson iteration. Comp. Meth. Appl. Mech. Eng., 20, 267-278.

Doughill J.W. (1976), On stable progressively fracturing solids. ZAMP, 27, 423-437.

Riks, E. (1979), An incremental approach to the solution of snapping and buckling problems. Int. J. Solids Structures, 15, 529-551.

Vermeer, P.A. (1978), A double hardening model for sand. Geotechnique, 28, 413-433.

Vermeer, P.A. (1979), A modified initial strain method for plasticity problems. In Proc. Third Int. Conf. Num. Meth. Geomechanics (ed. W. Wittke), 377-387.

Willam K.J. (1978), Numerical solution of inelastic rate processes, Computers and Structures, 8, 511-531.

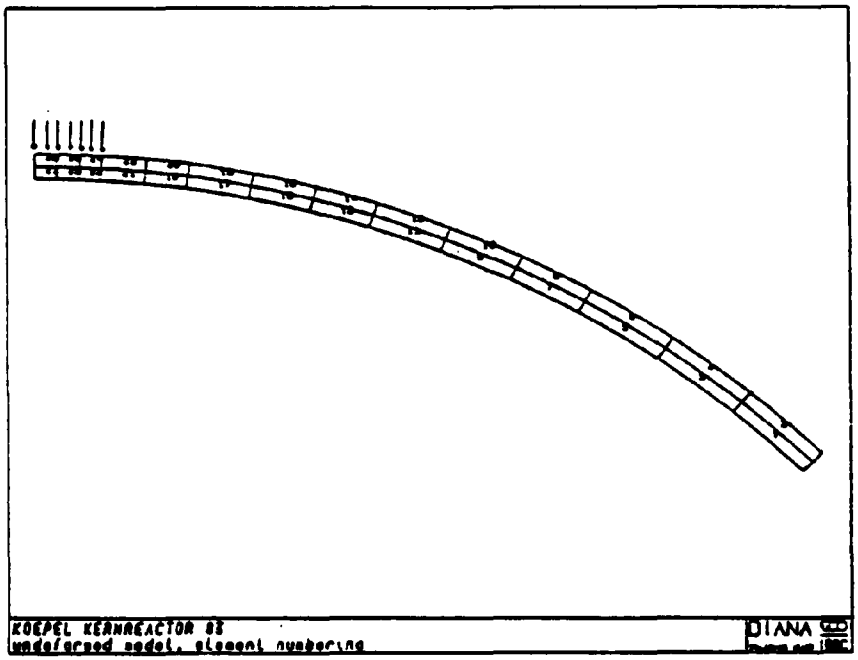

Figure 1. Finite element mesh of dome structure.

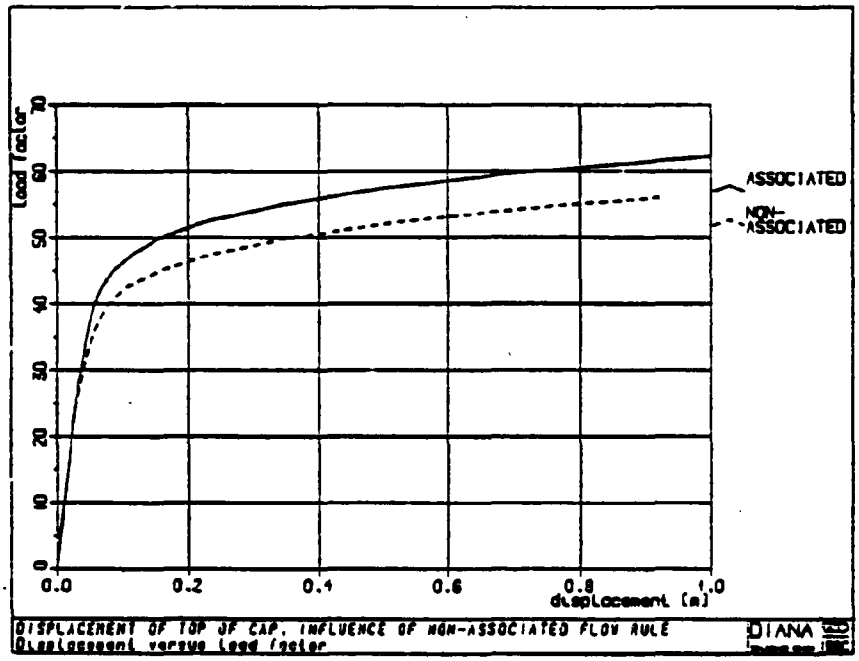

Figure 2. Load-deflection curve for associated and non-associated plasticity model.

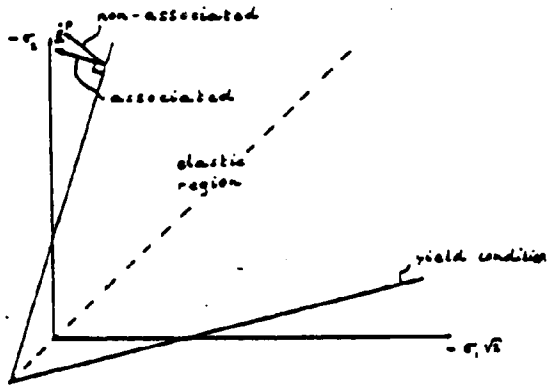

Figure 3. Graphical representation of non-associated plasticity model.

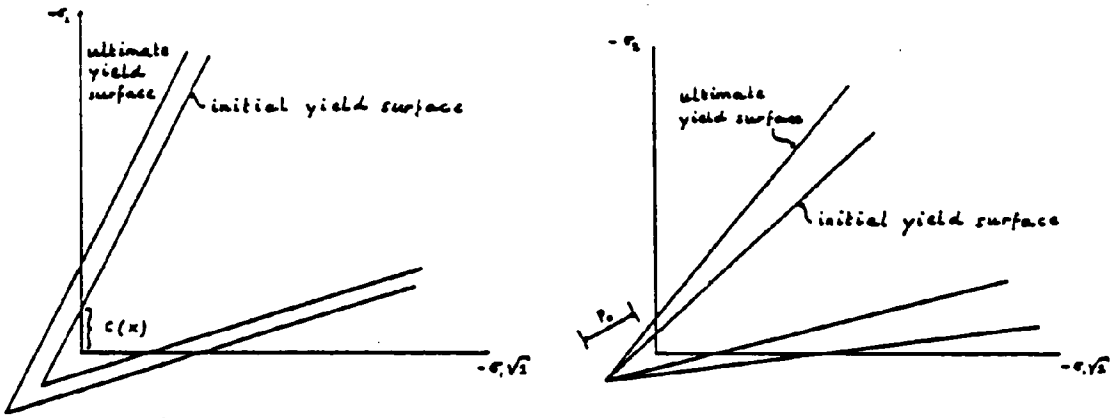

Figure 4. Representation of cohesion and friction hardening in the stress space.

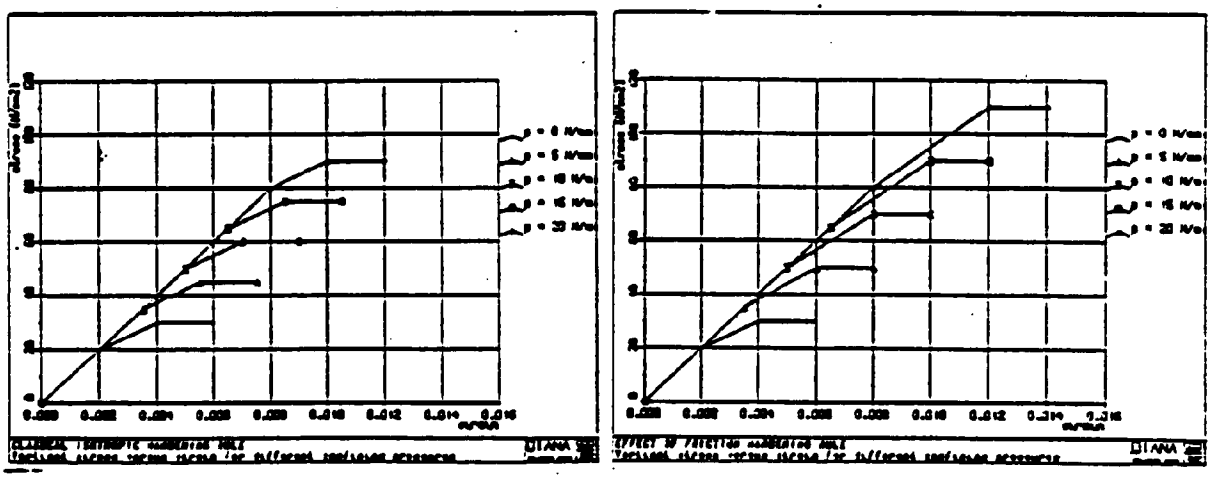

Figure 5. Response of concrete specimen at increasing confining pressure; (a) hardening on the cohesion (b) hardening on the friction angle.

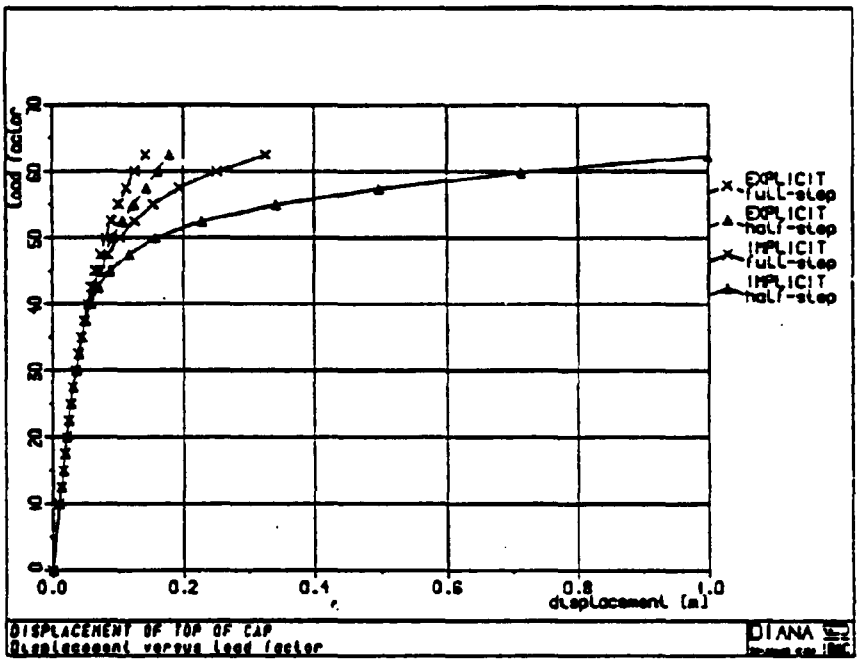

Figure 6. Load-deflection response of dome structure using different integration schemes.

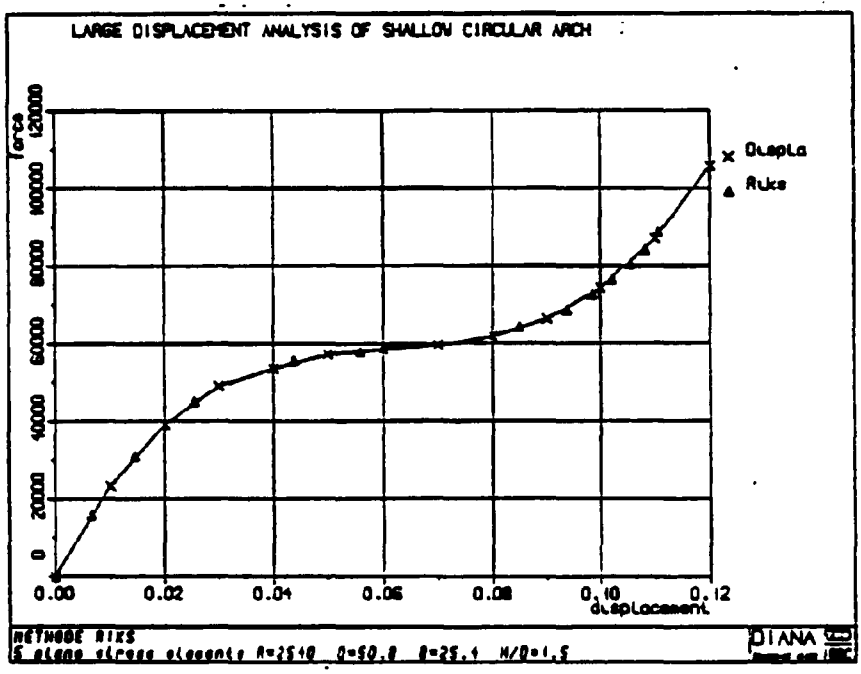

Figure 7. Load-deformation curve for a shallow cinrular arch, calculated by displacement control as well as by arch length control.

BOND BETWEEN CONCRETE AND REINFORCEMENT

Hans Groeneveld
Mato Dragosavić

INSTITUTE TNO FOR
BUILDING MATERIALS AND BUILDING STRUCTURES
Rijswijk, The Netherlands

In 1981 a physical model and a mathematical model for bond were outlined based on a rational approach of a triaxially loaded bond zone. Further a program of experiments was drawn for verification an quantification of the models.

Two series of tests were included:

a) Cast in bars loaded in tension. The differences with relation to other similar tests are a greater length of the specimen, introduction of several primary cracks and variation of bar diameter, concrete cover and concrete quality. Sustained and cyclic loading is involved.
b) Detail-tests on the bond zone, 0.5 ϕ thick and 3 ϕ long (ϕ = bar diameter). The concrete outside the bond zone is substituted by a metal tube. These tests make it possible to measure the axial bond stress and slip, as well as the consequent radial stress and displacement (the origine of longitudinal cracks).

In 1982 a lot of effort is spend on improving the test specimens, the loading procedure and the accuracy of the measurements.
In 1983 the main program of the experiments is being carried out.

Some of the first results are shown in the figures 1 to 4.

Figure 1 shows an example of the measured steel strains along the bar in a tensile specimen, before cracking and after one, two and three cracks occured. Figure 2 gives the corresponding axial bond stresses.

Figure 3 is an example of the measured axial bond stresses versus measured slip in a detail-specimen, due to monotonic and repeated loading. Figure 4 shows the corresponding radial bond stresses.

The meeting at the Delft University of Technology in June 1983, was, as well as former meetings, a good opportunity to exchange research data on bond with foreign institutes (Cornell a.o. from U.S., Germany and Italy). Various complications related to bond are discussed (e.g. compression and tension perpendicular to a reinforcing bar). The Dutch program is found promissing and necessary.

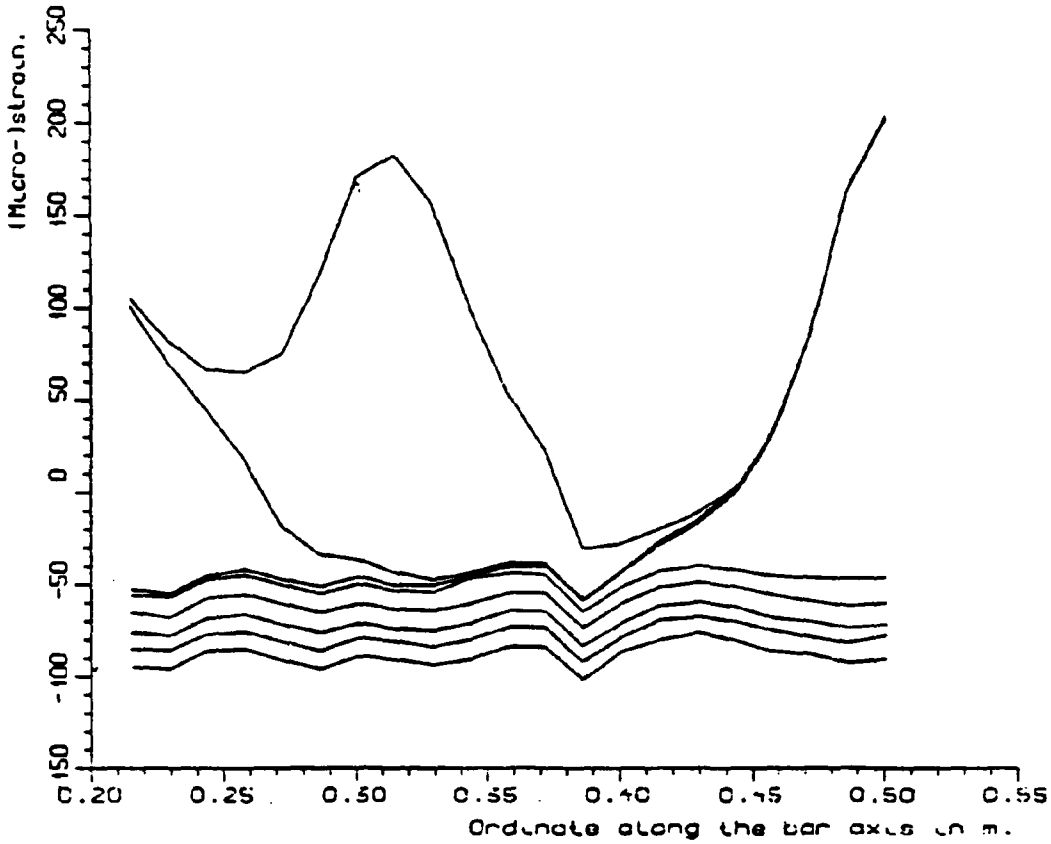

Figure 1: Tensile specimen; steel strains along the bar

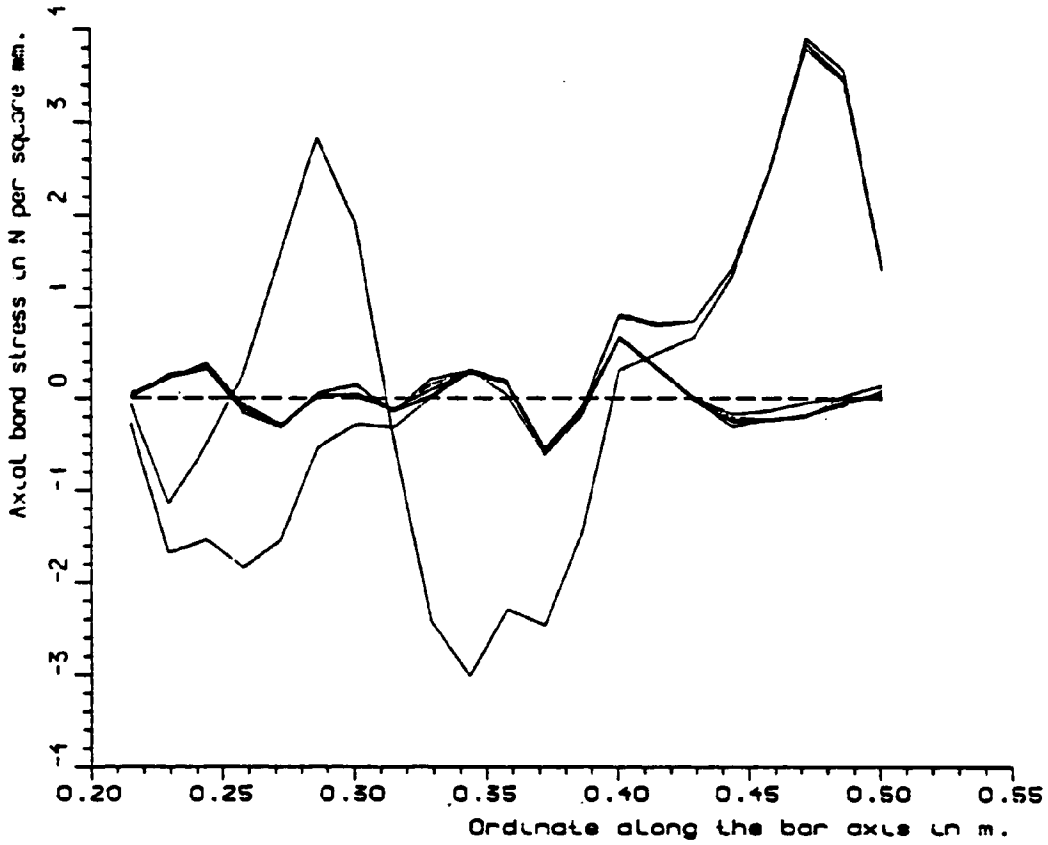

Figure 2: Tensile specimen; axial bond stresses along the bar

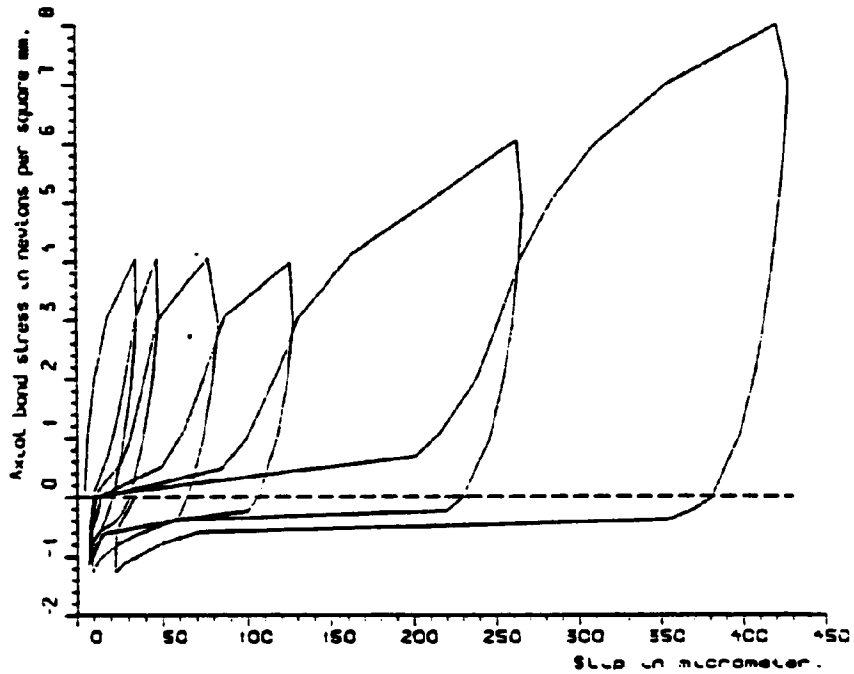

Figure 3: Detail-specimen; axial bond stress versus slip

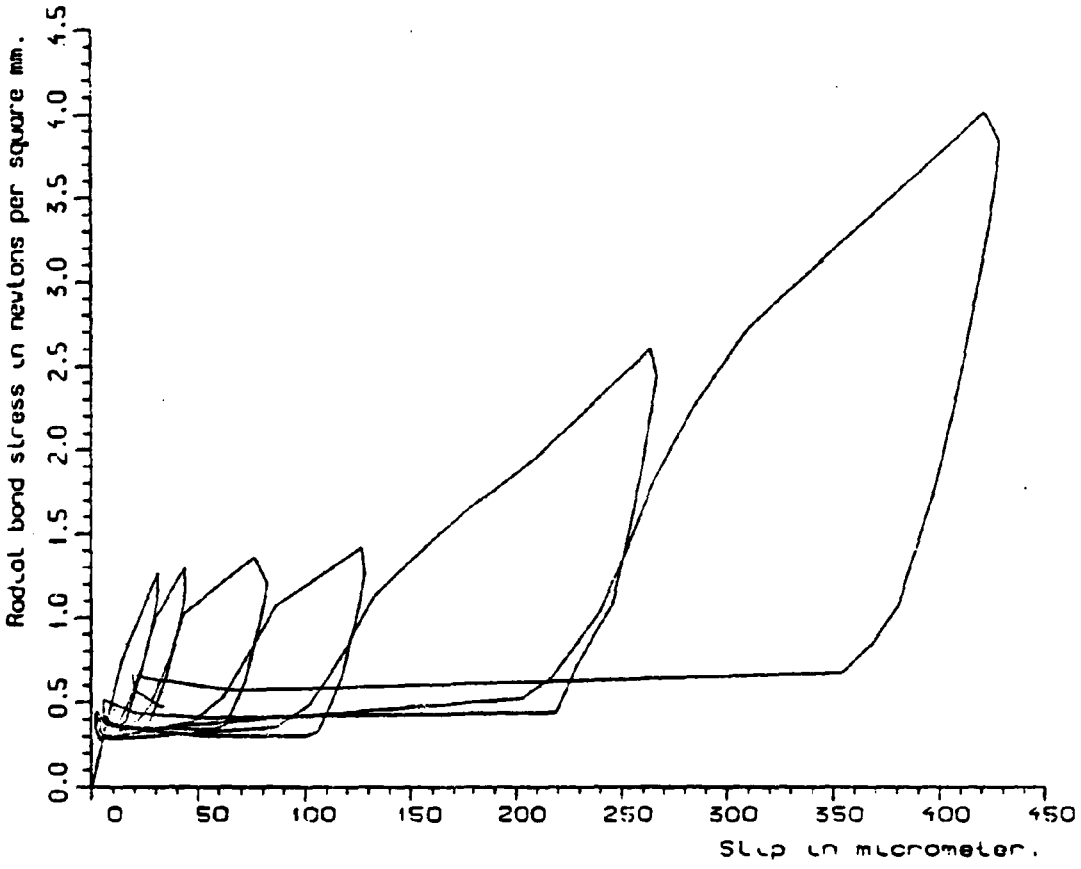

Figure 4: Detail-specimen; radial bond stress versus slip

SMEARED CRACK ANALYSIS OF SOME BENCHMARK PROBLEMS WITH DIANA

J.G. Rots, R.J. van Foeken, G.M.A. Kusters

Institute TNO for Building Materials and Building Structures
Rijswijk, The Netherlands.

Rijswijk, August 1983

SMEARED CRACK ANALYSIS OF SOME BENCHMARK PROBLEMS WITH DIANA

J.G. Rots, R.J. van Foeken, G.M.A. Kusters

Institute TNO for Building Materials and Building Structures
Rijswijk, The Netherlands.

INTRODUCTION

The finite element package Diana, developed at TNO-IBBC, offers the facilities of a non-linear analysis of concrete (or other material) structures. Several constitutive relations are available for modelling the diversity of the material behaviour of concrete under multiaxial stress states e.g. cracking, creep and crushing. The DIANA results of three types of benchmark problems with reference to crack modelling of concrete structures are discussed. For full details about the computations and backgrounds of the constitutive model the reader is referred to [4,5,6,7]. The benchmarks are:

- Mixed-mode crack propagation test
  At Cornell University experiments are performed on notched, unreinforced concrete beams [1]. We analysed beam C1. The notch and the load were placed in such a way that the beam was loaded non-symmetrically which leads to the arising of a mixed-mode crack in front of the notch. Between the two crack faces not only a crack opening displacement (mode I), but also a crack sliding displacement (mode II) occurs.

- Reinforced beams, subjected to four-point loading
  Three beams (A1, A2 and A3) out of a series of beams are studied which were tested at the Stevin Laboratory of the Delft University of Technology in the Netherlands in a researchprogram to investigate the influence of beam depth and crack roughness on the shear failure load [8]. The concrete beams have no shear reinforcement, only underside reinforcement. Beam A1 collapses by yielding of the reinforcement, whereas the beams A2 and A3 fail in shear by the arising of a diagonal tension crack prior to yielding of the reinforcement. In this summary the computations on the beams A1 and A2 are reported.

- Punch test
  A reinforced circular plate has been tested at the Stevin Laboratory of the Delft University of Technology. The failure mechanism is punch of the column prior to yielding of the reinforcement. The main problem of this benchmark is the occurrence of cracks in the radial and tangential directions.

CONSTITUTIVE MODEL

For the behaviour of uncracked concrete under tensile and compression loading an elasto-plastic model, based on an associated flow rule, has been adopted. Incidentally, the model has been extended by isotropic hardening.
To initiate a crack tension cut-off criteria are available, as shown in figure 1. Once the principal stresses exceed the tension cut-off criterion a crack is introduced, perpendicular to the direction of the principal tensile stress.
Within Diana the smeared crack concept is used. This concept spreads the effect of cracking over the entire volume that belongs to an integration point of the finite element.
Crack propagation is controlled by a fracture mechanics criterion that takes into account the 'tension-softening' effect. This effect reflects the gradual decrease of the tensile load carrying capacity, which is the result of the formation of micro-cracks in front of a macro-crack. We employ an adapted and extended version of the linear tension-softening model proposed by Bazant and Oh [3]. This model is organized around an equivalent concrete tensile stress-strain diagram, as shown in figure 2. Three regions can be distinguished (1) elastic, (2) partially cracked or micro-cracked and (3) fully cracked. The length of the descending branch ϵ_u is linked with the fracture energy G_f , see [5].
To simulate aggregate interlock we reduce the initial shear stiffness once cracks occur by using βG , where β is the shear retention factor ($0< \beta <1$) and G is the elastic shear modulus of uncracked concrete. For concrete good results are attained with $0.01< \beta <0.2$.

GENERAL REMARKS ON THE COMPUTATIONS

Eight-noded isoparametric plane stress elements have been used to represent the concrete. The elements are numerically integrated employing the four-point Gauss integration scheme. For information on the element formulation see Bathe [2].
The reinforcement is smeared out into a thin sheet having the same cross section as the actual reinforcement. Between the concrete and the reinforcement perfect bond is assumed.
The Modified Newton-Raphson scheme was adopted. As yieldcriterion the Drucker-Prager and the Von Mises criterion were used for concrete and reinforcement respectively. The tension cut-off criterion 2 is applied, see figure 1, which is in agreement with experimental findings.

MIXED-MODE CRACK PROPAGATION TEST, [6]

The experimental set-up of the notched unreinforced beam is shown in figure 3. The concentrated load was applied to the steel beam which distributes the load to the concrete beam. The finite element mesh can be recognized from figure 4, which shows a plot of the deformations. The steel beam was included into the mesh. In order to compute the beam behaviour not only before but also after the point at which the maximum load is reached, the computations were performed by controlling the displacement at the loading point.
The nonlinear response of the beam is presented in terms of load-CMSD curves, in which CMSD is the crack mouth sliding displacement as indicated in figure 4. The experimental as well as the computed load-deflection curves are shown in figure 5.
The computation appears to give a good approximation of reality. After the top there is a difference, viz. the experimental curve shows a faster decline than the computed curve. This is probably due to the fact that in the analysis many integration points suddenly cracked just after the top of the diagram was reached, which may have resulted in numerically inaccuracies. It should be said that the values of the fracture energy G_f, the shear retention factor β and in particular the assumption for the crack band width h affect the calculated curve, see [6].
The crack patterns corresponding to two CMSD levels, indicated in figure 5, are presented in figure 6. From the mesh only the part around the notch is shown. A distinction is made between the size of the actual strain at the gausspoints to investigate the occurrence of strain localization. Thick lines indicate cracks with strains larger than 0.0005, whereas normal lines indicate cracks with strains smaller than 0.0005. Many cracks appear to have small crack strains and may be interpreted as 'pseudo-cracks'. When we disregard these pseudo-cracks, the single crack of the experiment is clearly predicted by DIANA. The only difference is that the predicted path of the crack is somewhat too steep.
By studying this benchmark problem two main problems arise. First, the mixed-mode crack does not propagate parallel to the lines of the finite element mesh. This inevitably leads to a 'zig-zag' crack band path of which the width h is not constant but varies along the crack band path. Secondly, our tension-softening model assumes all supplied energy to be consumed in crack opening, whereas in reality also a part of the supplied energy will be consumed in crack sliding. A coupling between tension-softening and shear stiffness reduction is required. Both aspects need further study.

REINFORCED CONCRETE BEAMS, [4,7]

The finite element mesh and the geometrical properties of the beam A1 are shown in figure 7. On account of symmetry of the structure, the boundary conditions and the loading, it was sufficient to confine the analysis to one half of the structure. The computations were carried out displacement controlled at the loading point.
The experimental as well as the computed load-deflection curves of beam A1 are presented in figure 8. The computed behaviour resembles the recorded behaviour closely. In both cases failure occurs by yielding of the reinforcement. The predicted failure load differs only less than 10 % of the experimental one. The crack patterns of this beam are presented in figure 9. When the strain normal to the crack exceeds 0.001 the crack is marked by a thick line. Just like the previous benchmark, a considerable number of integration points appear to contain pseudo-cracks with very small crack strains. By disregarding these pseudo-cracks, the predicted crack patterns clearly visualize the dominant cracks occurring in the experiment.

The mesh and the geometrical properties of beam A2 are shown in figure 10. From figure 11 one may observe that the computed load-deflection curves are extremely sensitive to the choice of the shear retention factor. When using β -values higher than 0.1 numerical failure is governed by yielding of the reinforcement whereas β -values lower than 0.1 predict the beam to fail in shear prior to yielding of the reinforcement. The failure load corresponding to $\beta = 0.01$ and $\beta = 0.05$ reaches respectively 50% and 70% of the load that corresponds with yielding of the reinforcement. (For beam A3 similar results were obtained.) The low β -values (e.g. $\beta = 0.05$) appear to be the best approximation of reality since experimental failure was also brittle, due to the arising of an inclined diagonal tension crack prior to yielding of the reinforcement.
Figure 12 shows the crack patterns at two load levels ($\beta = 0.2$). Thick lines indicate cracks with normal strains larger than 0.00054. For this deeper beam A2 the dominant cracks are even more pronounced as they are for beam A1. Initially vertical flexural cracks arise near midspan. With increasing load however, we observe a transition from flexural cracking to diagonal cracking controlled by shear. In the final stage severe damage due to diagonal cracking is predicted, which is in close agreement with the experiment.

PUNCH TEST, [4]

The circular plate is an axialsymmetric structure, so we use an axialsymmetric element. For the reinforcement a grid-element was used by which the reinforcement is smeared out in two directions (radial and tangential) into a thin sheet. Between the concrete and the steel perfect bond is assumed.
The network of elements, the restraints and supports and the external loading of this structure are shown in figure 13. The load-deflection curve for the analysis and experiment are shown in figure 14. The crack patterns at different load levels in radial and in tangential direction are shown in figure 15. The calculation is discontinued after numerical instability occurs. The computed behaviour of the plate resembles the recorded behaviour closely.
The size of the crack strain in tangential direction is plotted in percentages at several Gausspoints. The dominant cracks in radial direction are marked by thick lines. The dominant crack strains vary from 0.002 to 0.006. The difference in the thickness of the lines gives an indication of the size of the calculated crack strain.
At none of the above calculations the yielding stress of the steel has been exceeded. Therefore the plate fails by punch.

CONCLUSIONS

With the current constitutive model used in the finite element package Diana good results are obtained to simulate the cracking of concrete. For a variety of benchmark problems satisfactory agreement with the experiments is attained with respect to load-deflection curves, failure mechanisms and dominant cracks which leads to ultimate failure of the structure.
The predicted crack patterns clearly reveal strain localization by considering only the large crack strains. Despite the fact that we use the smeared crack concept dominant cracks can be predicted satisfactory as shown in the above calculations.
Nevertheless, improvements are required. In particular the propagation of mixed-mode cracks, which occur in the notched unreinforced beam, the reinforced beams as well as in the punch test, should be paid attention to. Suggestions about an extension of the shear stiffness reduction concept and a coupling between tension softening and shear stiffness reduction are given in [6,7]. To analyse e.g. punching shear, the numerical treatment of two or three cracks in one integration point needs improvements, see [4].

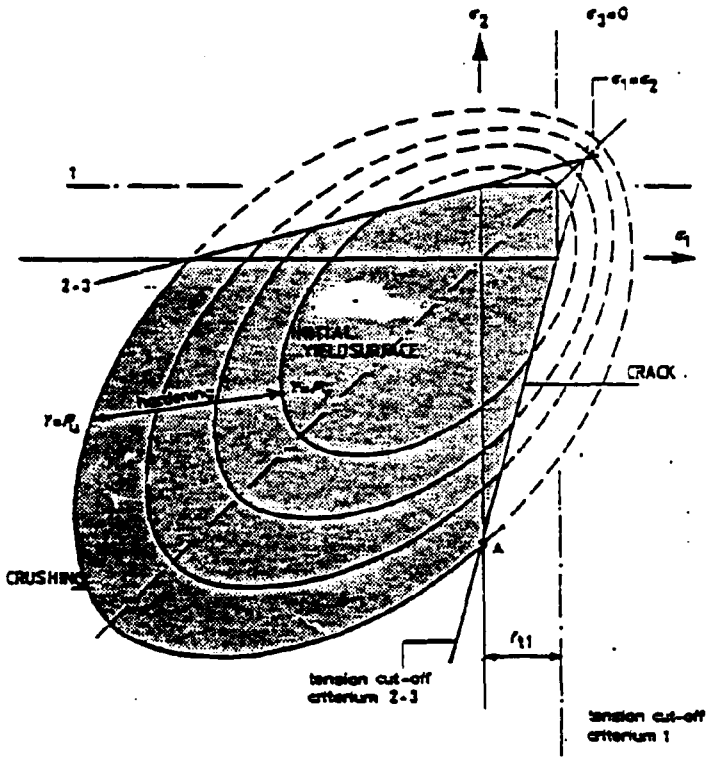

fig. 1 Tension cut-off criterion in combination with Drucker-Prager.

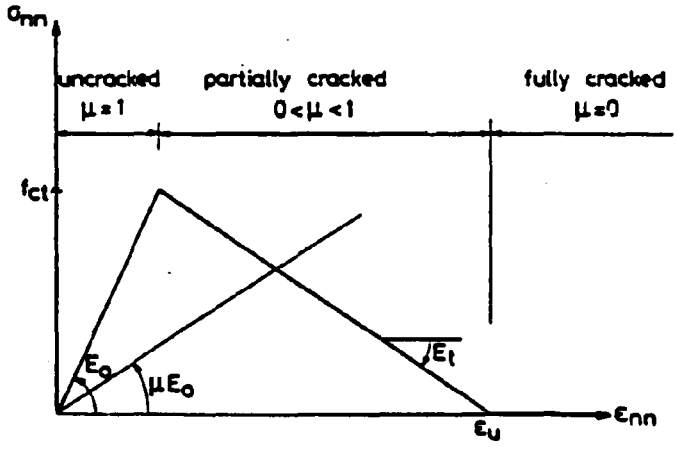

fig. 2 Tensile stress-strain relation.

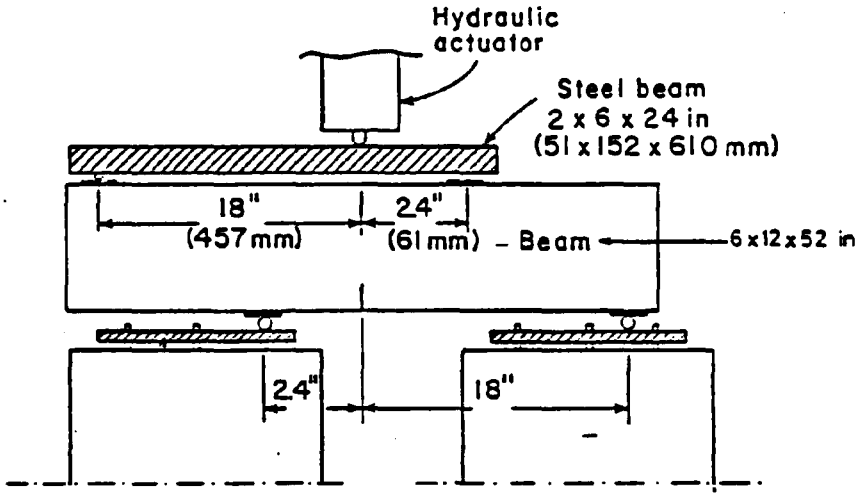

fig. 3 Experimental set-up of the mixed-mode crack propagation test.

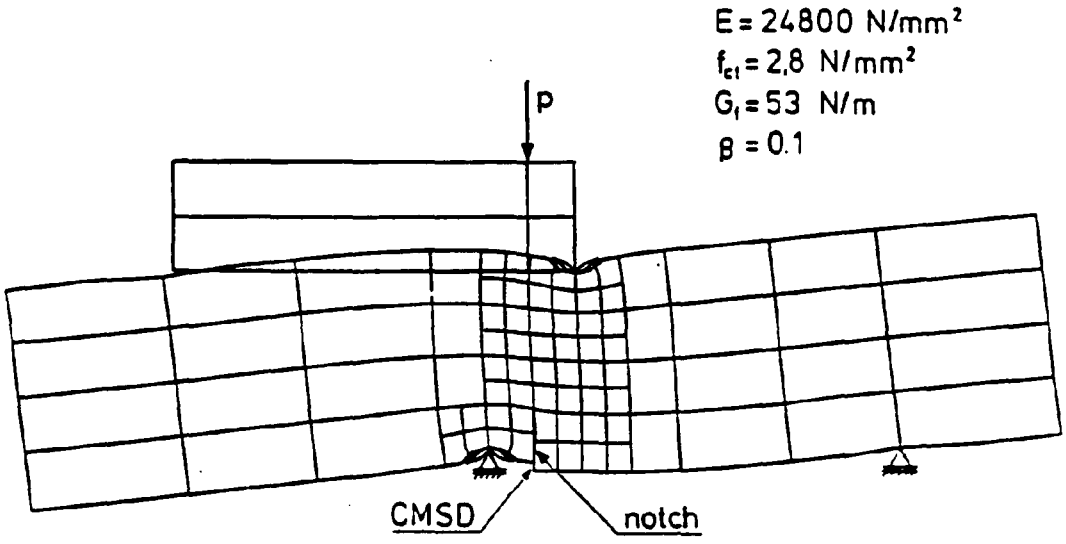

fig. 4 Finite element idealization of the mixed-mode crack propagation test.

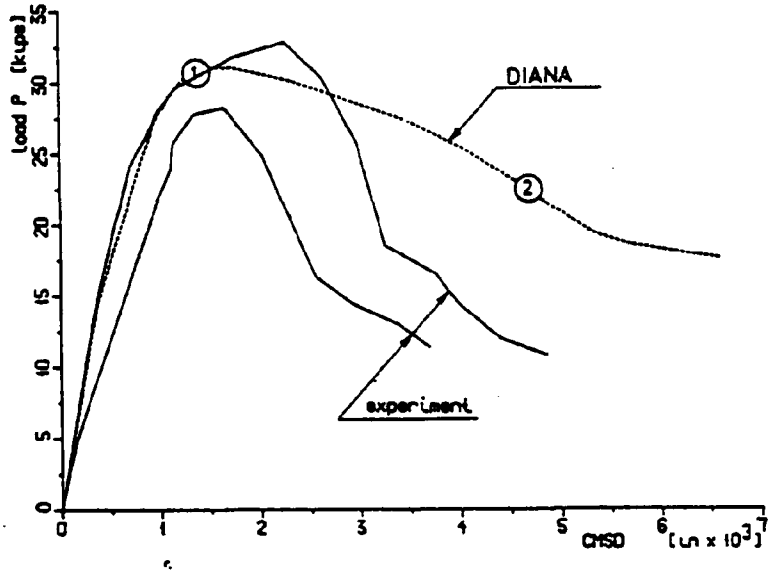

fig. 5 Experimental and computed load-deflection curves for the mixed-mode test.

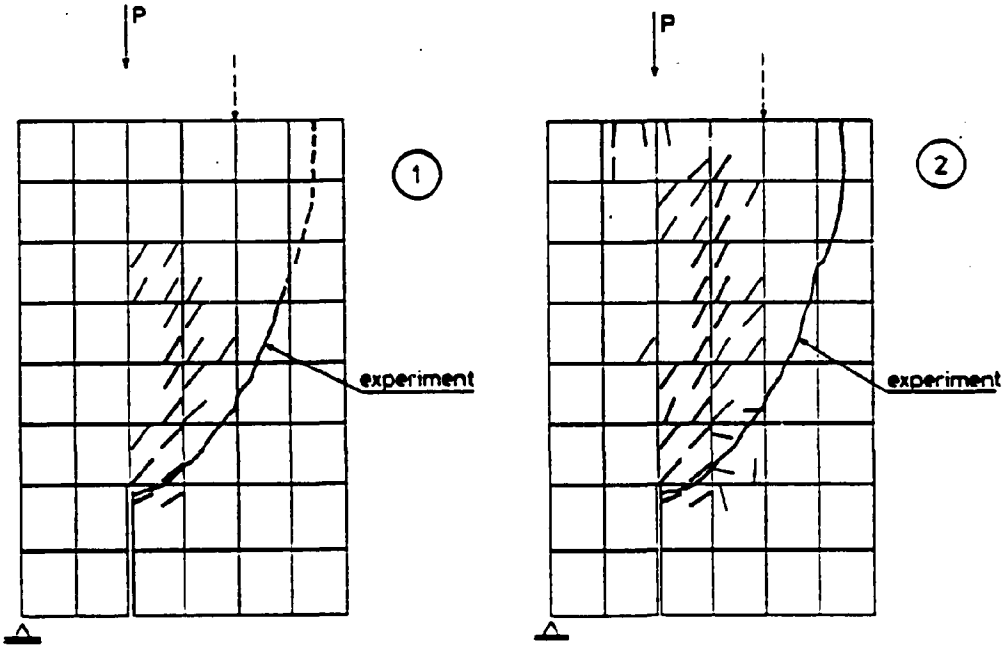

fig. 6 Crack patterns mixed-mode test at two CMSD levels.

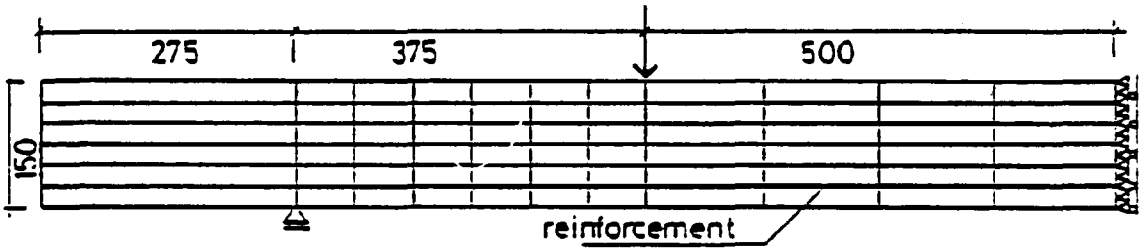

fig. 7 Geometrical properties of beam A1.

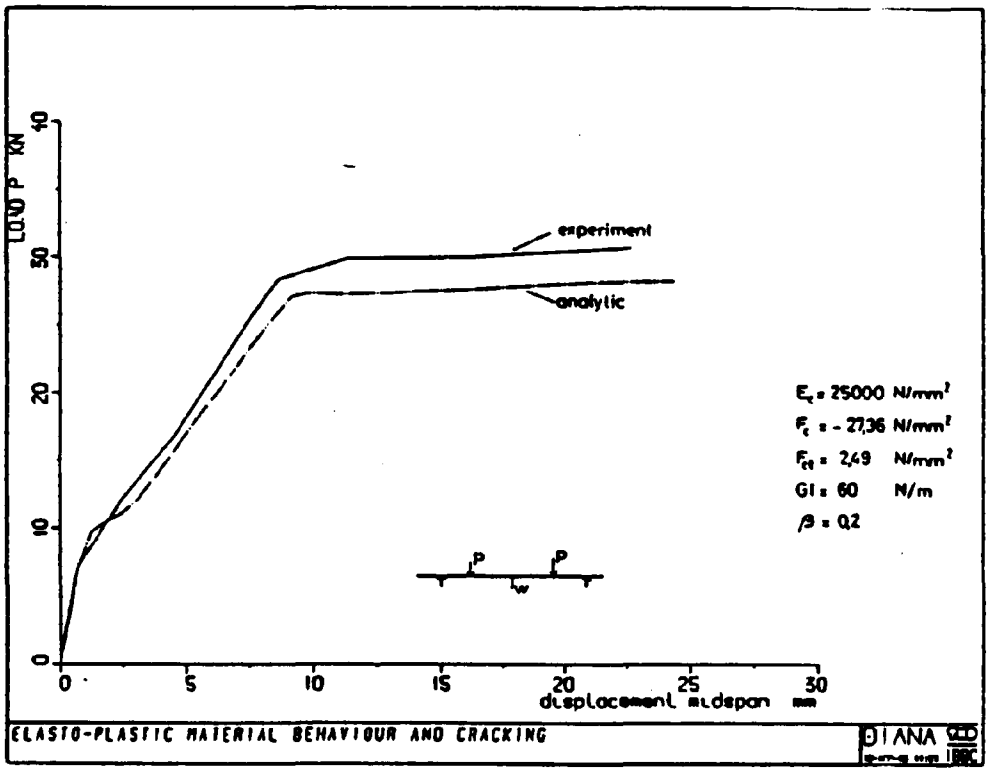

fig. 8 Experimental and computed load-deflection curves beam A1

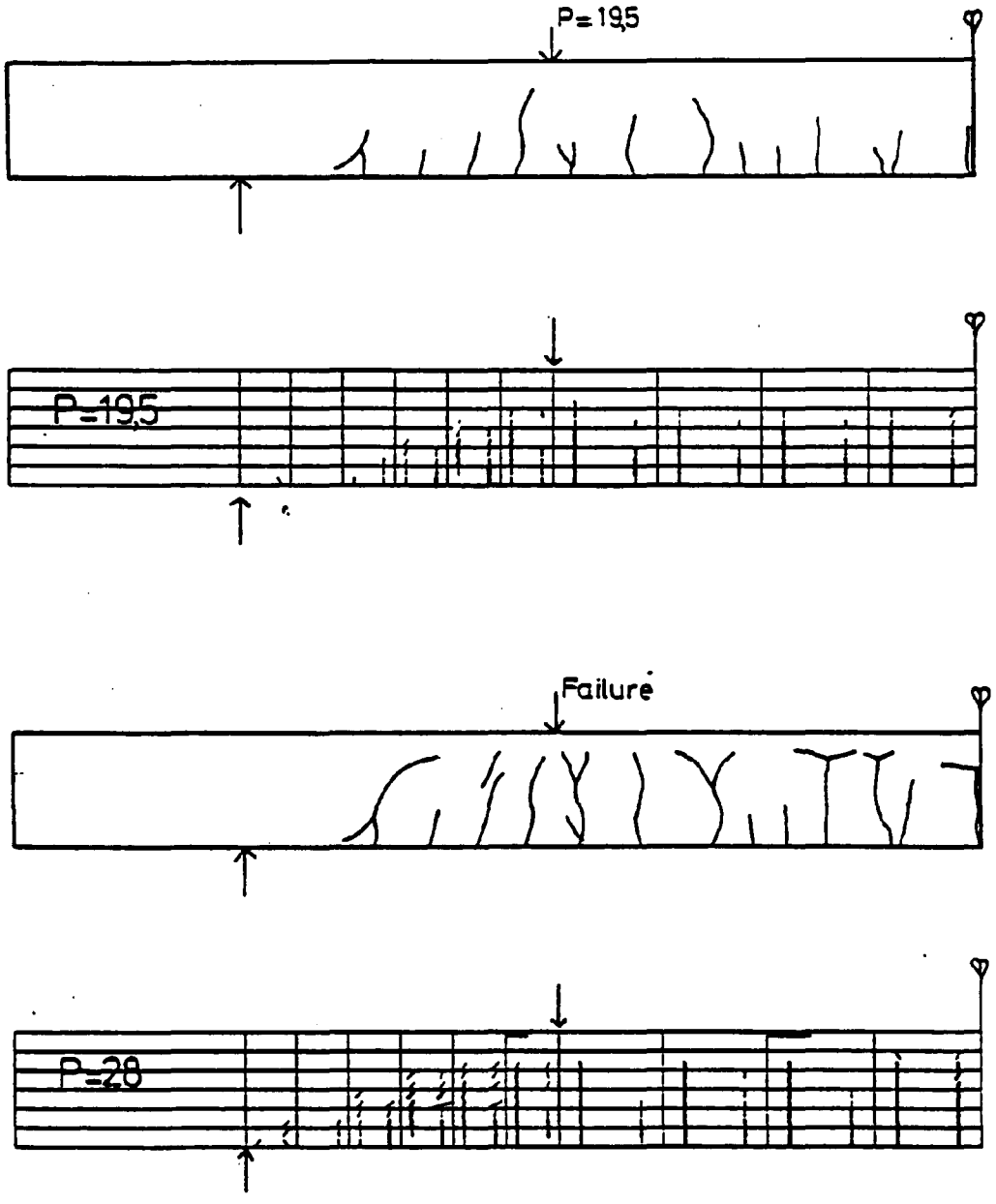

fig. 9 Crack patterns beam A1 at two load levels.

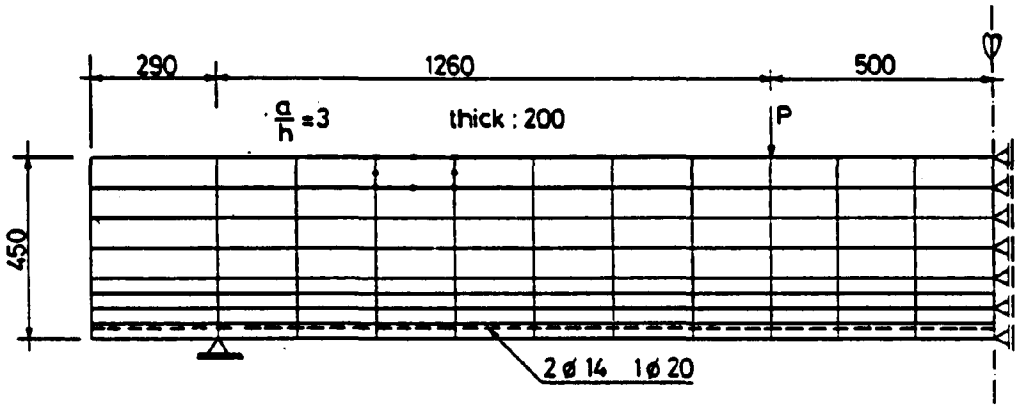

$E = 28000\ N/mm^2$

$G_f = 60\ N/m$ $f_{ct} = 2.5\ N/mm^2$

fig. 10 Geometrical and material properties of beam A2. (units in mm)

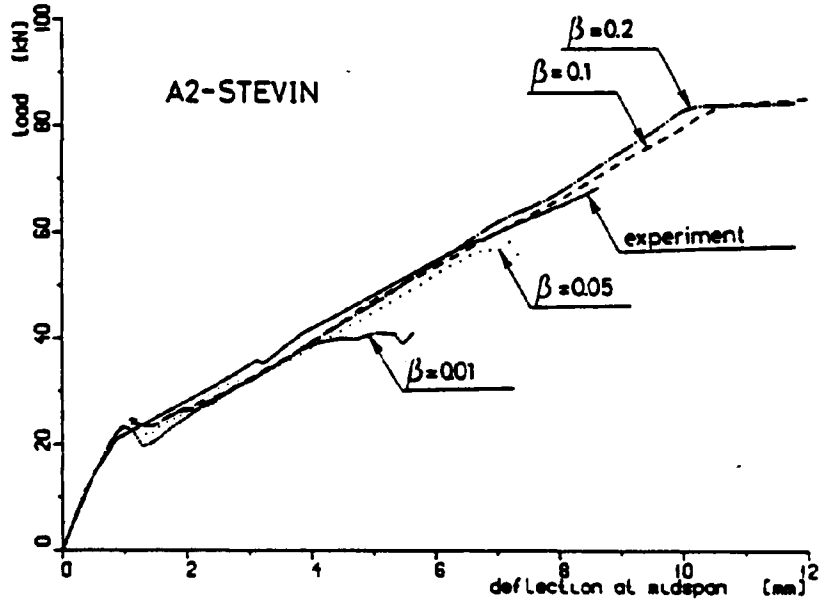

fig. 11 Load-deflection curves beam A2 for several β -factors

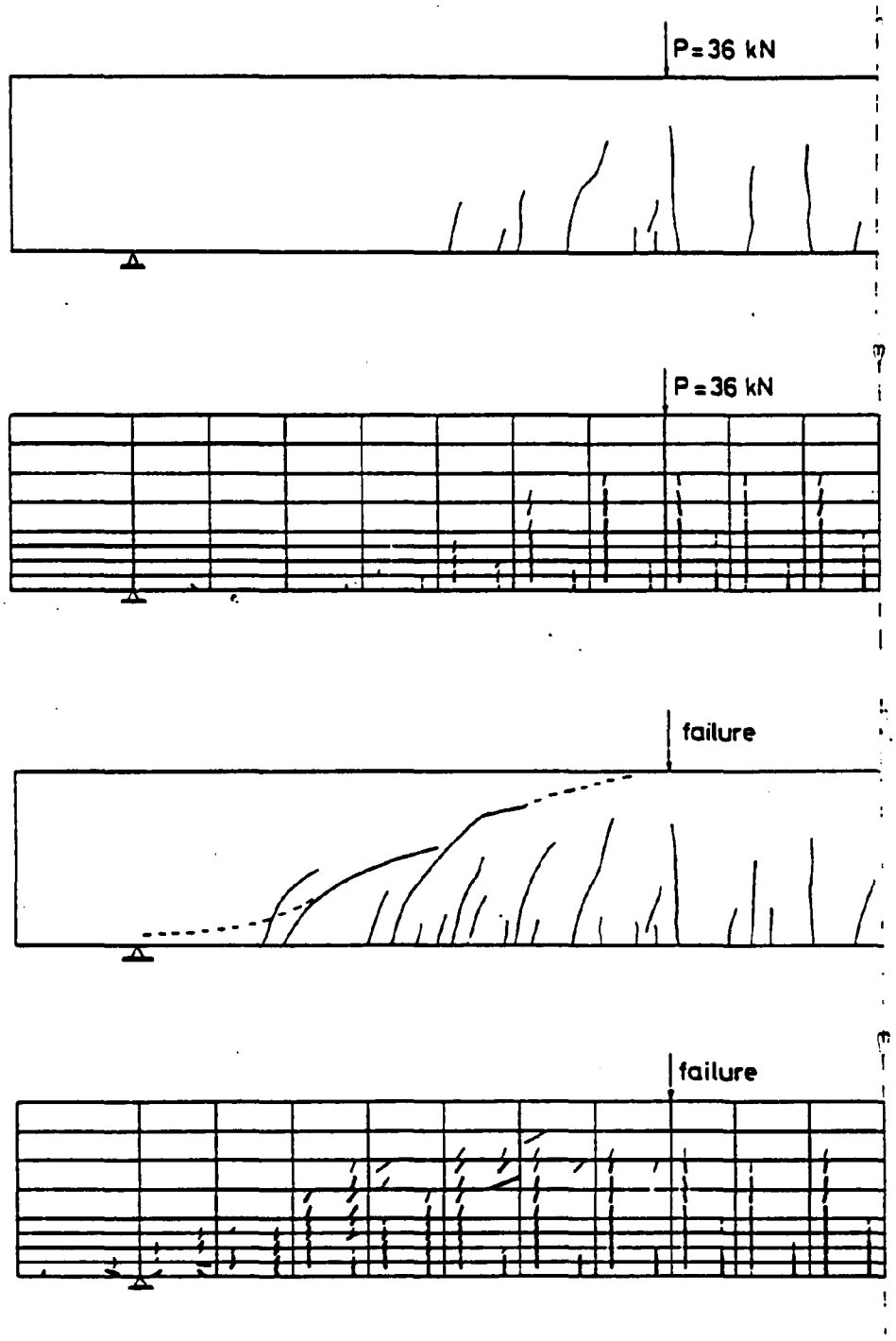

fig. 12 Crack patterns beam A2 at two load levels.

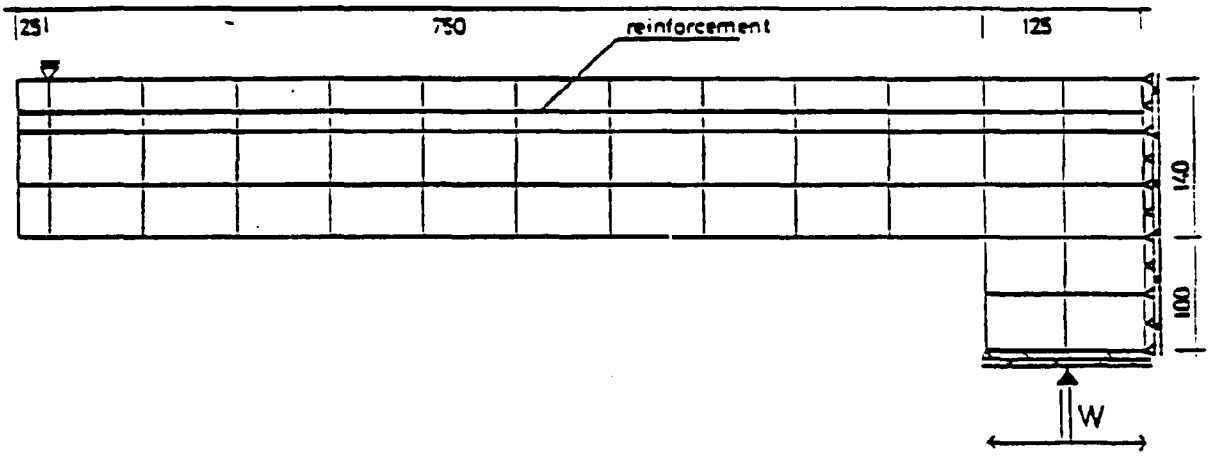

fig. 13 Geometrical properties of the punch plate.

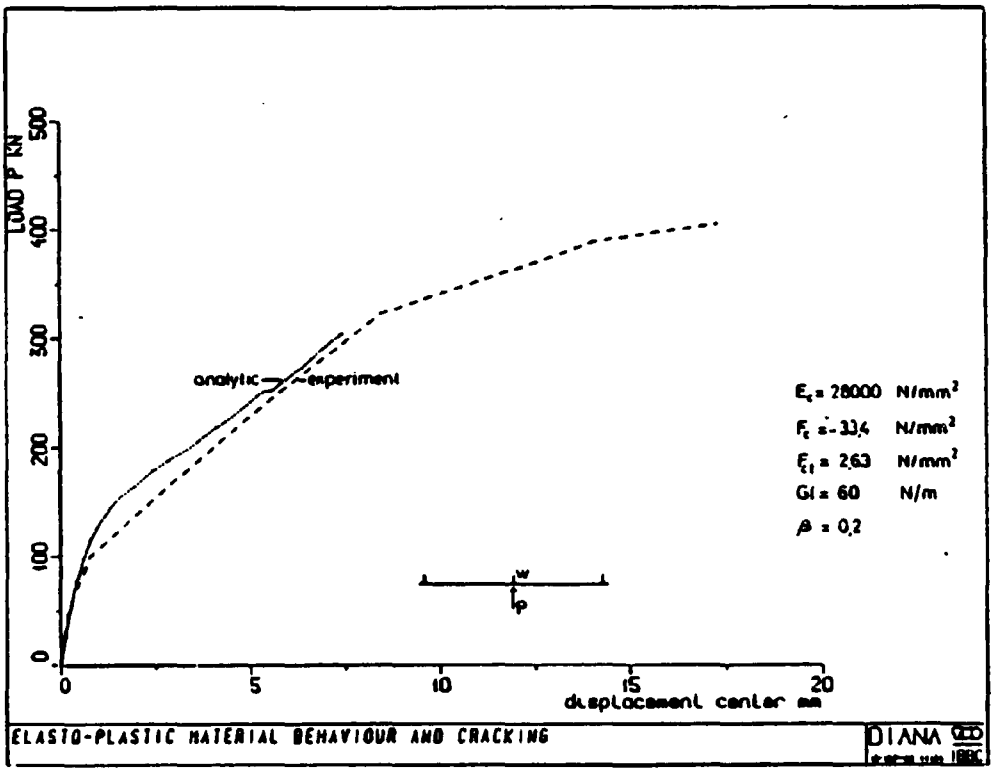

fig. 14 Experimental and computed load-deflection curve.

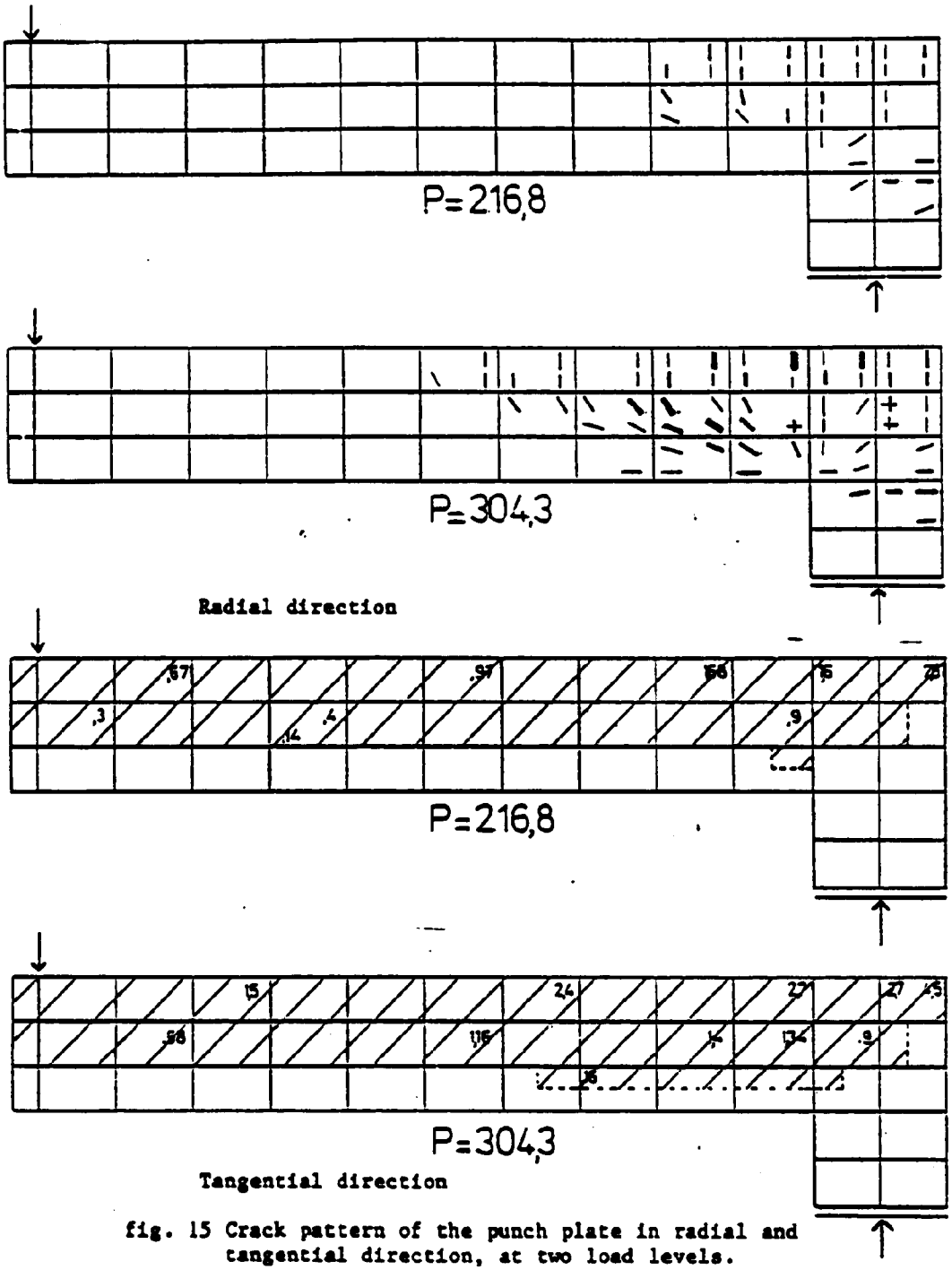

fig. 15 Crack pattern of the punch plate in radial and tangential direction, at two load levels.

REFERENCES

[1] Arrea M. and A.R. Ingraffea,
Mixed mode crack propagation in mortar and concrete.
Department of structural engineering report 81-13.
Cornell University, Ithaca, NY, 1982.

[2] Bathe K.J.
Finite element procedures in engineering analysis.
Prentice-Hall, New Jersey (1982).

[3] Bazant Z.P. and B.H. Oh
Concrete fracture via stress-strain relations.
Report 81-10/665c, Center for Concrete and Geomaterials,
Northwestern University (1981).

[4] Foeken R.J. van
The prediction of the crack pattern and the load-deflection behaviour of some benchmark problems with DIANA-NONLIN.
TNO-IBBC, report BI-83-40 (1983).

[5] Rots J.G.
Breukmachanicamodellen en hun toepasbaarheid voor beton.
TNO-IBBC, report BI-83-16 (1983), in Dutch.

[6] Rots J.G.
Analysis of crack propagation and fracture of concrete with DIANA.
TNO-IBBC report BI-83-26 (1983), in preparation.

[7] Rots J.G.
Prediction of dominant cracks using the smeared crack concept.
TNO-IBBC, report BI-83-39 (1983)

[8] Walraven J.C.
The influence of depth on the shear strength of ligthweigth concrete beams without shear reinforcement.
Report 5-78-4, Stevin Laboratory, Department of Civil Engineering, Delft University of Technology (1978)

THE USE OF THE ROUGH CRACK MODEL OF WALRAVEN AND THE FICTITIOUS CRACK MODEL OF HILLERBORG IN F.E. ANALYSIS

J. Blaauwendraad
Professor Civil Engineering
Delft University of Technology
The Netherlands

F.J.M. van den Berg
Research Assistent
Delft University of Technology
The Netherlands

P.J.G. Merks
Research Assistent
Rijkswaterstaat
NL - Utrecht

Program Micro/1

Structures of reinforced and unreinforced concrete in the cracked stage are analyzed numerically in two ways, either with discrete single cracks, or using the concept of smeared cracks. This paper regards applications of the program MICRO/1 for plane stress problems with discrete cracks. A finite element method is used which is based on an assumed stress field and natural boundary displacement (Lagrangian multipliers for the boundary tractions). So, differently from the standard FEM programs of the compatible type, the program MICRO is an equilibrium model, using boundary displacements as degrees of freedom. Essentially two different types of elements are used, namely triangular elements for the concrete and straight linear elements for the reinforcement. A reinforcement bar never crosses a triangular element, but instead is always positioned in between two elements. Bond behaviour is counted for by a nonlinear spring between the concrete and the reinforcement. Stresses in the triangles vary linearly over the region of the element. This corresponds with linearly varying boundary displacements, linearly varying bond stresses between the triangles and the straight reinforcement bars,and hence a parabolic distribution of the normal force in the bars.
Discrete cracks do not occur between the triangular elements, but run across the elements. In such a case a triangle is split in two parts, and additional degrees of freedom appear in the crack, namely for the crack opening and for the sliding of the two crack faces. In a cracked triangle the stresses can become discontinuous if necessary, and the same applies for the bond shear stress along the edge of a cracked element.

The constitutive relations of the concrete correspond with the model of Link, which has been extended with an appropriate tension cut-off criterion. The bond mechanism is a nonlinear spring, which behaves elastically up to a maximum shear stress, and shows softening for increasing slip behind that state. The behaviour of cracks can be discribed with the rough crack model

of Walraven and the fictious crack model of Hillerborg, Peterson c.s. The latter tension-softening concept has been adopted as the fracture mechanics option to account for the process zone of micro cracks around the crack "tip". This model is especially active if no reinforcement is applied.

Shear failure of reinforced concrete beams

The program has been applied to simulate the behaviour of reinforced concrete beams under shear loading. We consider the case in which main reinforcement is applied to carry the bending moments, but no shear reinforcement (stirrups) has been used. Furthermore we concentrate on the well-known fact that for such beams the shear capacity depends on the actual depth of the beam. Our starting point is a series of experiments which was carried out at the Stevin Laboratories of Delft University of Technology. From this series we selected two beams which correspond to each other such that the slenderness ratio a/h in the shear part of the beam has the same value (namely 3), however the depths differ considerably (respectively 125 mm and 720 mm). The beams have been shown in fig. 1. If model laws would apply, these beams should show the same ultimate nominal shear stress τ_u, which is the average shear stress at failure. The experiment however shows a value $\tau_u = 1.2$ *Mpa* for the shallow beam, and $\tau_u = 0.7$ *MPa* for the deep beam. So the shallow beam behaves far better. In fact this beam can be loaded until the main reinforcement starts to yield because the full plastic moment has been reached, producing a ductile failure behaviour. The deep beam cannot be loaded that far. Long before the reinforcement yields, brittle failure occurs in the shear part of the beam. The two beams are welcome bench-mark problems because of their expected simularity and still so different behaviour.

The wanted material properties of the concrete to be fed in the program MICRO/1 are the cylindrical compression strength, the tensile strength, the modulus of elasticity and Poissons ratio. These quantities have been taken from the experimental data. The rough crack model of Walraven is related to the cube compression strength, which is also known from the experiment. The fictituous crack model of Hillerborg has not been applied in these analyses. Due to the presence of the crack arresting main reinforcement, the fictituous crack model is less important in this case. The data for bond have been chosen on basis of experience. The adopted data are regularly used values for normal concrete and ribbed reinforcement bars. In this short note we just show a comparison between the load-deflection diagrams found in the test and resulting from the analysis (fig. 1). The ductile and brittle failure is produced satisfactorily. Crack patterns, not shown here, do also correspond quite well.

Mixed mode fracture in unreinforced notched beam

The program has also been applied to the problem of crack propagation in an unreinforced beam. Starting point in this case is a series of tests at Cornell University for mixed mode crack propagation in notched beam under pure shear. One of the tests is shown in fig. 2. A curvilinear crack develops and a typical diagram occurs for the load versus the crack mouth sliding displacement (CMSD).

In the analysis we used data for the tensile strength, compression strength, elasticity modulus and Poisson's ratio which are derived from the experiment. For the fracture mechanics release energy G_f two values $35\ N/m$ and $100\ N/m$ have been adopted. The results (fig. 2) show that the ultimate load can be computed rather accurately, but not the softening branch. Part of the difference between the test and the analysis may be due to different definitions of CMSD.

Conclusions

The rough crack model of Walraven in F.E. Analysis of the shown reinforced concrete beams yields good computational results. Used in combination with the fictitious crack model of Hillerborg also promising results were reached for failing unreinforced notched beams.

References

1. Grootenboer, H.J., Leijten, S.F.C.H., Blaauwendraad, J.: Concrete Mechanics, Numerical models for reinforced concrete structures in plane stress, Heron, vol. 26, 1981, no. 1c.

2. Walraven, J.C., Reinhardt, H.W.: Concrete Mechanics, Theory and experiments on the mechanical behaviour of cracks in plain and reinforced concrete subjected to shear loading, Heron, vol. 26, 1981, no. 1a.

3. Hillerborg, A. and Petersson, P.E.: Fracture mechanical calculations, test methods and results for concrete and similar materials. Advances in Fracture Research, 5th international conference of fracture, Cannes (ed.C.Francois), p. 1515-1522 (1981).

4. Walraven, J.C.: Het afschuifdraagvermogen van grindbeton en lichtbetonliggers zonder schuifwapening, Cement nr. 1, 1979.

5. Arrea, M., Ingraffea, A.R.: Mixed-mode crack propagation in mortar and concrete, Report 81-13 Cornell University, 1982.

6. Van den Berg, F.J.M., Merks P.J.G.: Interaction of rough crack model and fictitious crack model in program MICRO/1. F.E. Analysis of beams subjected to shear. Report BSW 83- Rijkswaterstaat, Structural Research, Utrecht, Netherlands, 1983.

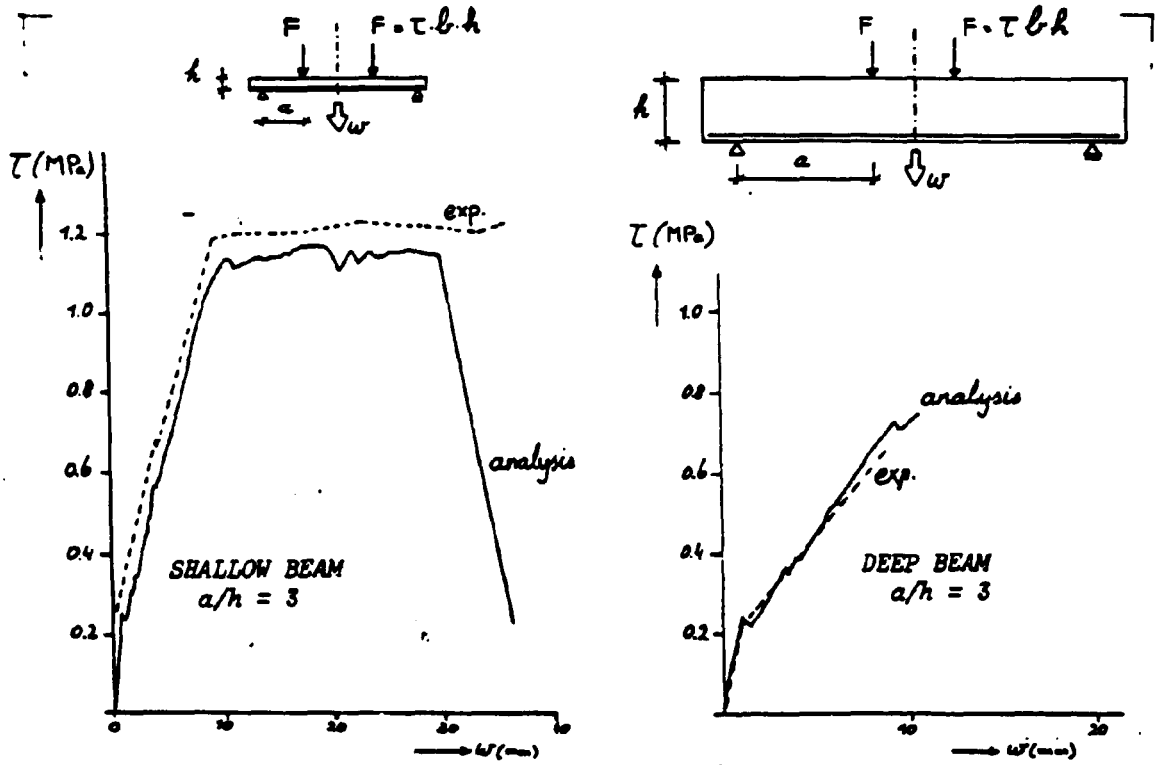

Figure 1 Two beams with the same shear slenderness $a/h = 3$, but the actual depths of the beam differ about a factor 6. The failure type is ductile for the shallow beam and brittle for the deep beam.

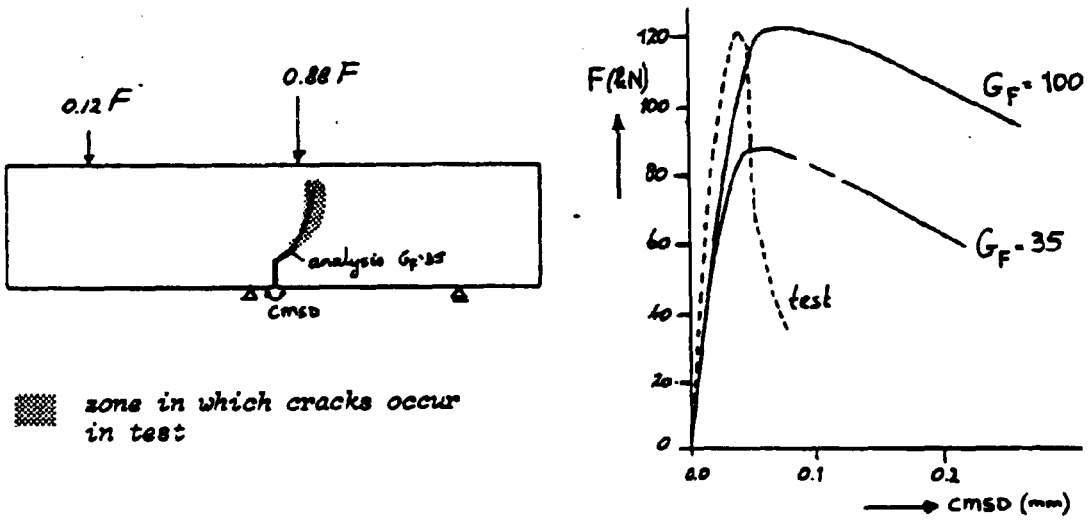

Figure 2 Unreinforced notched beam in pure shear. In this mixed mode fracture problem a curved crack trajectory occurs.

SUMMARY REPORT: MEETING AT DELFT UNIVERSITY OF TECHNOLOGY, NETHERLANDS, JUNE 23 and 24, 1983.

by David Darwin*

BENCH MARK PROBLEMS

Work at the University of Kansas centered on three problems: The unreinforced beam, the reinforced beam, and the tension panel. The results obtained in preparation for the meeting are briefly summarized.

Several variations of the material models were used to investigate the effects of the modeling parameters on the behavior of the finite element representations.

For most of the studies, concrete was modeled as linear elastic in compression and as linear elastic in tension, until the cracking stress was attained. Upon reaching the tensile strength, a smeared crack representation was used. In some cases, the tensile stress was reduced abruptly to zero and in others a linear strain softening branch (referred to as tension stiffening) was used. In the reinforced concrete beams, a nonlinear representation for concrete in compression (2,3) was also investigated. When used, steel was modeled as a uniaxial material with a bilinear stress-strain curve. Perfect bond between steel and concrete was assumed.

Four node linear isoparametric elements and two node truss elements were used for concrete and steel, respectively.

Following the formation of a crack the modulus of elasticity was set equal to zero and a shear retention factor, $\beta = 0.4$, was used.

Unreinforced Beam: Notched four point bend specimens were used to study mixed mode crack propagation in mortar and concrete at Cornell University. The tests are described in Reference 1. In our study, we considered the beams in Series B, shown in Fig. 1, along with the finite element model.

The material properties used in the analysis are given in Table 1. The concrete was represented as linear elastic in both tension and compression, with three methods of representing tensile failure: tensile strength = $7.5\sqrt{f'_c}$, no tension stiffening, tensile strength = $7.5\sqrt{f'_c}$ with linear tension stiffening, and tensile strength = $4.5\sqrt{f'_c}$ with linear tension stiffening. No unloading was permitted once a crack formed, i.e., when tension stiffening was used, positive strains resulted in a reduced stress, but negative strains resulted in no stress change. The load vs. crack mouth slip displacement curves

---

* Professor of Civil Engineering, University of Kansas, Lawrence, KS 66045

for the three cases are illustrated in Fig. 2. The model using the low tensile strength plus tension stiffening proved to be the best. The fracture energy, G_f, was close to typical values for concrete only for this case.

The results clearly indicate that tensile strength alone is not satisfactory to correctly represent this structure. Both fracture energy and tensile strength must be considered. Allowing the material to unload once it is on the descending branch is also important. Without unloading, a broad band of cracks is formed instead of allowing the cracks to localize. The crack path was also steeper than obtained in the tests (Fig. 3). This was also observed for other results presented at the meeting and may be due to 1) the lack of a rough crack model to represent crack dilatancy and 2) the fact that the test was cyclic and the finite element models attempted to obtain the envelope curve with monotonic loading. An accumulation of residual strain in cyclic tension may result in the difference in the calculated and the actual crack trajectories.

Reinforced Beams: A series of normal weight and lightweight reinforced concrete beams were tested by Walraven at Delft University of Technology (4) to study the influence of depth on the shear strength of beams without stirrups. The beams all had the same reinforcing ratios and shear-span to depth ratios. Two of the beams with normal weight concrete, A1 and A3 were studied. The material properties used for the beams are given in Table 2. The finite element representations are in Fig. 4.

The load-deflection curves for beam A1, the shallowest of the group, are illustrated in Fig. 5. Concrete is represented as linear in compression. Separate representations, both with and without tension stiffening, are illustrated. The failure of this beam is apparently governed by yielding of the reinforcing, and both representations are reasonably close to the test results. The small amount of linear tension stiffening does improve the match with the experimental results.

Three variations of the concrete model were used to study beam A3, the deepest of the three beams. A3 failed in shear during the test. Both linear and nonlinear compression were used without tension stiffening and linear compression was used with tension stiffening (Fig. 6). Both of the representations without tension stiffening give results which are reasonably close to the experimental curve, but which tend to slightly underestimate the flexural cracking load. The use of tension stiffening greatly overestimates the

stiffness and strength of the structure. The reason for this can largely be assigned to the large amount of tension stiffening used, coupled with the large size of the elements, which translates into a very high fracture energy.

All three representations have the drawback that they do not represent the failure mode of the specimen. This shortcoming may be assigned to the lack of inclusion of a model for bond in the finite element representation. The critical shear crack in the test specimen indicated the possibility of a bond failure. In the finite element models, the state of stress in the concrete alone does not indicate incipient material failure in the compression zone. All three models are ultimately too stiff.

Tension Panel: A tension panel tested at Cornell University as a portion of a study on shear transfer was used as a "blind" bench mark problem. Material properties for the model are given in Table 3. The finite element model and load-deflection curve are illustrated in Fig. 7 and 8. The model did not use tension stiffening.

Due to the limited time, only a portion of the load-deflection curve was obtained. The curve contains a linear portion prior to major cracking, which ensued at a load of about 10 kips. The load-deflection curve flattens out and then subsequently increases in stiffness. Cracks occurred predominately at the transverse reinforcing bars where the concrete section is reduced (Fig. 9). There was, however, some spurious cracking in the elements, probably due to the coarse grid and the lack of stress relief with the large linear strain quadrilaterals used.

BENEFITS OF THE VISIT

The bench mark problems gave my graduate students and me the opportunity to participate in an intense and stimulating investigation. The meeting allowed me to make new contacts and become aware of new research, especially work on cyclic tension, tensile fatigue and creep and shear strength of reinforced concrete. The importance of cracking in structural response and what we do not know about cracking were strongly emphasized.

The meeting exposed a number of important questions that need to be answered. What is the behavior of concrete in cyclic tension? How much shear is transmitted parallel to a crack? What is the fracture energy for mixed mode cracks, and how is this represented using a smeared crack representation? What is the correct fracture energy for Mode I cracks, and what are the effects on tensile strength of cycling into compression?

The program allowed me to advance the level of my work a great deal in a short amount of time. I feel that I am much more aware of the problems involved and have been stimulated to pursue a number of different approaches to obtain the answers.

REFERENCES

1. Arrea, Manrique and Ingraffea, Anthony R., "Mixed-Mode Crack Propagation in Mortar and Concrete," Report No. 81-13, Department of Structural Engineering, Cornell University, Ithaca, N.Y., Feb. 1982, 143 pp.
2. Darwin, David and Pecknold, David A., "Analysis of Reinforced Concrete Shear Panels under Cyclic Loading," Journal of the Structural Division, ASCE, Vol. 102, No. ST2, Feb. 1976, pp. 355-369.
3. Darwin, David and Pecknold, David A., "Nonlinear Biaxial Stress-Strain Law for Concrete," Journal of the Engineering Mechanics Division, ASCE Vol. 103, No. EM2, April 1977, pp. 229-241.
4. Walraven, J. C., "The Influence of Depth on the Shear Strength of Lightweight Concrete Beams without Shear Reinforcement," Report 5-78-4, Stevin Laboratory, Delft University of Technology, The Netherlands, 36 pp.

TABLE 1 Material Properties for Four Point Bend Specimen (Series B)

Property	Value
Concrete	
Compressive Strength	6.600 ksi (45.5 MPa)*
Young's Modulus	3600 ksi (24.8 GPa)*
Cracking Stress	0.365 ksi (2.52 MPa)**
	0.609 ksi (4.20 MPa)***
Poisson's Ratio	0.18*

* Experimental

** $f'_t = 4.5\sqrt{f'_c}$

*** $f'_t = 7.5\sqrt{f'_c}$

TABLE 2 Material Properties for Beams A1 and A3

Property	Value
Steel	
Young's Modulus	29000 ksi (200 GPa)
Yield Stress	64 ksi (440 MPa)
Concrete--Beam A1	
Compressive Strength	4.464 ksi (30.8 MPa)*
Young's Modulus	3808 ksi (26.3 GPa)**
Cracking Stress	0.361 ksi (2.49 MPa)***
Poisson's Ratio	0.2
Concrete--Beam A3	
Compressive Strength	4.543 ksi (31.3 MPa)*
Young's Modulus	3842 ksi (26.5 GPa)**
Cracking Stress	0.386 ksi (2.66 MPa)***
Poisson's Ratio	0.2

* f'_c = .9 x Ave. Cube Strength

** $E = 57\sqrt{f'_c}$

*** f'_t = Ave. Splitting Strength

TABLE 3 Material Properties for Tension Panel

Property	Value
Steel	
Young's Modulus	29000 ksi (200 GPa)
Yield Stress	60 ksi (414 MPa)
Concrete	
Compressive Strength	3.800 ksi (26.2 MPa)
Young's Modulus	3500 ksi (24.1 GPa)*
Cracking Stress	0.280 ksi (1.93 MPa)**
Poisson's Ratio	0.2

* $E = 57\sqrt{f'_c}$

** $f'_t = 4.5\sqrt{f'_c}$

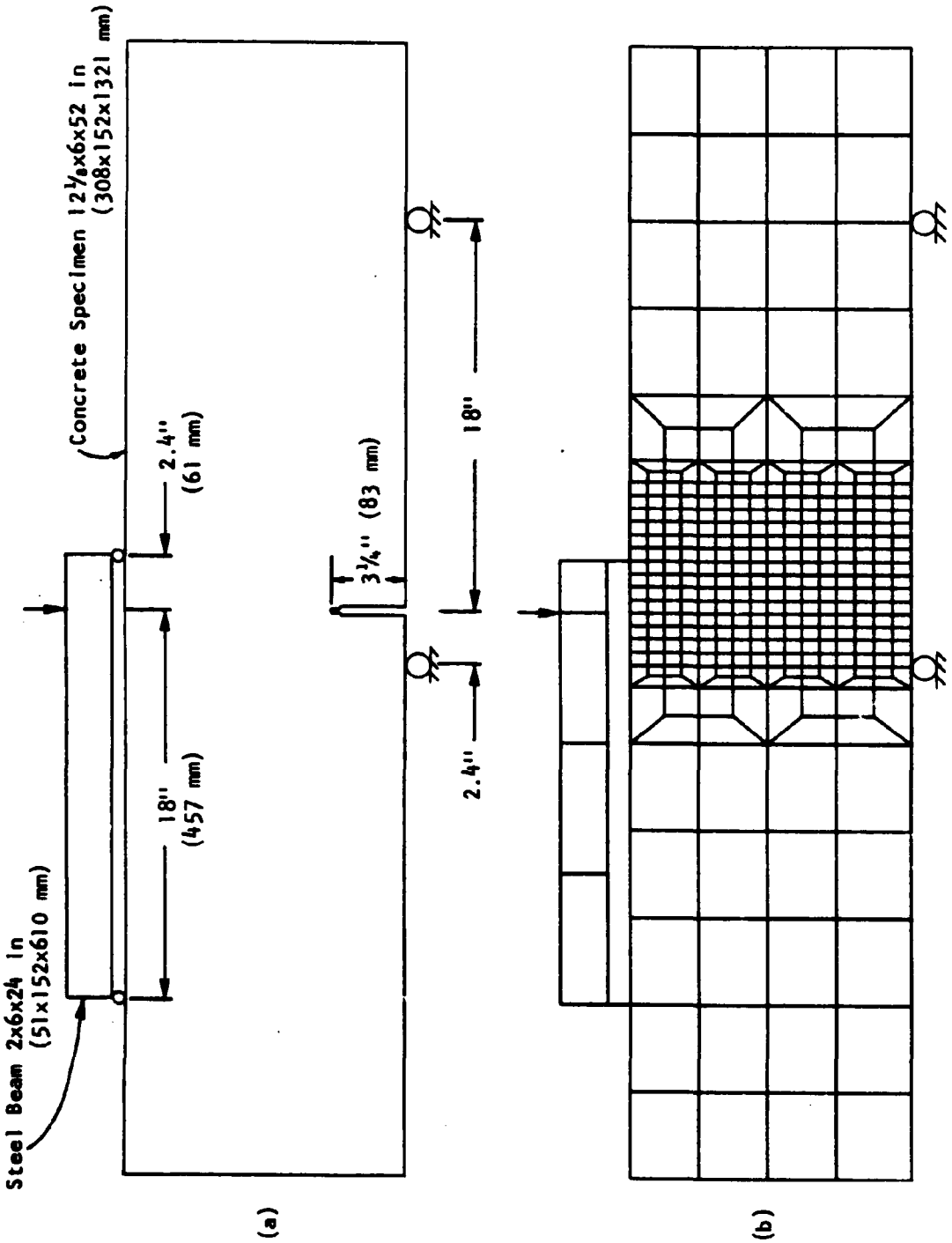

Fig. 1 - Cornell Mixed Mode Fracture Specimen (Series B): (a) Specimen Geometry and Loading Configuration, (b) Finite Element Model

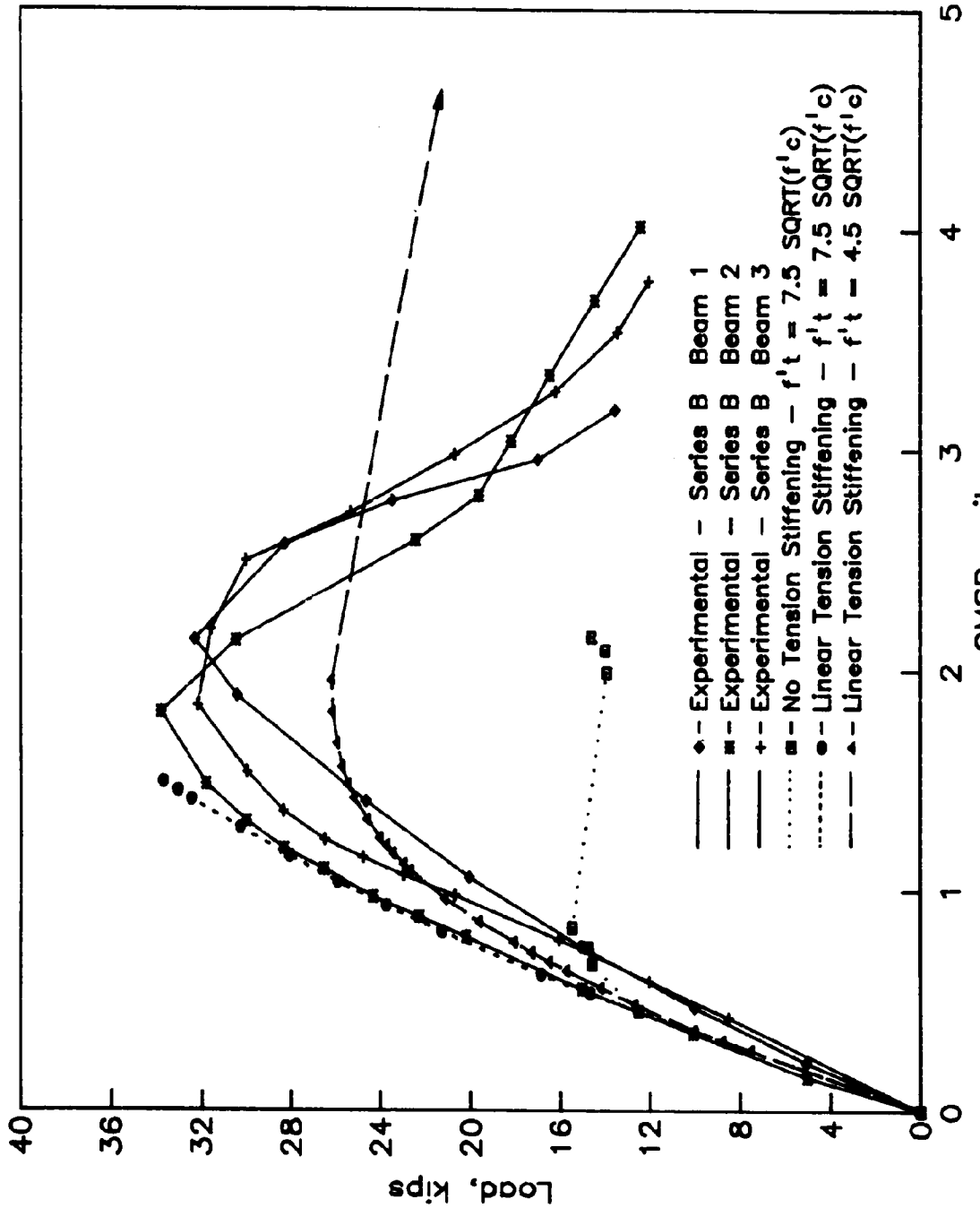

Fig. 2 - Load-Crack Mouth Sliding Displacement Curves for the Series B Fracture Specimen
(1 kip = 4.45 kN, 1 mil = 25.4 μm)

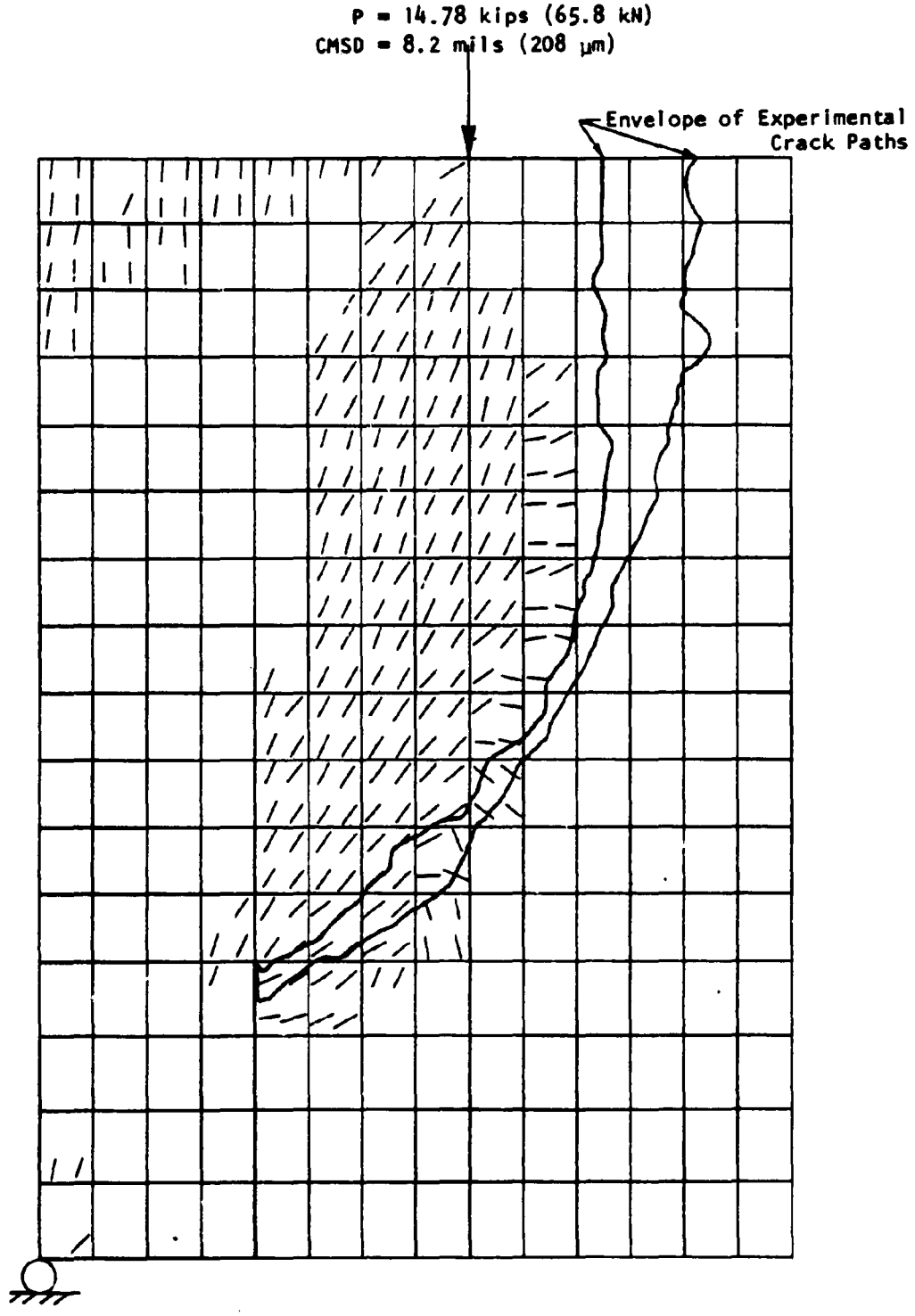

Fig. 3 - Crack Path for Model with Linear Tension Stiffening, $f'_t = 4.5\sqrt{f'_c}$

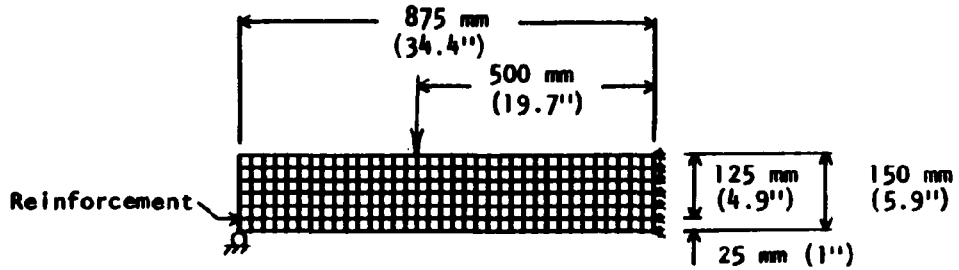

(a) Beam A1: t = 200 mm (7.9") ρ = 0.8%

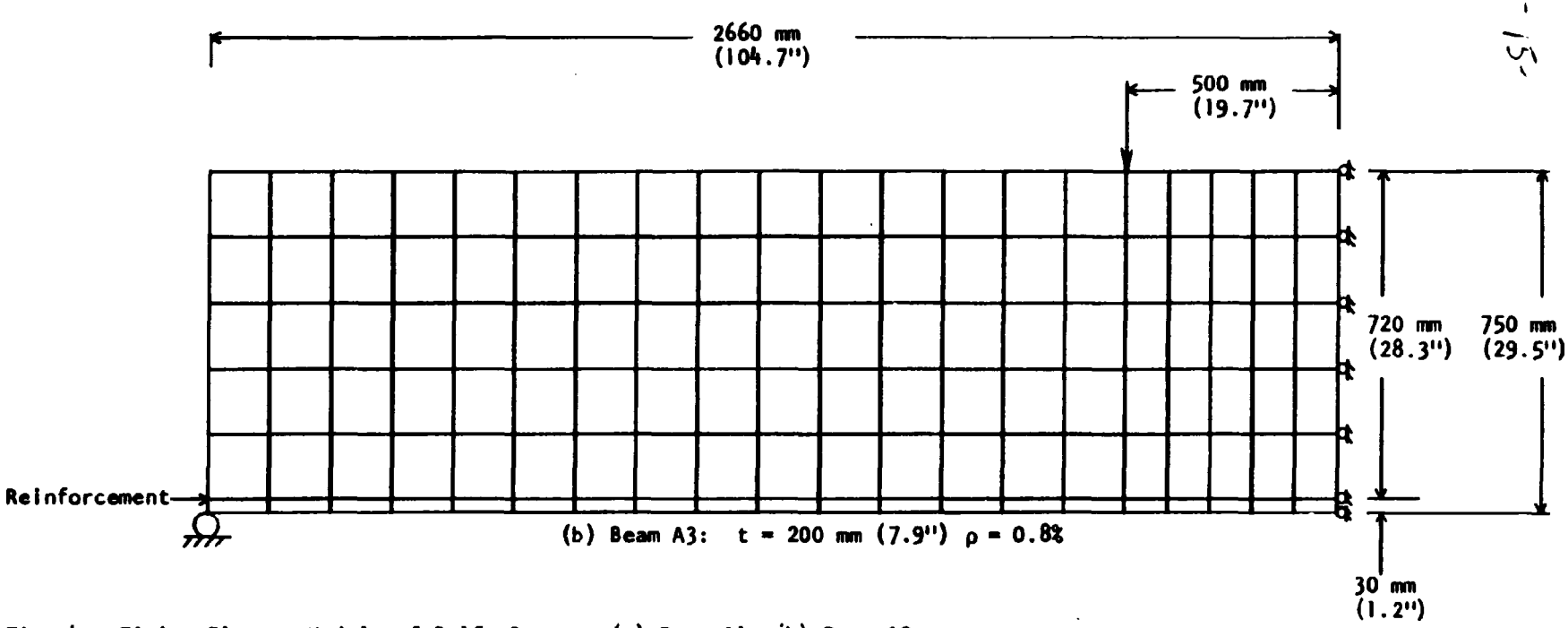

(b) Beam A3: t = 200 mm (7.9") ρ = 0.8%

Fig. 4 - Finite Element Models of Delft Beams: (a) Beam A1, (b) Beam A3

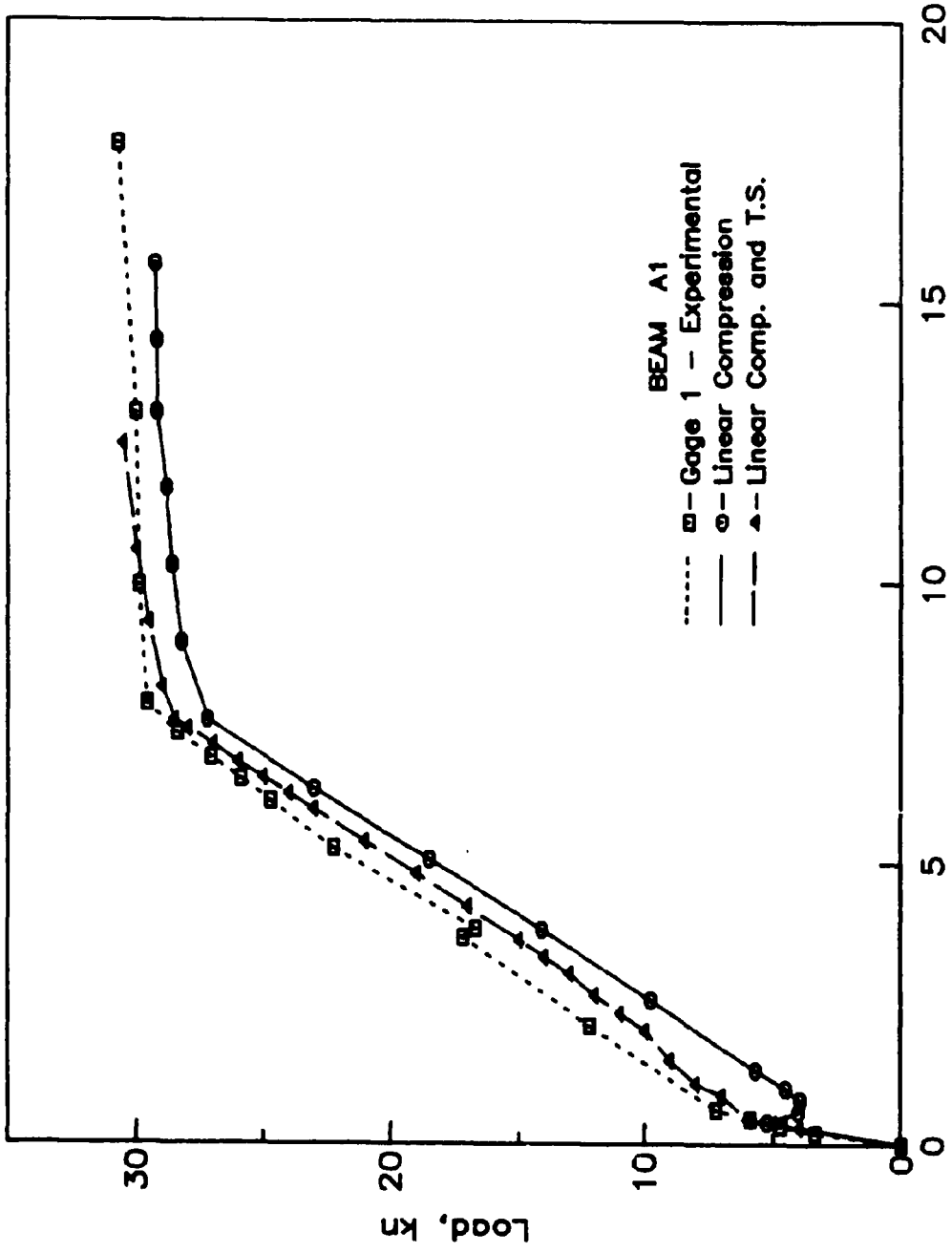

Fig. 5 - Load-Deflection Curves for Beam A1 (1 kN = .225 kips, 1 mm = .039 in)

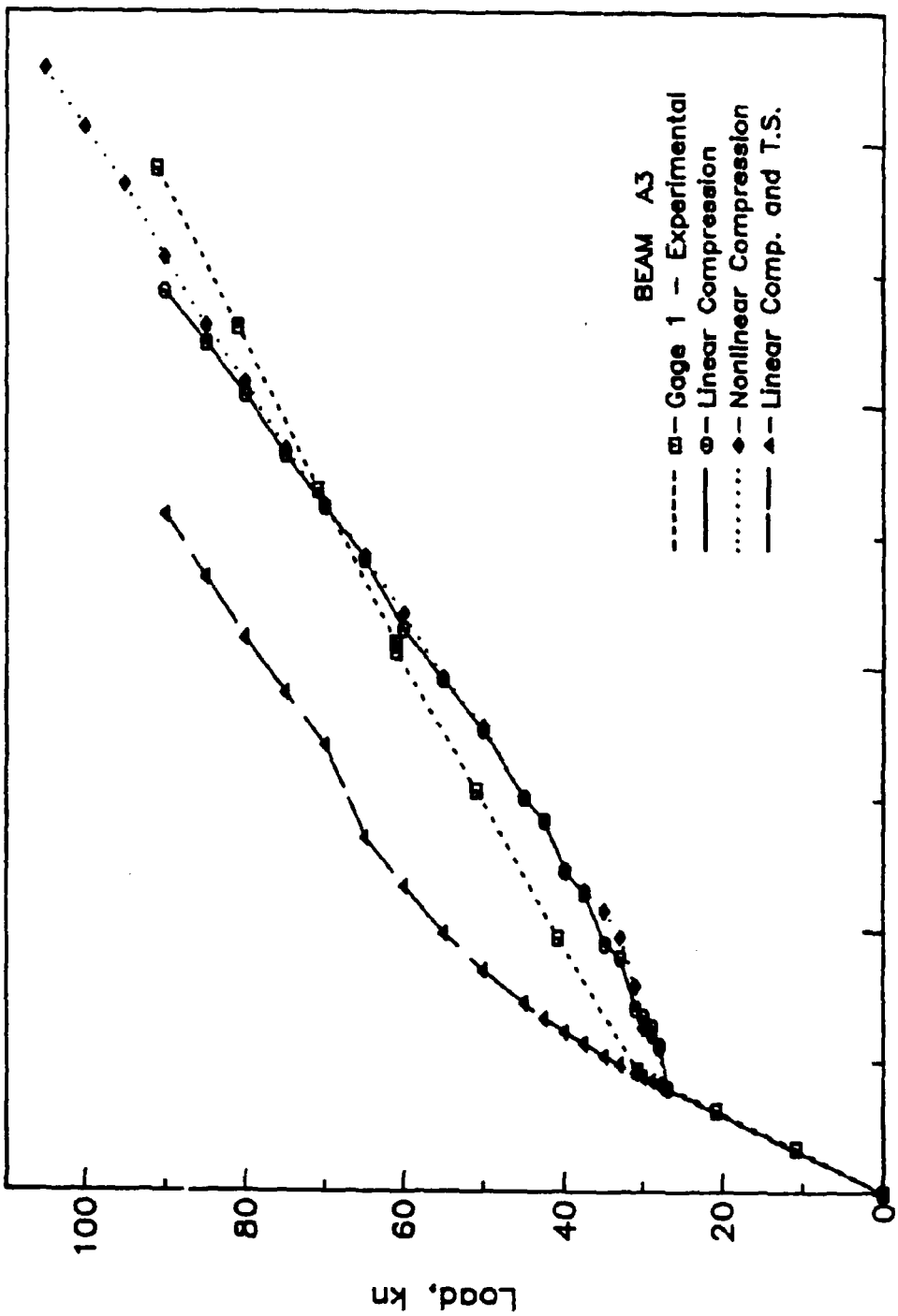

Fig. 6 - Load-Deflection Curves for Beam A3 (1 kN = .225 kips, 1 mm = .039 in)

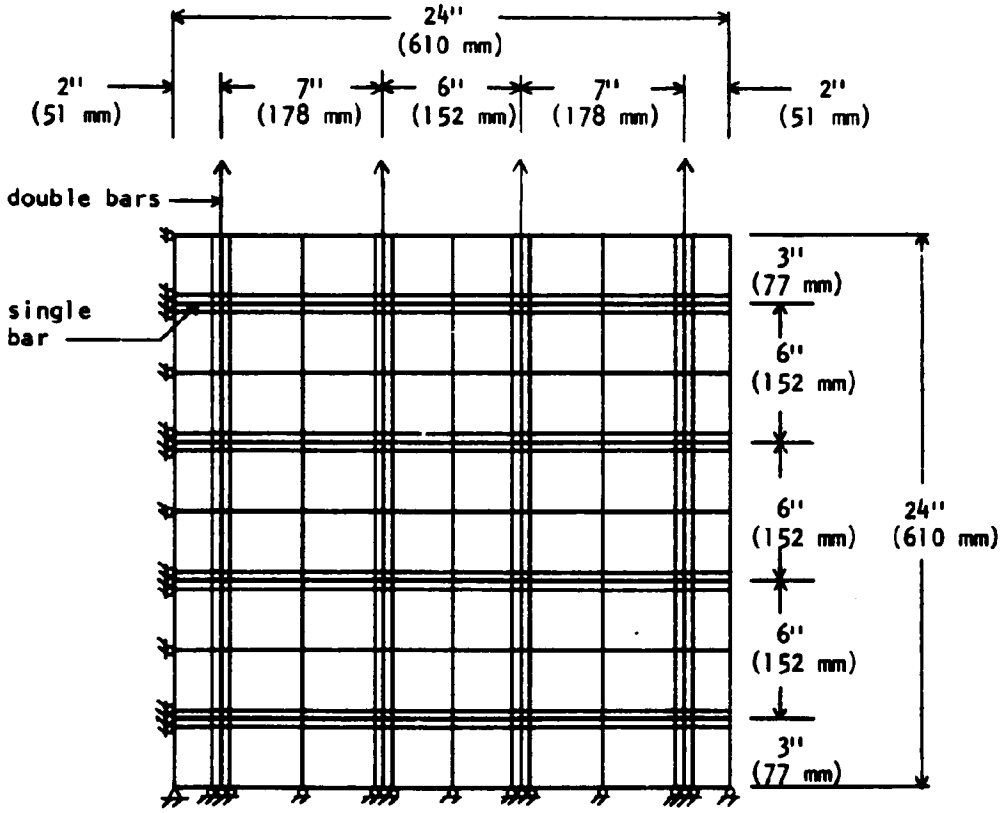

Fig. 7 - Finite Element Model of the Tension Panel

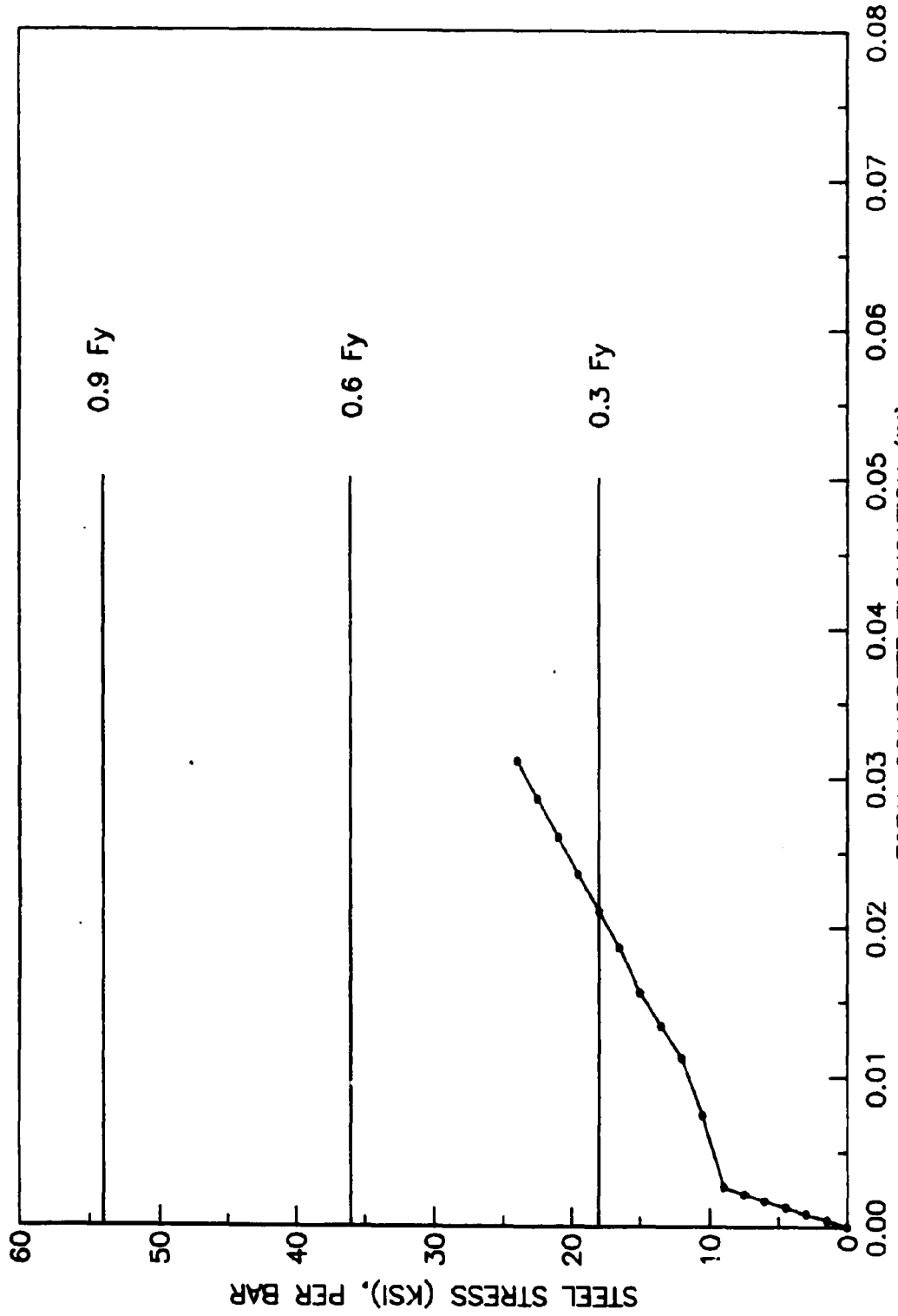

Fig. 8 - Load-Deflection Curve for the Tension Panel (1 ksi = 6.89 mPa, 1 in = 25.4 mm)

Steel Stress per Bar = 10.5 ksi (72.4 mPa)
Total Concrete Elongation = .00745 in (.19 mm)

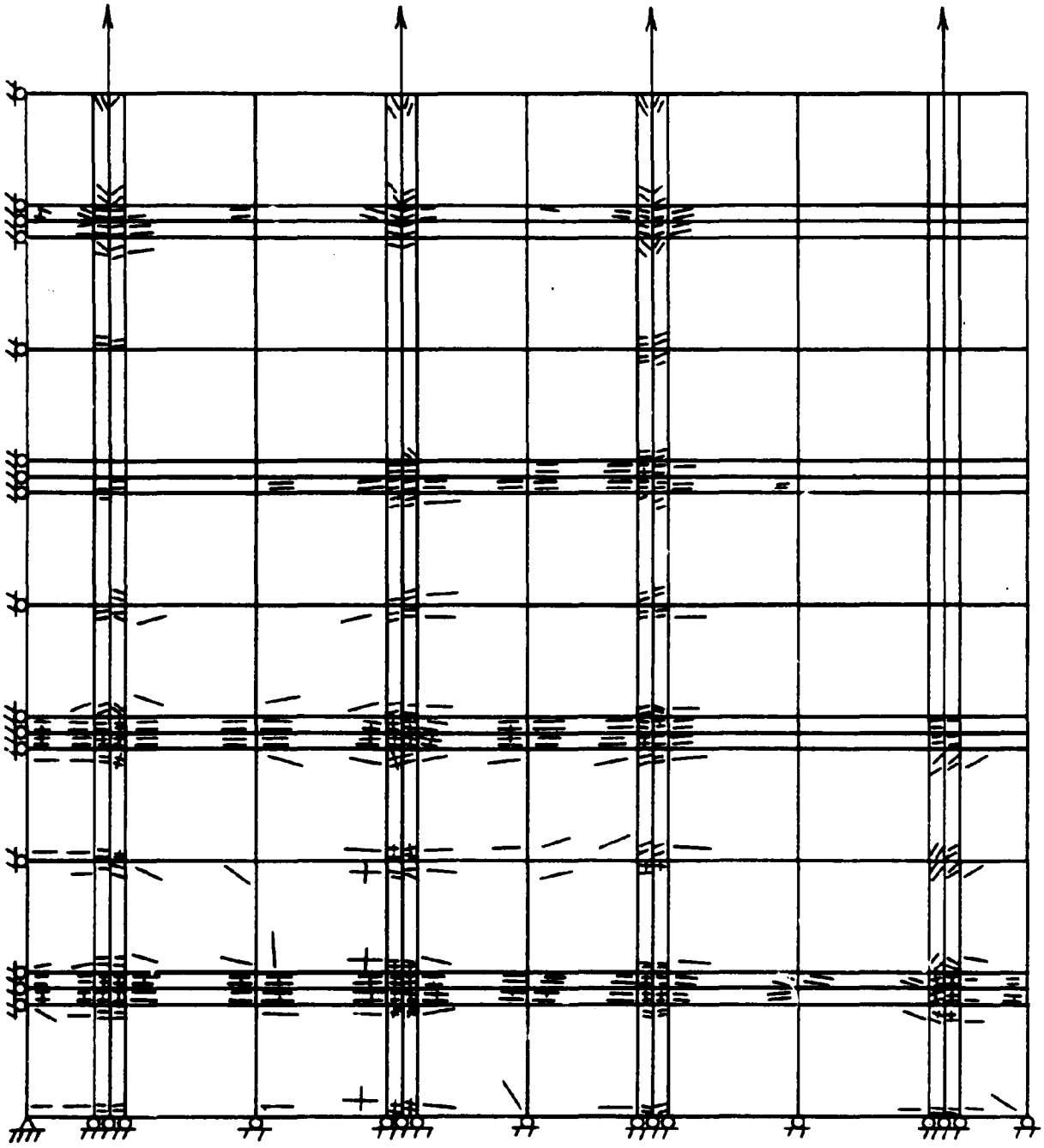

Fig. 9 - Crack Pattern for the Tension Panel

COMPUTATIONAL ASPECTS OF CONCRETE MECHANICS

Kaspar J. Willam

US-Dutch Cooperative Research Symposium

Delft University of Technology, Delft, June 22-24, 1983

CONTENT

1. COMPARATIVE EXAMPLE PROBLEMS

Four plain and reinforced concrete problems were distributed to the participants of the US-Dutch Symposium in order to verify different computational approaches in comparison to experimental results. Two examples were selected at UC-Boulder for presentation at the symposium. The results of these two numerical predictions are briefly summarized below.

At this stage it is important to keep in mind that the material properties of most problems were defined at best in terms of stiffness and strength parameters such as E and f'_c. There was no extensive material test data made available which could be used to calibrate the material parameters for the nonlinear computational studies. Therefore, the different numerical investigations were forced to adopt parameter values for their particular material formulation in a rather arbitary fashion which resulted in considerable variations from one study to another.

1.1 Tension Panel

This test example was selected by Dr. Gergely at Cornell University in order to assess the prediction capabilities of different computational strategies for reinforced concrete components subjected to tensile load histories. The geometry and material properties of the reinforced concrete panel are summarized in Fig. 1.1, whereby only f'_c = 3.8 ksi and f_y = 60 ksi were specified in the original description.

Since our computational strategy is geared towards a "smeared" cracking approach, a macroscopic viewpoint was adopted, in which the entire 48" x 48" panel was idealized by a single biquadratic plane stress element QUAMC9. The X- and Y-reinforcements were lumped into equivalent bar elements which were connected to the pertinent degrees of freedoms of the quadritateral concrete element assuming perfect bond. The load history was originally

specified in terms of the steel stress in the Y- reinforcement with a monotonic increase to $\sigma_y = 0.6\ f_y$, subsequent unloading and reloading thereafter. Fig. 1.2 shows the corresponding finite element idealization of the tension panel at hand, whereby the load-unloading history was specified in terms of prescribed Y-displacements Δ. Three parameter studies were carried out in order to assess the influence of the tension softening of concrete on the overall load carrying capacity of the reinforced concrete structure.

Fig. 1.3 shows the results of the elastic-perfectly plastic material model for the steel and concrete behavior in terms of the total reactive Y-force which comprises both steel and concrete components versus the overall elongation Δ in the Y-direction. We recognize a considerable load-carrying contribution of the concrete if fully ductile behavior is assumed in tension (upper bound solution). Note that the initial load strategy yields large permanent deformations upon unloading according to the unloading concept with the initial elastic stiffness of both concrete and steel constituents.

Fig. 1.4 illustrates the response prediction of the perfectly brittle concrete model while the steel behavior was again described by an elastic-perfectly plastic formulation. We observe that the brittle post-peak behavior of the concrete leads to an abrupt discontinuity in the load-deformation behavior which is fully reproduced by the displacement control of loading (lower bound solution). Since the actual tests were run under load control rather than displacement control, no such discontinuity could be observed in the experiment. The simple unloading strategy with the initial elastic stiffness of both steel as well as concrete components leads again to large irreversible deformations. In contrast, a refinement of the tensile-unloading strategy according to the concrete strain of the cracked cross-section would lead in this case

to full recovery of deformations and no permanent set. This would certainly lead to larger disagreements with the experimental observations by Dr. Gergely than the irreversible deformations predicted by the simple unloading strategy shown in the figure (upper bound of permanent set).

Fig. 1.5 finally exhibits the computational results of the most representative material formulation which includes the tension-softening of the concrete in the post-peak regime. Because of the lack of material test data, an arbitray choice was made for the rupture point $\varepsilon_r = 0.0016$ which corresponds to a fracture energy value of $U_f = 3.36$ k in. The discontinuous character of the response curve corresponds to that of the experiments reported by Dr. Gergely, except for the decrease from the cracking limit at 160 k to 134 k which cannot be captured in the experiment under load-control. The simple unloading strategy with the initial elastic stiffness, again overestimates the permanent set. However, it agrees better with the experimental results than the prediction of zero permanent deformation by the more refined strategy which entirely disregards the concrete stiffness in tension after the tensile strain has exceeded the rupture value $\varepsilon_1 \geq \varepsilon_r$.

In this context it was intriguing that the experimental data presented by Dr. Gergely during the symposium showed a curious contractive Y-deformation in the initial tensile loading regime, because the actual measurements were taken between the Points B-B of Fig. 1.1 on the top surface of the concrete, rather than in the midsurface. Clearly, the two-dimensional plane stress idealization is unable to account for the out-of-plane distortions caused by the particular load transfer mechanism from the reinforcement into the concrete.

Acknowledgement

I would like to thank Mr. Afshar Jalalalian who carried out the computa-

tional and analytical study of the tension panel in partial fulfillment of his Master thesis. The numerical investigation was based on the finite element program SMART (1) which was originally developed at ISD, in Stuttgart. Because of the relatively simple configuration, the reinforced concrete panel was analyzed independently by hand calculations in order to verify the finite element predictions and to give credence to the computational results.

1.2 Notched Shear Beam

This plain concrete example was selected by Dr. Ingraffea at Cornell University in order to evaluate the capabilities of the smeared versus the discrete failure approach in predicting shear failure. In this case, a high strength plain mortar beam with a 2.75 in center notch was primarily subjected to shear by the loading frame shown in Fig. 2.1 (Series A, Beam #2). As a result of the loading mechanism, the critical failure zone was limited to a 7.2" wide strip in the midspan region near the blunt notch. The experimental results were specified in terms of the overall loading force of the hydraulic actuator and the crack-mouth-sliding-displacement -CMSD, i.e. the shearing deformation across the crack flanks. The material properties of the high strength mortar were specified for an age of t = 150 days although actual testing was carried out 400 days after casting.

$f'_c = 8.8$ ksi

$E = 3800$ ksi and $\nu = 0.21$

Note the unusually high value of the uniaxial compressive strength of the mortar and the relatively low stiffness. Aside from the minimal material information we observe that the govering control parameter, the CMSD deformation across the notch, is an extremely sensitive quantity which can not be monitored directly by the finite element displacement formulation. In fact, the computations were carried out under displacement control of the vertical

component of the loading frame under the hydraulic actuator, Point A. Fig. 2.2 shows the plane stress idealization with 137 biquadratic quadrilateral QUAMC9 and 36 linear strain triangles TRIMC6 in the mesh transition region. Two spring elements were used to model the roller supports of the steel loading beam which was idealized with two elements in order to account properly for the load transfer into the actual specimen. Altogether, 1373 DOF were used for the spatial discretization of the notched mortar beam and the loading set-up. The actual bearing platens were also included in the idealization in order to avoid excessive cracking at the supports. This was especially important because the LVDT - measuring device for the CMSD was attached only 0.9" away from the edge of the 2" x 4" x 0.5" bearing plate at the left support.

Two parameter studies were carried out in order to gain insight into the influence of the softening formulation for combined tensile cracking and frictional slip. The underlying material formulation has been described before (2), here we should mention that a crack width parameter was included recently (3) in order to reduce the mesh size dependence of the smeared failure prediction. At this stage, the tensile and cohesive strength parameters in the Mohr- Coulomb model with tension cut-off shown in Fig. 2.3 degrade independently of each other. They are described by softening formulations of the tensile strength f_t' versus major principal strain ε_1 and the cohesion c versus the shear strain γ_n in the prevalent slip-plane of the Mohr- Coulomb criterion.

Fig. 2.4 shows the material parameters which were adopted in the case of the linear softening model, the results of which are compared in Fig. 2.5 with those of a perfectly brittle assumption for the post-peak behavior of the tensile as well as cohesive strength properties.

The experimental results exhibit extremely brittle post-peak behavior, whereby the unloading and reloading curves suggest that the actual fracture mechanism is a rate process with a viscous component. The computational results for the linear softening model exhibit reasonable agreement in the stiffness and the maximum load-carrying capacity, but far too large ductility. This can only be partly attributed to the difficulties with the indirect monitoring of the CMSD-control over the vertical displacements of the loading beam and the numerical or rather financial difficulties in getting a fully converged solution the (iteration limit was 20 with a convergence threshold of 0.001 in the relative displacements). The numerical predictions of the brittle model show some improvements with regard to both strength and ductility, however, the brittle post-peak behavior of the actual mortar beam was not reproduced satisfactorily. Although there are several possibilities to refine the present softening model in terms of a combined fracture energy formulation for cracking and frictional slip the post-peak regime of the test beam # A2 is highly unstable. Therefore, it is prudent to resort to a bifurcation analysis since the smeared approach replaces the discontinuous crack phenomenon by a continuous degradation of strength.

The following figures show typical results of the computational study using the brittle softening model. Fig. 2.6 shows the nodal displacement vectors and thus, the prevalent motion of the center of beam # A2 at load step No. 3 which corresponds to an actuator force of P_{fe} = 21.3 kips when the peak value is reached. The vector plot helps to visualize the driving action at the roller support of the steel beam and the splitting motion in the mortar beam along the blunt notch at midsection. The apparent discontinuity of displacements is a measure of the CMSD deformation. The deformed mesh in Fig. 2.7 clearly illustrates the tangential motion of the notch

flanks. Moreover, the deflection of the bottom fiber at the left support shows the considerable influence of the bearing platen on the CMSD-value. In the original description of this example problem, the size of this bearing platen was not specified. Therefore, the results of the linear softening model are somewhat on the stiff side because of the particular choice of the platen geometry.

Fig. 2.8 shows the distribution of principal stresses in the center of the beam. The compressive strut action clearly demonstrates the load transfer from the steel loading beam into the left hand support at the bottom. It is intriguing that the prefabricated notch hardly affects the overall stress distribution and that the main failure mechanism develops due to excessive tensile cracking parallel to the direction of the principal minor stress rather than frictional slip. This is hardly surprising if we consider the extremely high value of initial cohesion, c_0 = 2.05 ksi, which results immediately from the high compressive strength, f'_c = 8.8 ksi. Therefore, the suggested shear failure is in reality a tensile failure mode which is also responsible for the brittle nature of the structural post-peak regime.

The last two figures supplement the behavioral study of the brittle softening model. Fig. 2.9 illustrates the deformed mesh at the final load step No. 8 in the post-peak regime when the actuator force has decreased to P_{fe} = 14.8 kips. The plot which uses the same scale as Fig. 2.7 demonstrates the splitting motion across the depth of the mortar beam. Fig. 2.10 shows the associated distribution of principal stresses for comparison with that at the peak load in Fig. 2.8. The compressive strut action is apparent from the distribution of the minor principal stresses. Note the large stress redistribution at the top right next to the support of the loading beam.

The full release of stresses in this zone agrees with the final crack pattern which was observed by Dr. Ingraffea during testing.

Acknowledgement:

I would like to thank Mr. Bryan Hurlbut who carried out the computational study of the notched mortar beam within an individual study.

2. CURRENT CONCRETE RESEARCH AT CU-BOULDER

At present, there are three research projects being actively pursued on various aspects of concrete mechanics.

2.1 Numerical and Experimental Study of Direct Shear Test:

Within the AFOSR project on "Finite Elements and Localized Failure", the current computational strategies are re-evaluated for predicting the failure propagation in structural components. In particular, tensile cracking and frictional slip modes of failure are studied with the aid of the direct shear test. The computational work is accompanied by an extensive experimental test phase with the large capacity direct shear apparatus developed at CU Boulder. The MTS-servo control provides full insight into the peak and post-peak behavior of mortar and concrete specimens subjected to different ratios of normal to tangetial shear loading. The project is directed by Dr. K. Willam and Dr. S. Sture as principal investigators. Preliminary results of this work on tensile and cohesive softening were published in refs. (4,5,6) and are presently summarized in the form of a Master Thesis (3).

2.2 Triaxial Load History Study of Plain Concrete:

Within the NSF project on "Response of Concrete to Multiaxial Load Histories", the behavior of concrete was studied for different load histories in triaxial compression. Guided by the "simple" formulation

presented in ref. (7) a large number of tests were carried out with the cubical cell device developed at CU-Boulder. Preliminary results were published in refs. (8,9), while the entire test data is presently compiled in an extensive research report (10). The test results indicated a strong interaction between hydrostatic and deviatoric behavior which led to a refinement of the simple theory (11). The project was directed by Dr. K. Gerstle and expired in December 1982. Funding for a subsequent research project on triaxial concrete behavior is presently proposed to NSF in order to develop a unified approach for the full range of tension-compression behavior which includes the post-peak regime.

2.3 Biaxial Behavior of Fiber Reinforced Concrete

Within the AFOSR project on "Load History Effects of Steel Fiber Reinforced Concrete Properties" the biaxial behavior of cubical reinforced concrete specimens is studied primarily in the tension-compression regime. To this end, the cubical cell device was extended to accommodate brush bearing platens for tensile load histories. Both strength and nonlinear deformation behavior are explored in order to assess the effect of steel-fibers. The project is directed by Dr. H-Y Ko, Dr. C. C. Feng and Dr. S. Sture. Preliminary results were reported in ref. (12) while the detailed results of the project were compiled in the recent report (13).

3. ASSESSMENT OF COOPERATIVE RESERACH PROGRAM

The cooperative reserach program between the US and Dutch institutions was extremely useful. It provided insight into current research activities in concrete mechanics in both countries and led to a lively exchange of ideas among leading experts during the informal meetings in Delft and Atlanta. A brief assessment of the exchange program follows below.

3.1 Annual Meetings

The regular meetings in Holland and the USA led to intensive contacts among prominent members of the research community. The format of a closed workshop gave all participants an opportunity to raise questions and express their opinion in a personalized atmosphere. Therefore, it was easier to focus on the open problems and to share sometimes negative experiences with the ongoing experimental and computational research. The main advantage of the informal meetings was, in my view, the mutual exchange of ongoing research activities and the stimulating discussion of "hot" topics, such as fracture energy concepts and prevalent softening formulations.

3.2 Comparative Example Problems

The closed workshop atmosphere was instrumental for the formulation of example problems which served to verify the different computational approaches proposed by individual researchers in the light of experimental evidence. The purpose of this comparative study was to challenge the current numerical strategies with a broad spectrum of example problems. In principle, this type of an international competition was an excellent idea. However, there were two aspects which influenced the outcome of the individual contributions, the difference in resource allocations and the loose description of the example problems. We all recognize that a nonlinear finite element analysis still imposes considerable demands on manpower and computer resources even if we can restrict ourselves to the execution of existing software programs. Therefore it is unrealistic, at least for academic institutions in the USA, to pursue four example problems with several parameter variations without any external funding. Although the outcome of nonlinear finite element studies is determined to a large extent by the underlying material model and the particular choice of material parameters, little information was made available

on the material properties of the comparative example problems. Therefore, a wide variety of results were obtained by the different contributors, each of which resorted to additional sensitivity studies in order to explore the effect of ill-defined material parameters on the computational results.

3.3 Recommendations for Future Cooperation

As indicated before, the exchange of information and the stimulating discussions are extremely valuable. Some of the experimental research activities of our Dutch colleagues along the line of the fracture energy studies in Delft, and the triaxial load history studies in Eindhoven, are of particular interest of our own work. Therefore, I recommend to follow up the outgoing cooperative research with a similar activity along that line. I propose to widen somewhat the number of participants and to include current researchers in the field of concrete mechanics from other European countries, but to retain the closed workshop format. On the other hand, it would be worthwhile to focus on one particular topic in each research meeting and to prepare the ground with comparative example problems, the results of which could be published in a joint report for public distribution.

4. REFERENCES

1. SMART I - Users Manual, ISD Report No. 186, University of Stuttgart, 1976.

2. Argyris, J.H., Faust, G., and Willam, K.J., "Limite Load Analysis of Thick-Walled Concrete Structures - A Finite Element Approach to Fracture", Comp. Meth. Appl. Mech. Eng., Vol. 8, (1976), pp. 215-243.

3. Christensen, J., "Computational and Experimental Investigation of Concrete Failure in Shear", M.S. Thesis, Dept. CEAE at University of Colorado, Boulder, 1983.

4. Christensen, J., Ickert, K., Stankowski, T., Sture, S. and Willam K., "Numerical Modeling of Strength and Deformation Behavior in the Direct Shear Tests", Proc. Int. Conf. Constitutive Laws of Engineering Materials, C.S. Desai and R.H. Gallagher eds., Tucson, AZ., (1984), pp. 537-544.

5. Christensen, J. and Willam, K., "Finite Element Analysis of Concrete Failure in Shear", AFOSR Symp. on The Interaction of Non-Nuclear Munitions with Structures, U.S. Air Force Academy, Colorado Springs, (1981), pp. 101-106.

6. Gould, M.C., "Development of a High Capacity Dynamic Direct Shear Apparatus and its Application to Testing Sandstone Rock Joints", M.S. Thesis, Dept. of CEAE at University of Colorado, Boulder, 1982.

7. Gerstle, K.H., "Simple Formulation of Biaxial Concrete Behavior", Jnl. A.C.I., Vol. 78, No. 1, (1981), pp. 62-68.

8. Gerstle, K.H., "Simple Formulation of Triaxial Concrete Behavior, Jnl. A.C.I., Vol. 78, No. 5, (1981), pp. 382-387.

9. Scavuzzo, R., Cornelius, H.V., Gerstle, K.H., Ko, H.-Y. and Stankowski, T., "Simple Formulation of Concrete Response to Multiaxial Load Cycles", Proc. Int. Conf. Constitutive Laws for Engineering Materials, eds. C.S. Desai and R.H. Gallagher, Tucson, AZ, (1983) pp. 421-426.

10. Scavuzzo, R., Stankowski, T., Gerstle, K., and Ko, H.-Y., "Experimental Stress-Strain Curves for Concrete Under Multiaxial Stress Histories, report to be published at Dept. CEAE, University of Colorado (1983).

11. Stankowski, T., "Concrete under Multiaxial Load Histories", M.S. Thesis, Dept. CEAE of University of Colorado, Boulder, 1983.

12. Ko, H.-Y., Meier, R.W., Egging, D.E., Sture, S., Feng, C.C., "Constitutive Properties of Steel Fiber Reinforced Concrete in Multiaxial Loading", AFOSR Symp. on the Interaction of Non-Nuclear Munitions with Structures, U.S. Air Force Academy, Colorado Springs, (1981), pp. 71-76.

13. Meier, R.W., Ko, H.-Y., Sture, S. and Feng C.C., "The Strength and Behavior of Steel Fiber-Reinforced Concrete Under Combined Tension Compression Loading", Report to AFOSR, University of Colorado, Boulder, 1983.

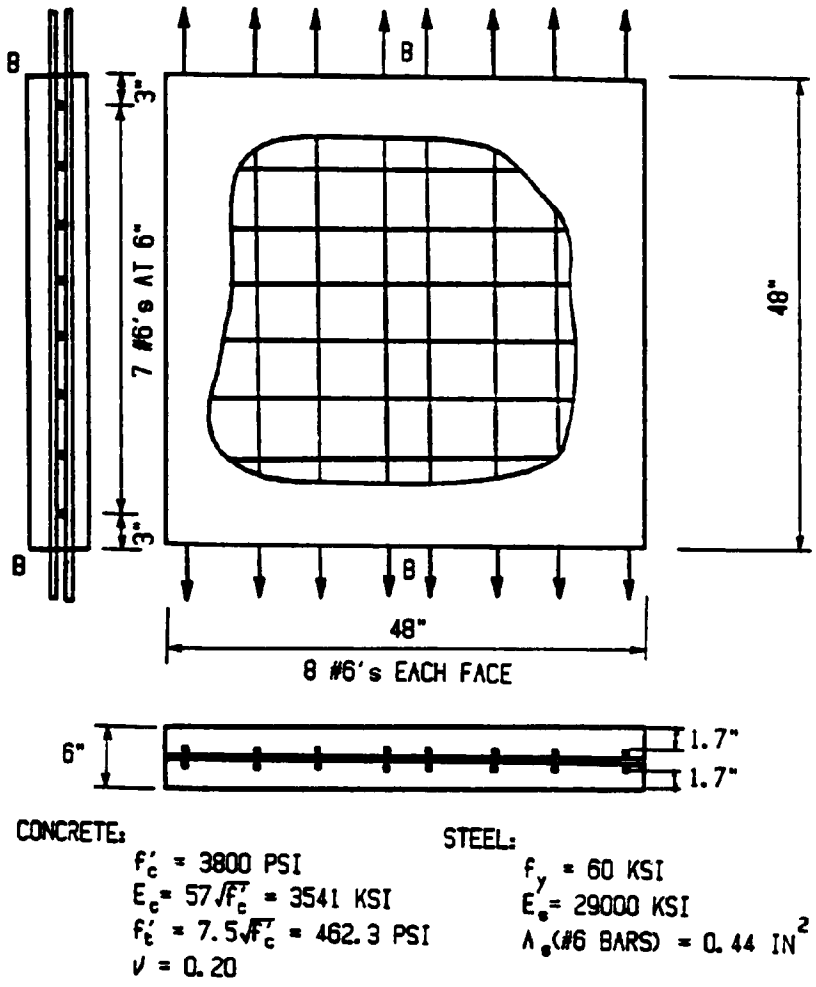

FIG. 1.1 REINFORCED CONCRETE TENSION PANEL PROBLEM DESCRIPTION

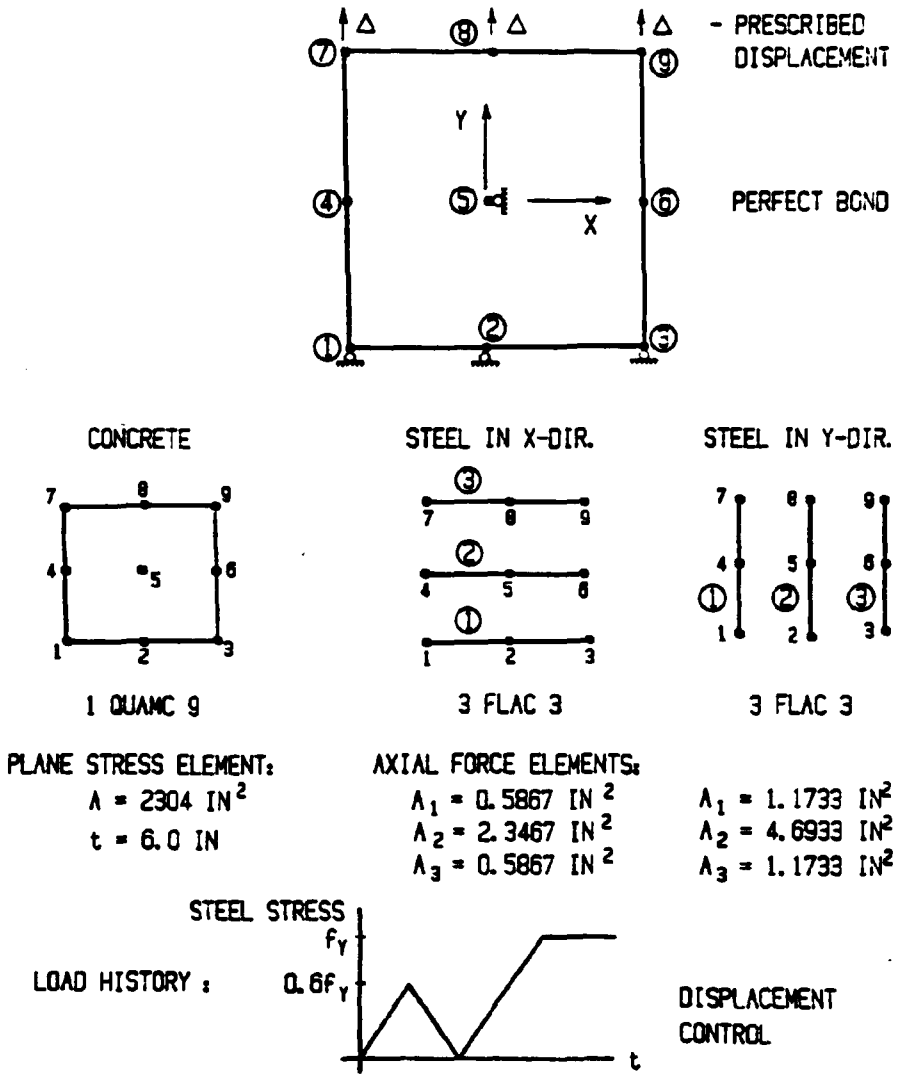

FIG. 1.2 REINFORCED CONCRETE TENSION PANEL PROBLEM IDEALIZATION

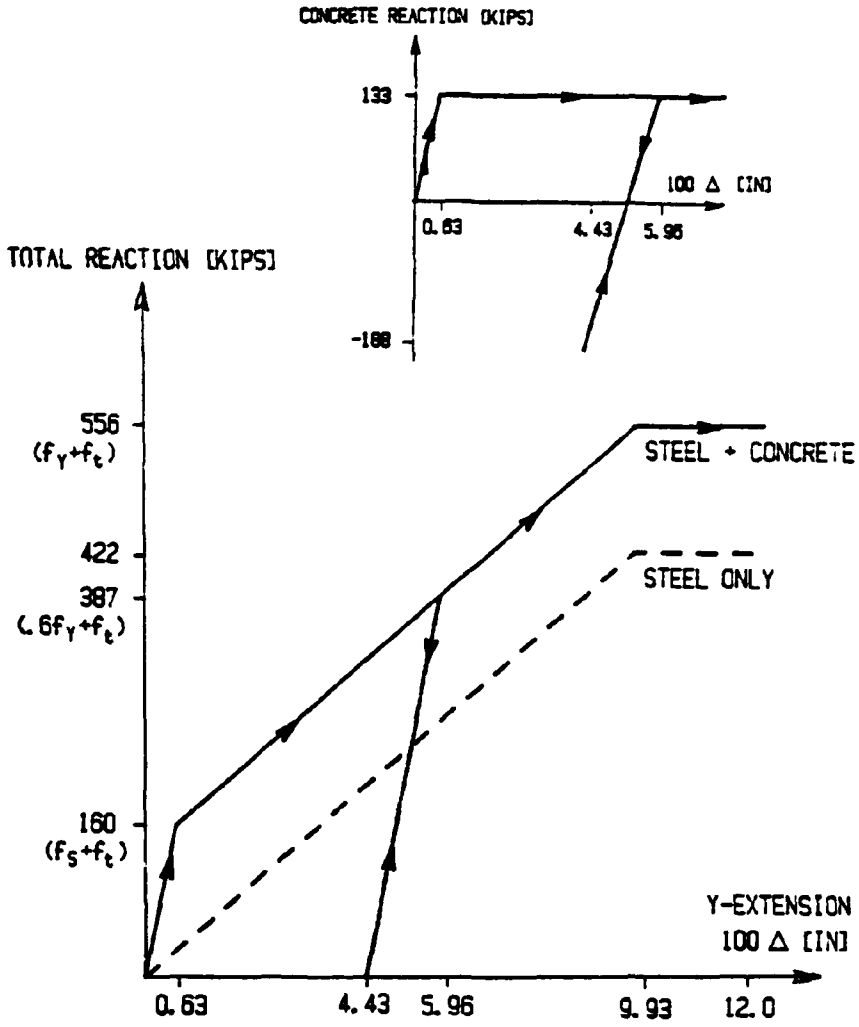

FIG. 1.3 REINFORCED CONCRETE TENSION PANEL

DUCTILE CONCRETE MODEL

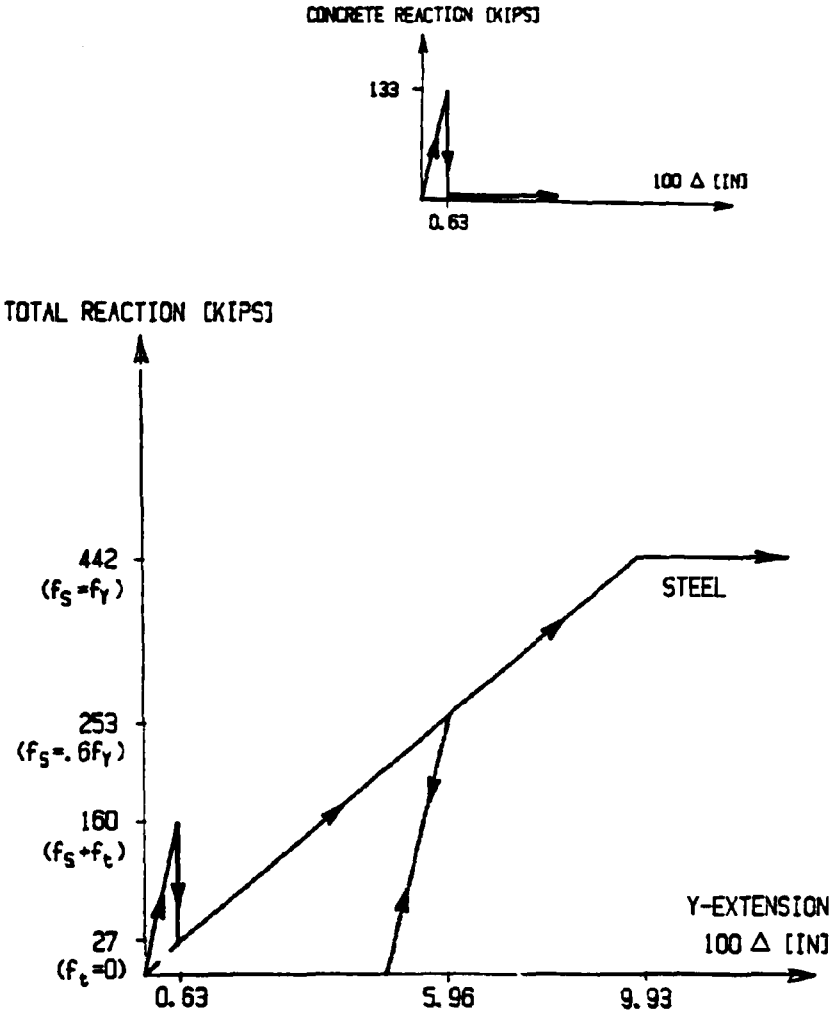

FIG. 1.4 REINFORCED CONCRETE TENSION PANEL

BRITTLE CONCRETE MODEL

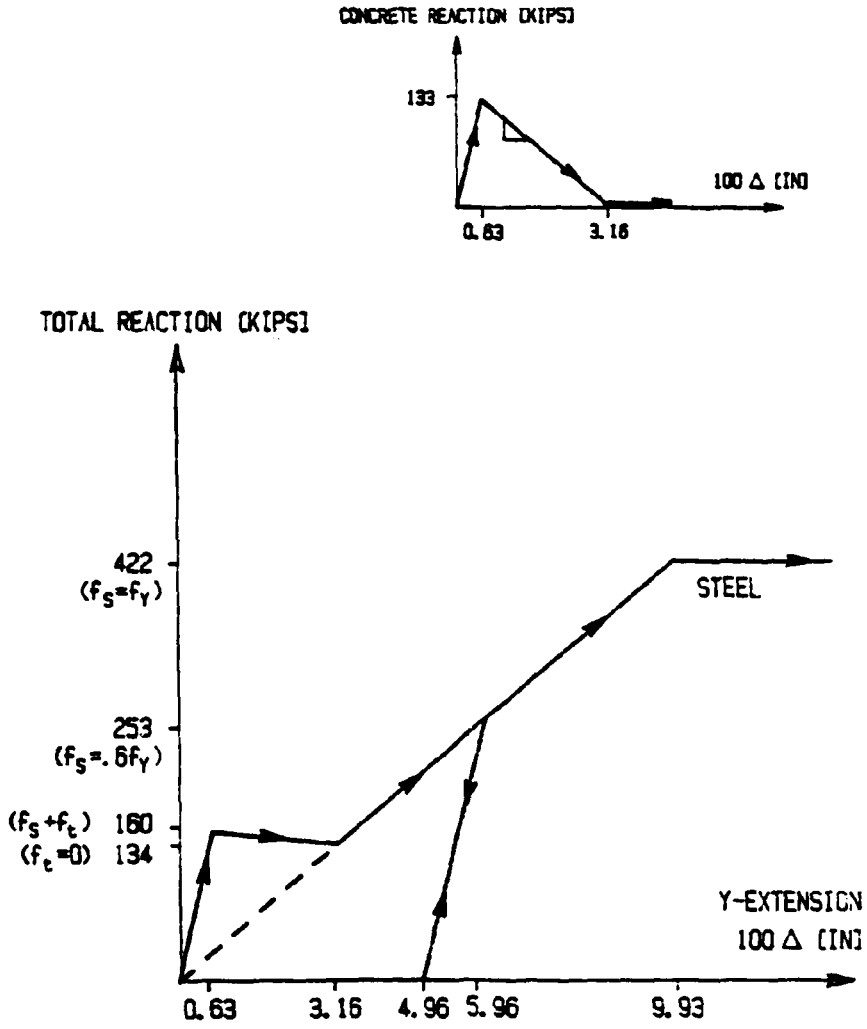

FIG. 1.5 REINFORCED CONCRETE TENSION PANEL SOFTENING CONCRETE MODEL

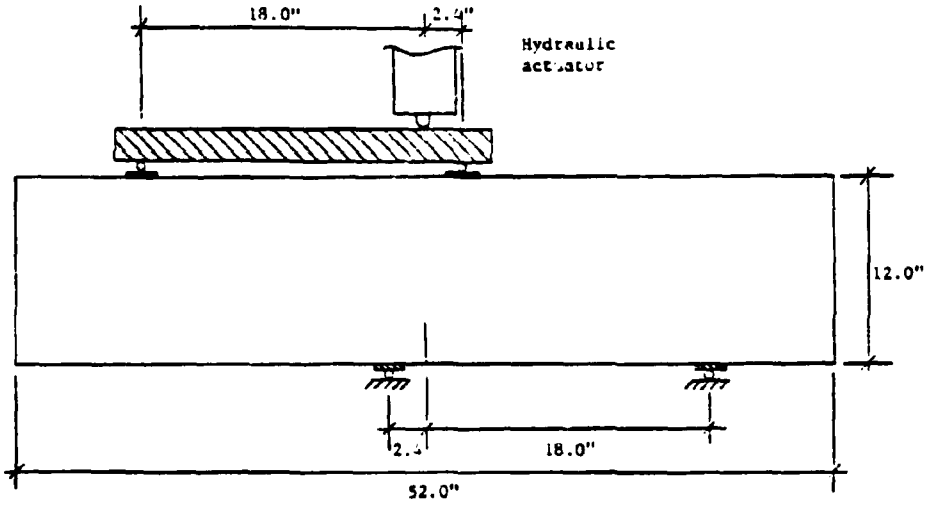

Loading Configuration

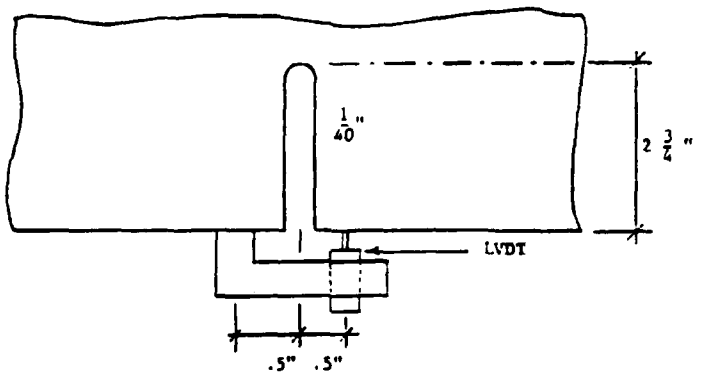

Notch Configuration
and
CMSD Measurement

FIG. 2.1 GEOMETRY AND LOADING CONFIGURATION OF NOTCHED MORTAR BEAM

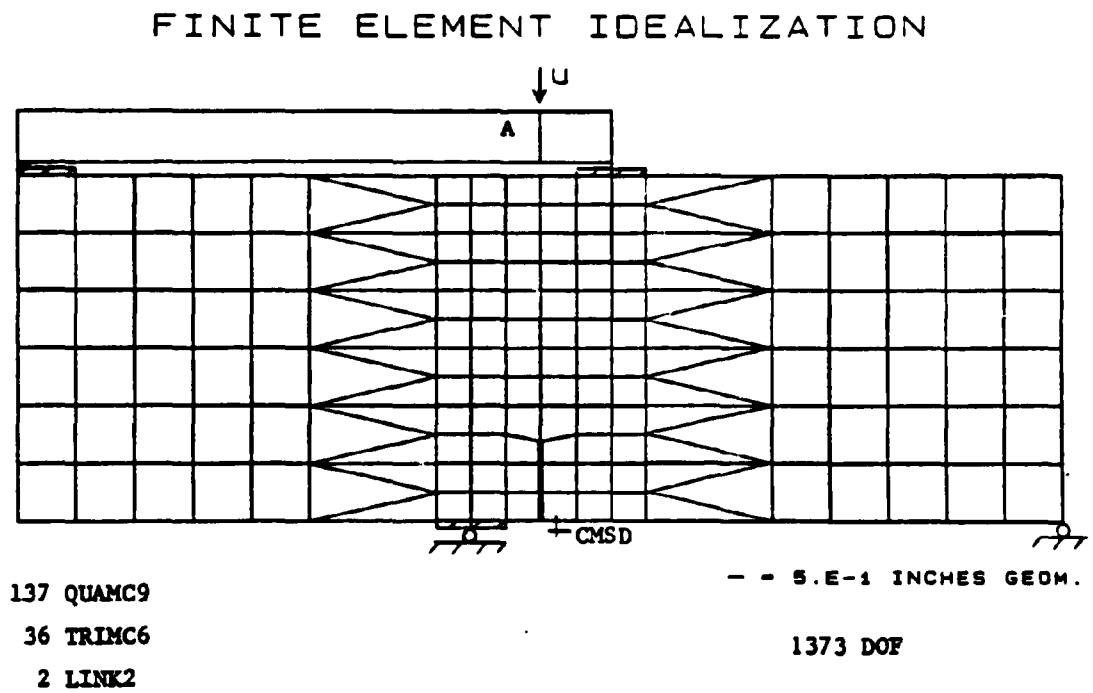

FIG. 2.2 FINITE ELEMENT IDEALIZATION OF NOTCHED MORTAR BEAM

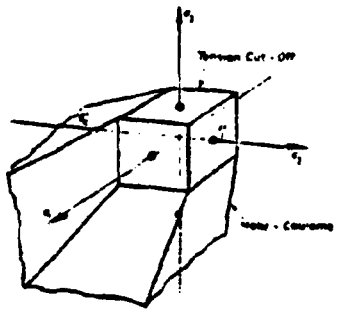

TRIAXIAL FAILURE SURFACE

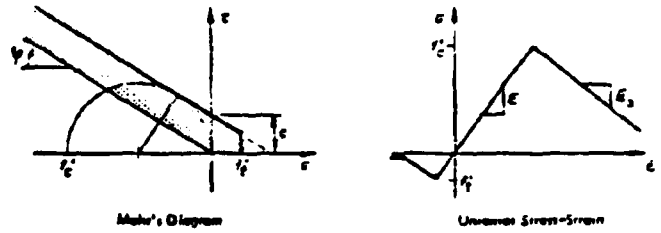

TENSION AND COHESIVE SOFTENING

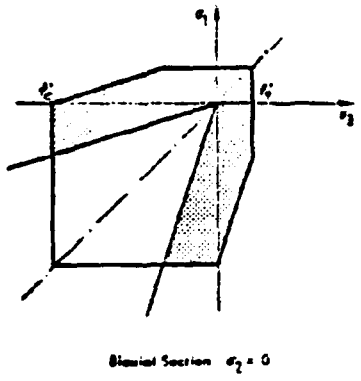

FIG. 2.3 MOHR-COULOMB MODEL WITH TENSION CUT-OFF

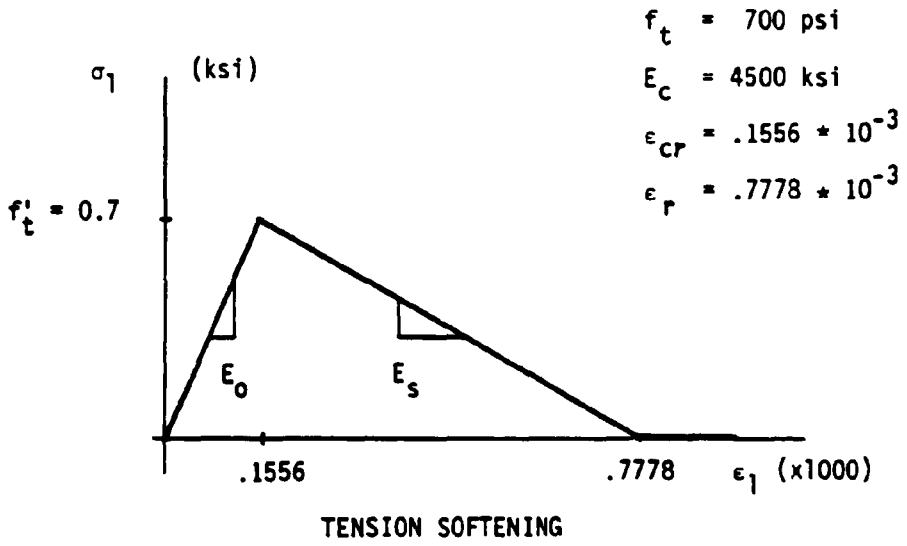

TENSION SOFTENING

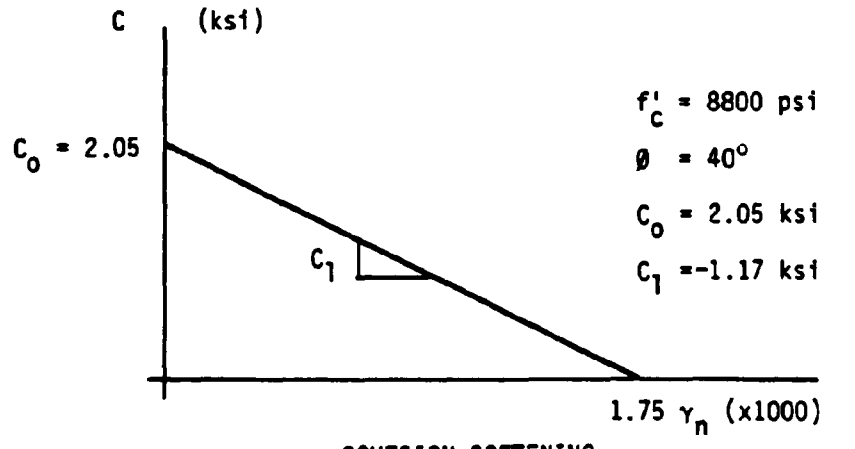

COHESION SOFTENING

FIG. 2.4 MATERIAL PROPERTIES OF HIGH-STRENGTH MORTAR

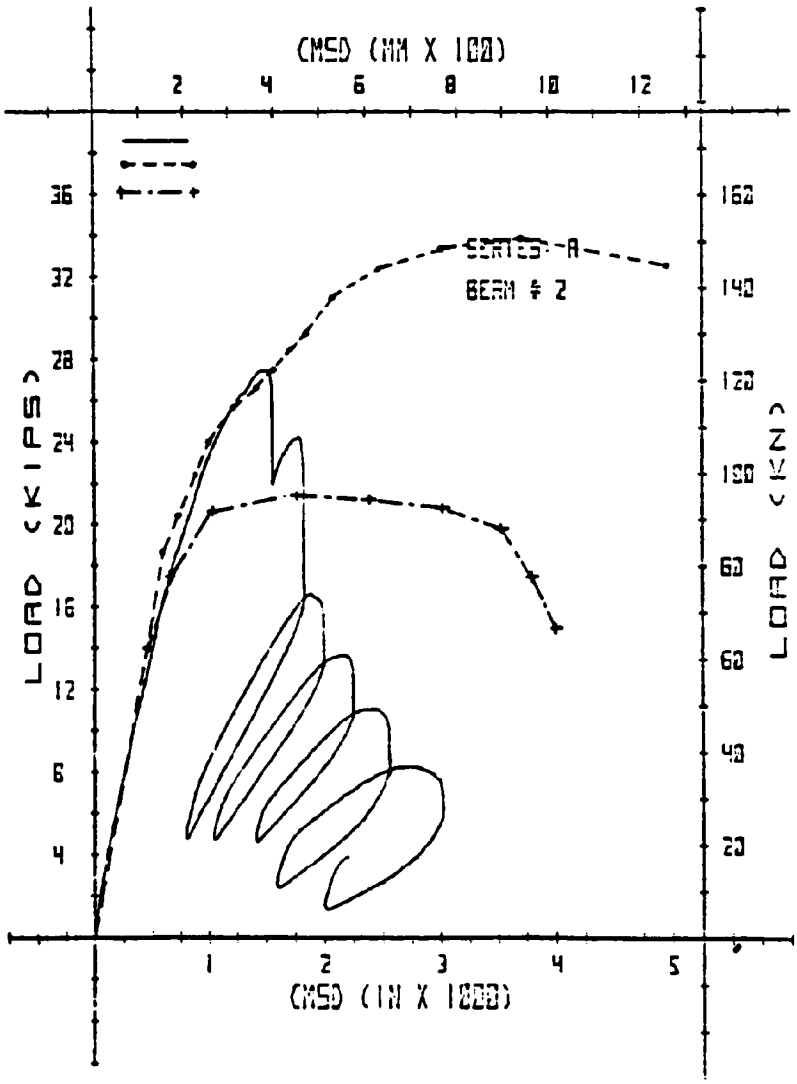

FIG. 2.5 LOAD VERSUS CRACK-MOUTH-SLIDING-DISPLACEMENT

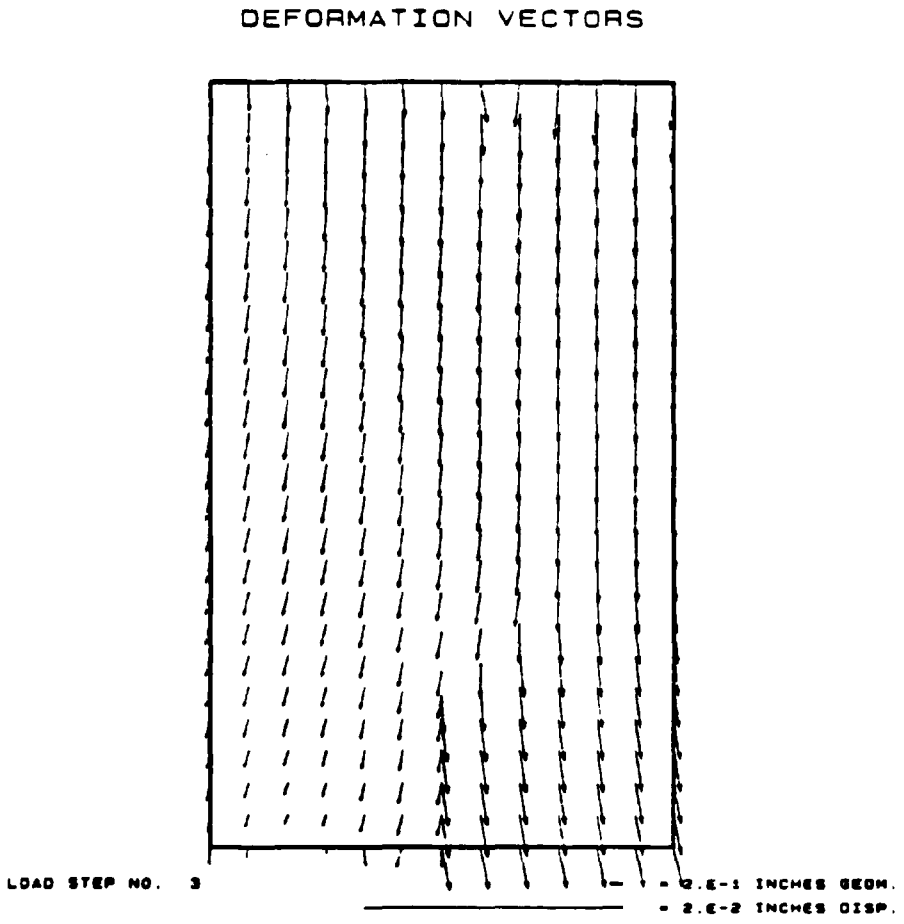

FIG. 2.6 MOTION OF NOTCH AREA AT PEAK LOAD P_p = 21.2 kips

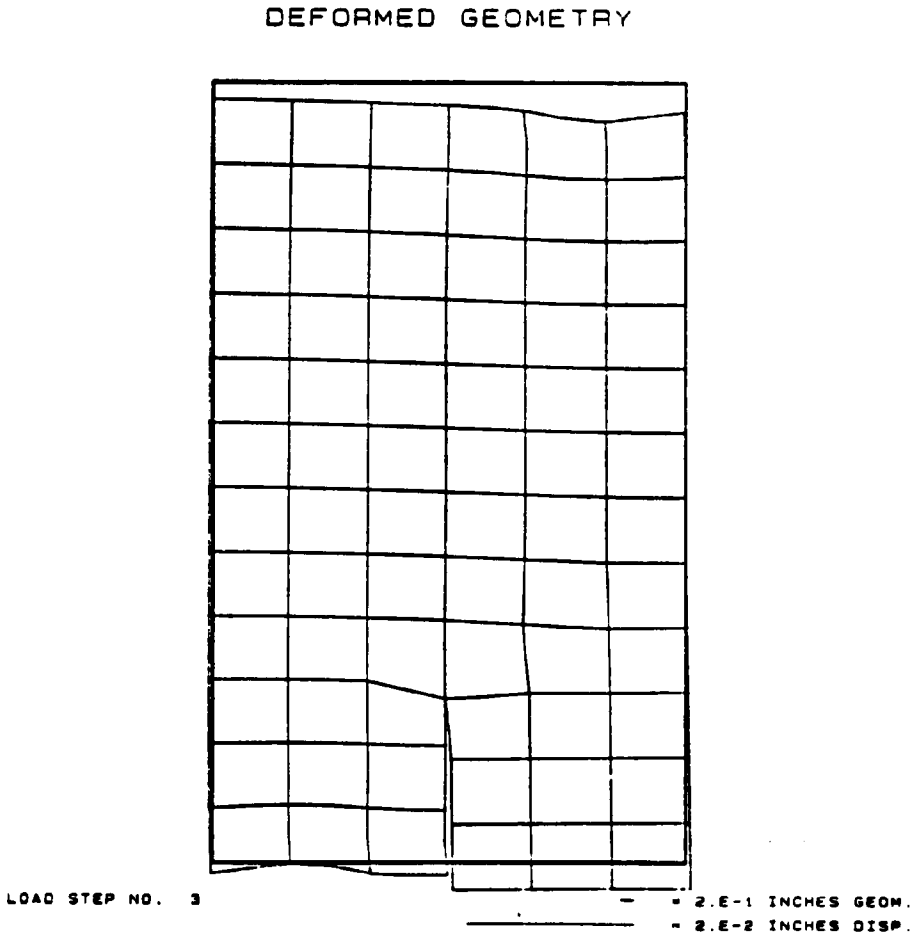

FIG. 2.7 DEFORMED MESH AT PEAK LOAD P_p = 21.3 kips

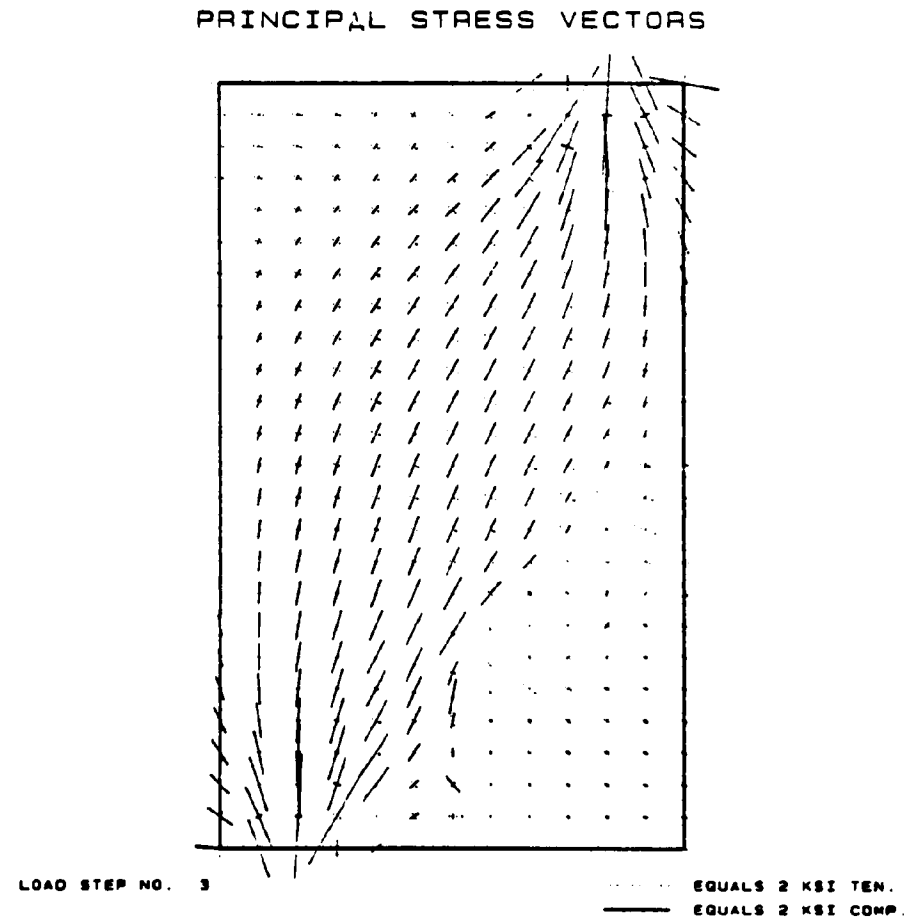

FIG. 2.8 PRINCIPAL STRESS DISTRIBUTION AT PEAK LOAD P_p = 21.3 kips

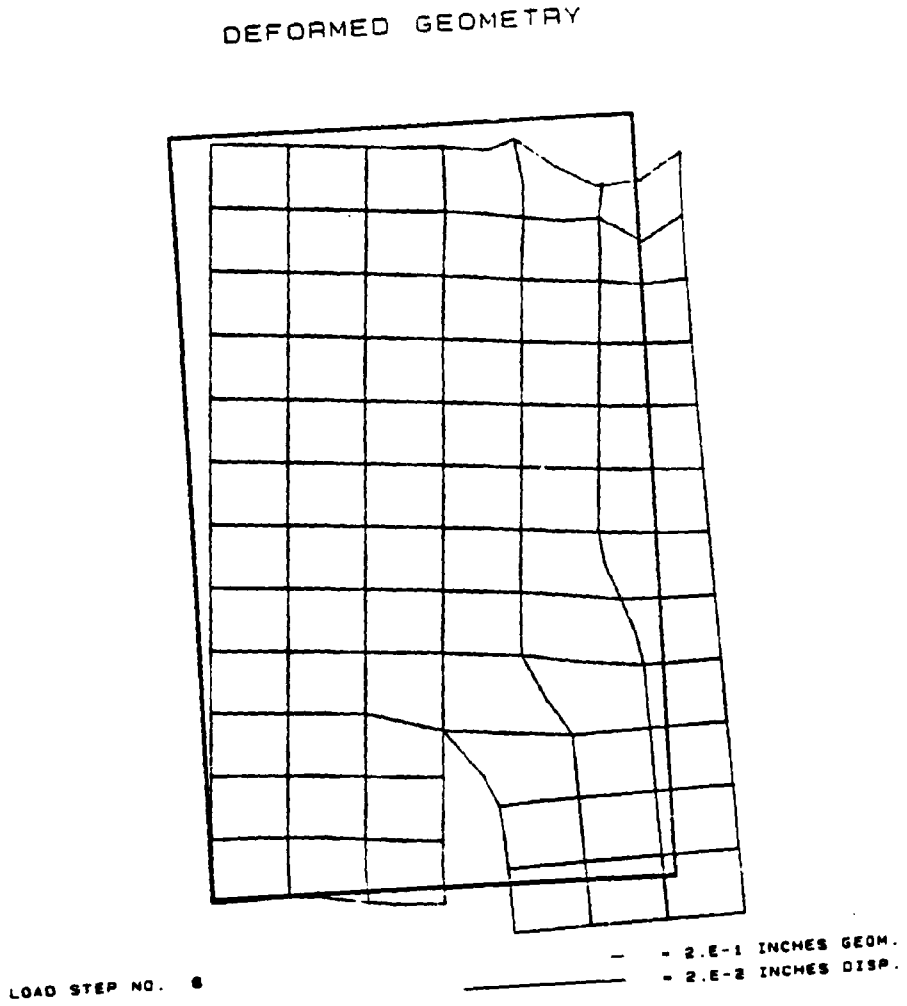

FIG. 2.9 DEFORMED MESH AT RESIDUAL LOAD P_r = 14.8 kips

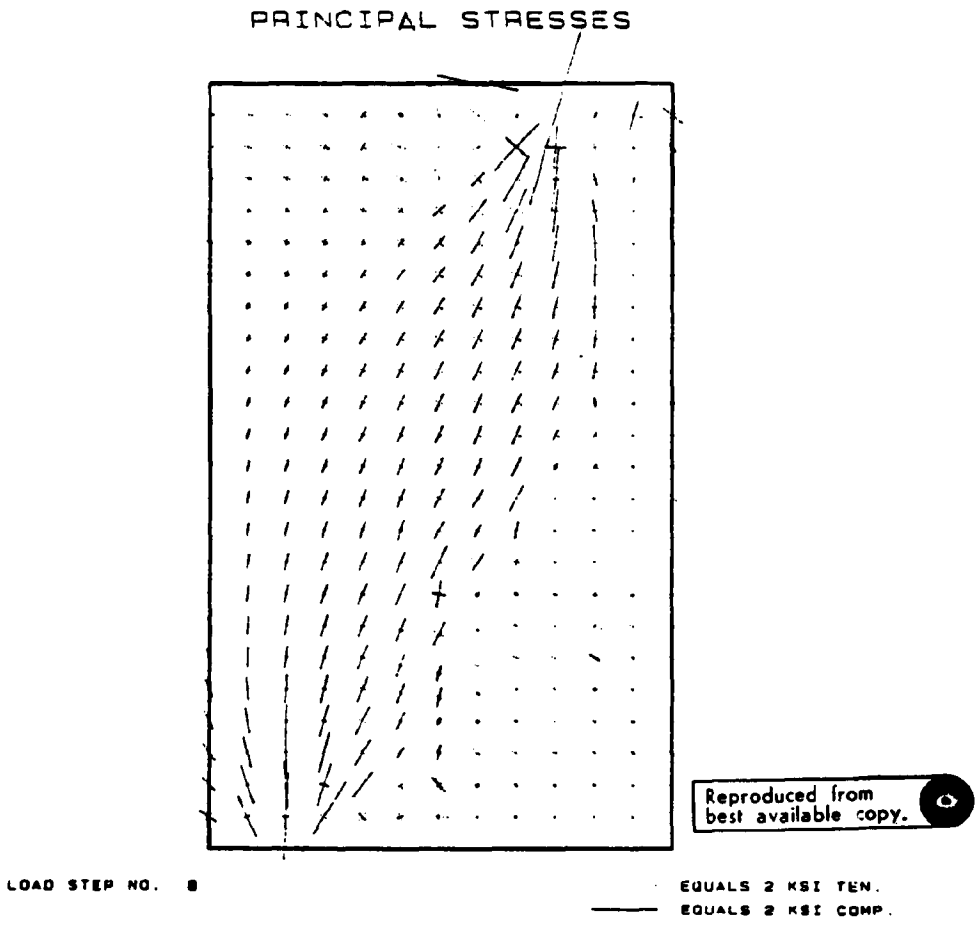

FIG. 2.10 PRINCIPAL STRESS DISTRIBUTION AT RESIDUAL LOAD P_r = 14.8 kips

The Fracture Mechanics of Concrete

Anthony R. Ingraffea
Cornell University

The proper fracture mechanics to be applied to crack propagation in concrete is determined by scale effects:

- How large is the process zone compared to the smallest critical dimension of the structure under consideration?

First, some definitions:

- Process zone ≡ that area accompanying crack propagation in which inelastic material response is occurring.
- Critical dimension ≡ the length of the crack itself, including its process zone, or, if it is smaller, the distance from the crack tip to the nearest free surface or reinforcing bar.
- Crack ≡ is not used here in its classical sense, as a complete discontinuity in both traction and displacement fields. Rather, it is used to describe an effective crack which consists of a length of true crack (in the classical sense) preceded by its process zone.

Next, some assumptions:

- It is assumed that the only constitutive modeling required for process zone description in pure Mode I is the stress-versus-crack-opening-displacement (COD) relation which can be obtained from a displacement-controlled direct tension test (Ref. 1). This relation is, in fact, the post-peak stress-COD curve measured in such a test. A range of such process zone softening models used in the present analyses is shown in Figure 1.
- The previous assumption implies that normal stress continues to be transferred across a displacement discontinuity which may or may not be visible to the naked eye. It is assumed that this stress

transfer is due to aggregate bridging and the undulating, three-dimensional nature of the opposing crack surfaces (Ref. 2).

- It is assumed that the process zone localizes, due to the rapid softening behavior shown in the models of Figure 2, into a very narrow band ahead of the true crack tip. In fact, for the purposes of finite element analysis, all softening is confined to one-dimensional interface elements lying in the crack plane ahead of the true crack tip (Ref. 3).

Given these observations and assumptions, it is natural to ask:

- How large must the critical dimension be for the application of linear elastic fracture mechanics (LEFM) to be valid? Or, rephrased, how long is the process zone?
- How sensitive is the process zone length, r_p, to structural geometry and the constitutive model which drives it?
- For a problem of effectively infinite domain, what is the steady-state process zone length for a given constitutive model?

This last question is addressed in the analysis of the structure shown in Figure 2. The structure is, except for its finite dimension, the same as that used by Griffith (Ref. 4) in developing the fundamental relationships of LEFM. To facilitate analysis over a wide range of crack lengths, two meshes, shown in Figures 3 and 5 were used. Both employed quadratic order, isoparametric quadrangles, triangles, and interface elements. Detail A of the first mesh, Figure 4, shows a typical interface element placement along the crack path.

Figures 6 and 7 show displaced shapes at two post-peak load levels. The shaded areas are actually the elongated interface elements comprising the process zone.

The complete load-displacement prediction is shown in Figure 8. The pre-peak nonlinearity due to process zone development ahead of the initial true crack is clearly shown.

The development of the process zone and the trailing, true crack is shown by way of crack opening profiles in Figure 9. Recall from Figure 1 that, for the constitutive model employed here, a COD of 0.005 inch is required to completely relieve normal stress transmission through the process zone.

Figure 9 can be used to trace the development of a steady-state process zone length. As shown in Figure 10, for this structure and this process zone constitutive model, the steady-state length is about 37 inches and this requires the development of a true crack length of about 60 inches.

The implications of this result are as follows:

- For LEFM to be applicable for this structure, a true crack length of at least 370 inches, 10 times the steady-state process zone length, would be required (Ref. 5).
- The steady-state process zone size estimate,

$$r_p \approx \frac{1}{3\pi}\left(\frac{K_{Ic}}{f_T}\right)^2$$

often used for concrete and rock is a gross underestimate. Note that Model D corresponds to a K_{Ic} of about 900 psi $\sqrt{\text{in}}$, and that a Young's modulus of 3×10^6 psi was used in this analysis.

REFERENCES:

1. Petersson, Per-Erik, "Crack Growth and Development of Fracture Zones in Plain Concrete and Similar Materials," Report TVBM-1006, Division of Building Materials, Lund Institute of Technology, Lund, Sweden, 1981, 174 pp.

2. Catalano, David M. and Ingraffea, Anthony R., "Concrete Fracture: A Linear Elastic Fracture Mechanics Approach," Research Report 82-1, Department of Structural Engineering, Cornell University, Ithaca, NY, Nov. 1982, 161 pp.

3. Ingraffea, Anthony R., Gerstle, Walter H., Gergely, Peter, and Saouma, Victor, "Fracture Mechanics of Bond in Reinforced Concrete," Journal of Structural Engineering, ASCE, Vol. 110, No. 4, April 1984.

4. Griffith, A. A., "The Phenomena of Rupture and Flow in Solids," Phil. Trans. Roy. Soc., Series A221, 1921, pp. 163-198.

5. Saouma, V., Ingraffea, A. R., and Catalano, D., "Fracture Toughness of Concrete: K_{Ic} Revisited," Journal of the Engineering Mechanics Division, ASCE, Vol. 108, No. EM6, 1982, pp. 1152-1166.

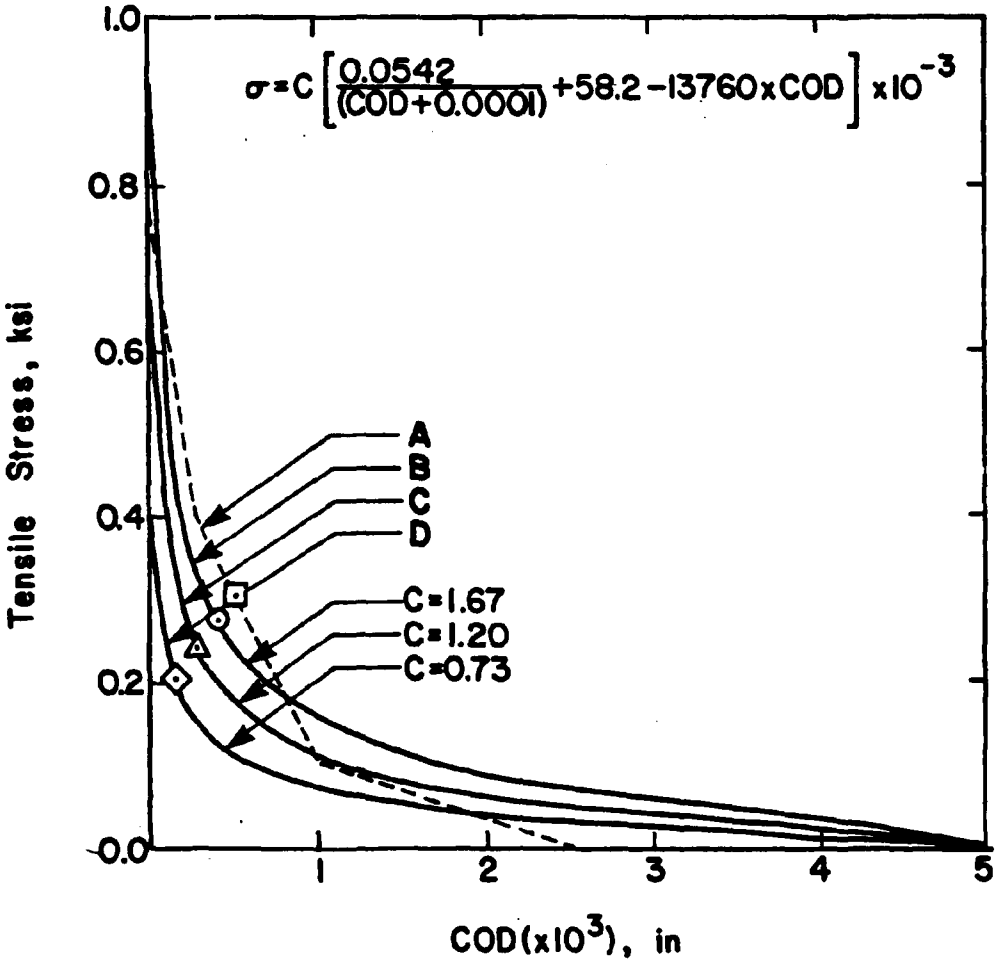

Figure 1. Process Zone, r_p, Softening Models

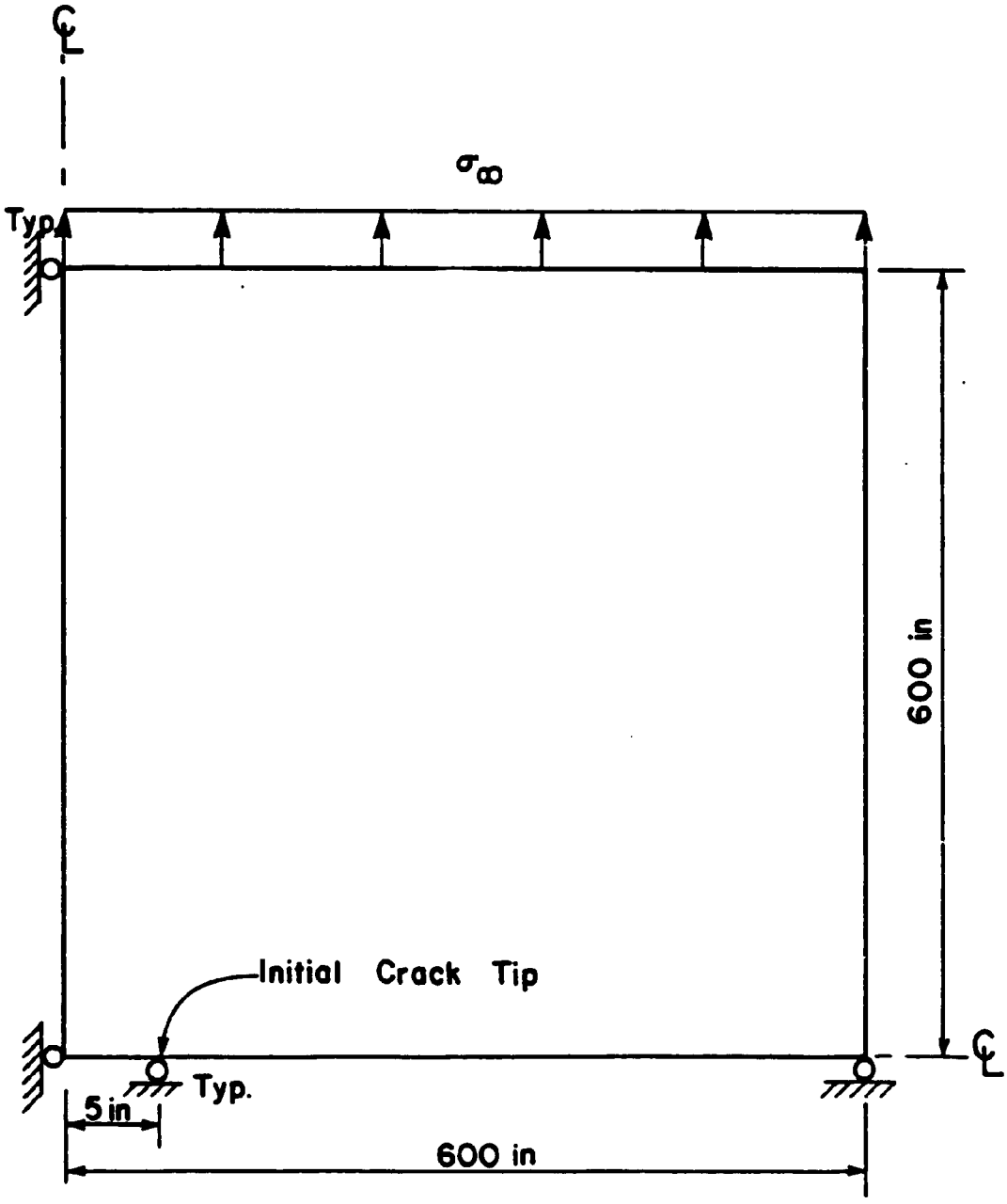

Figure 2. One-Quarter of Center-Cracked Plate (not to scale)

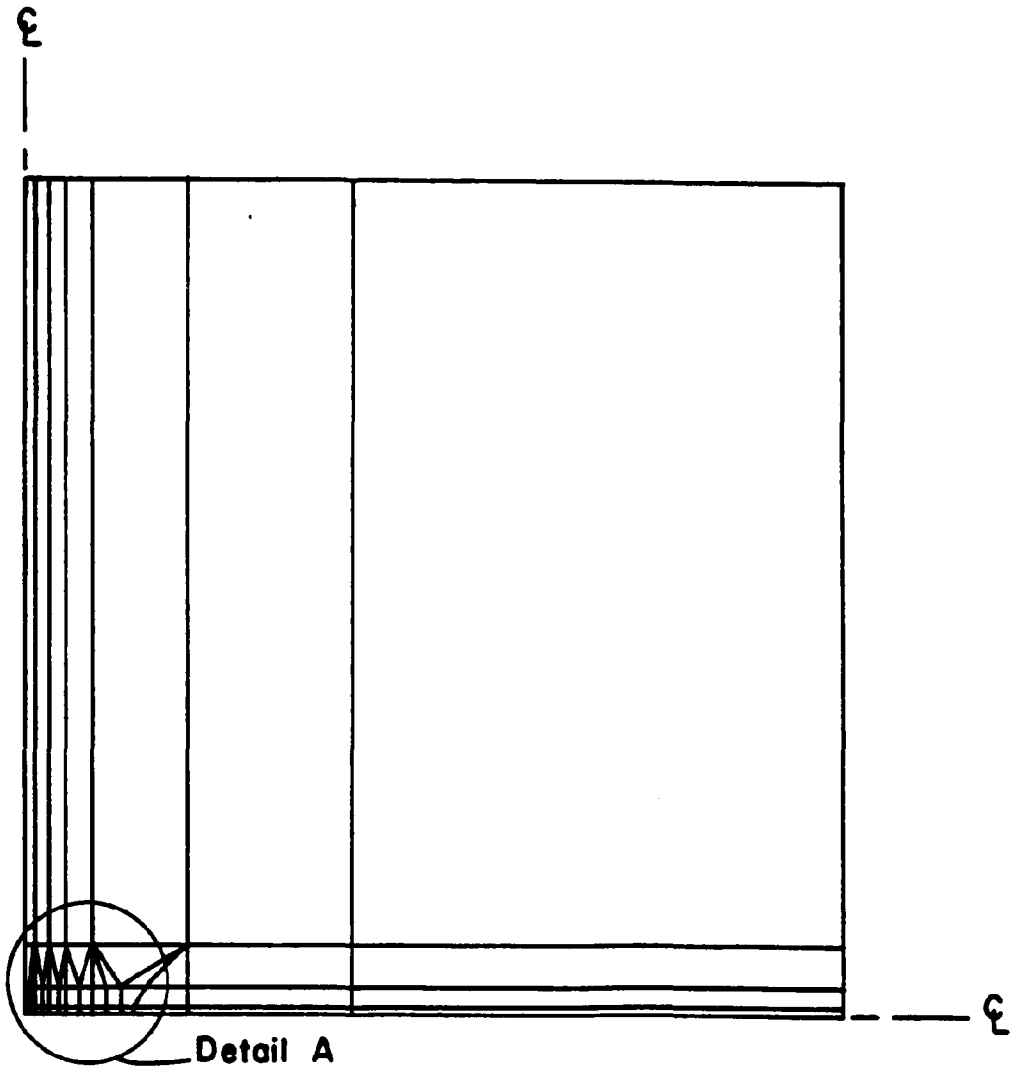

Figure 3. Mesh 1

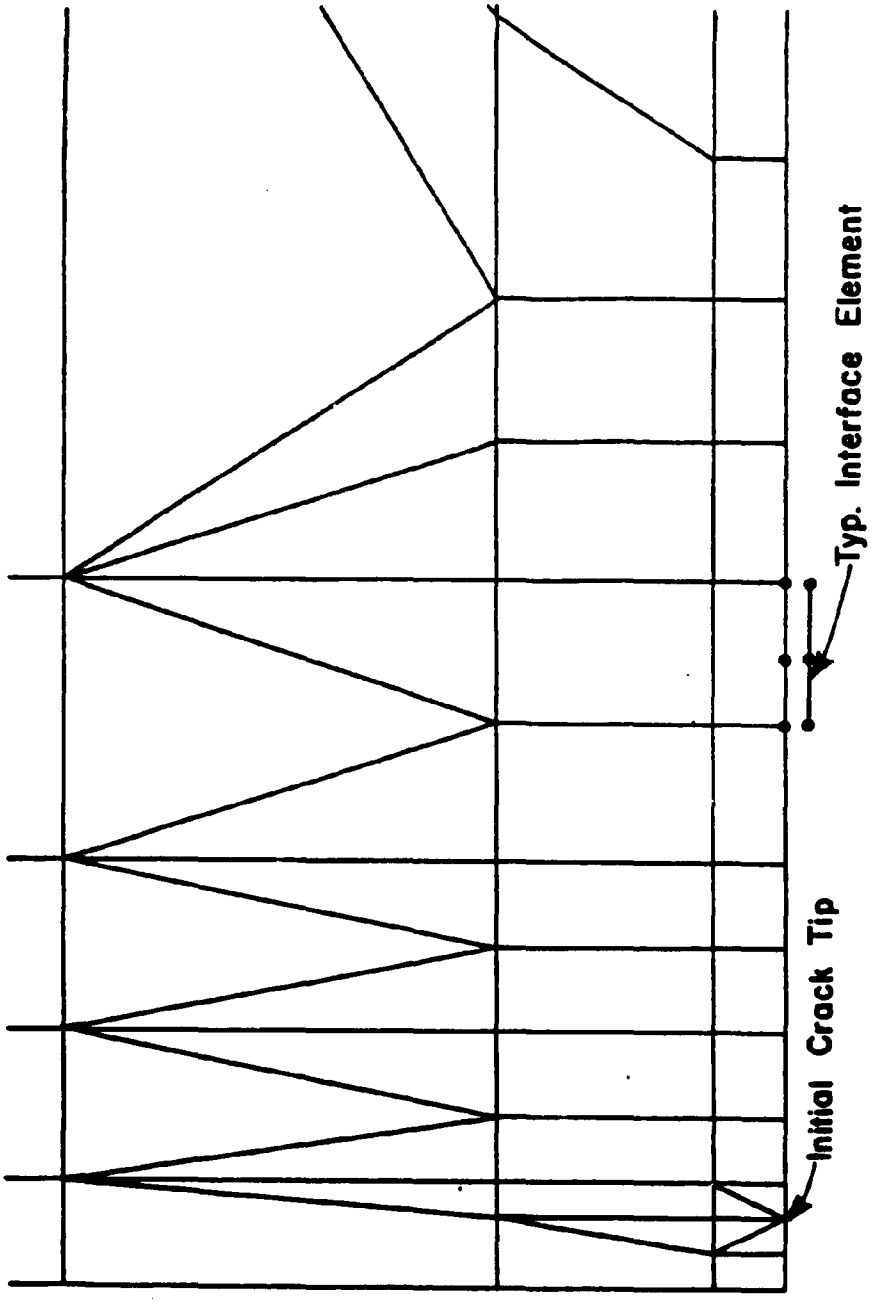

Figure 4. Detail A of Mesh 1

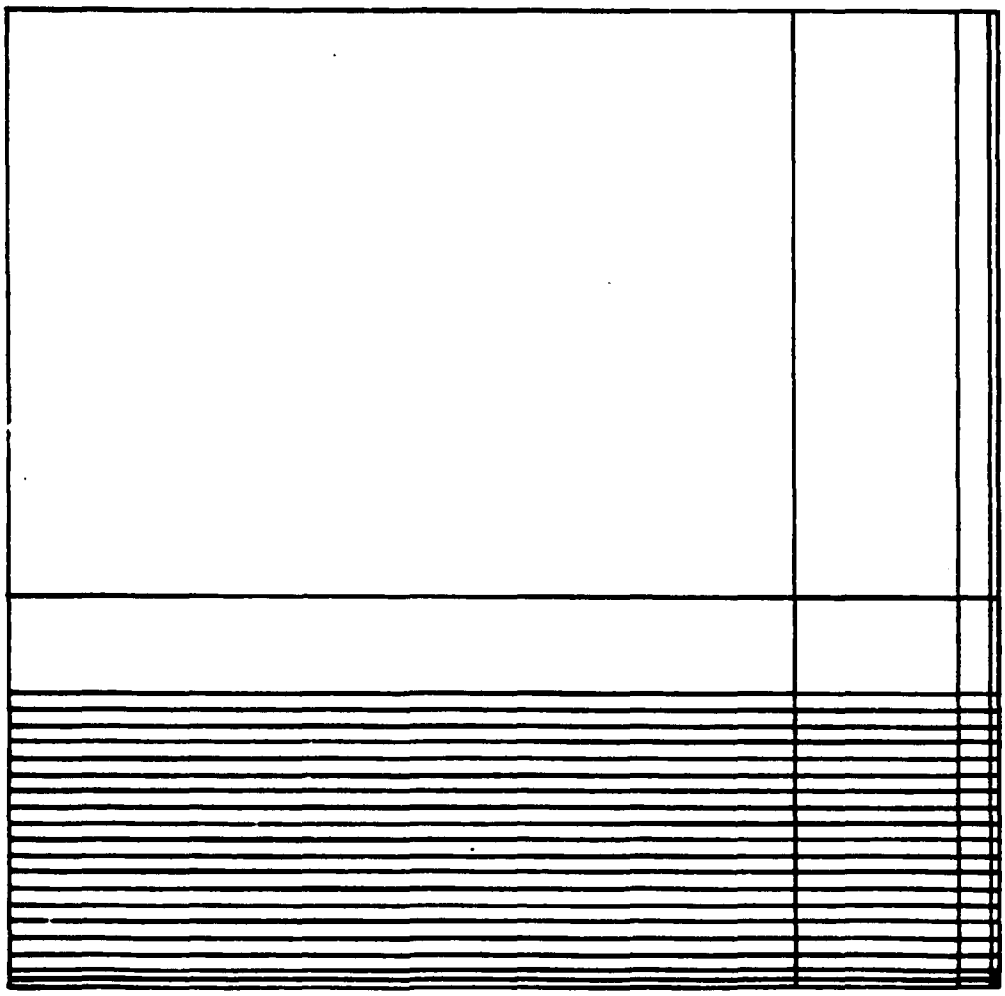

Figure 5. Mesh 2

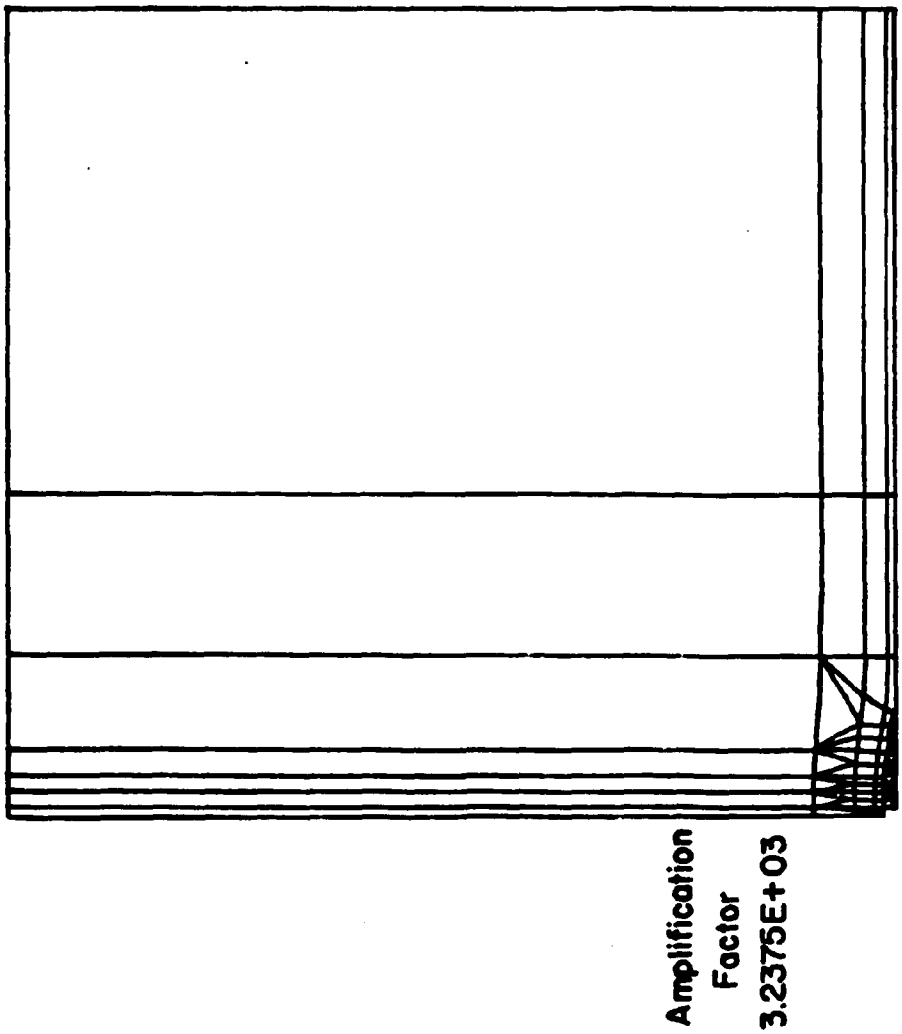

Figure 6. Displaced Shape for σ_∞ = 75 psi

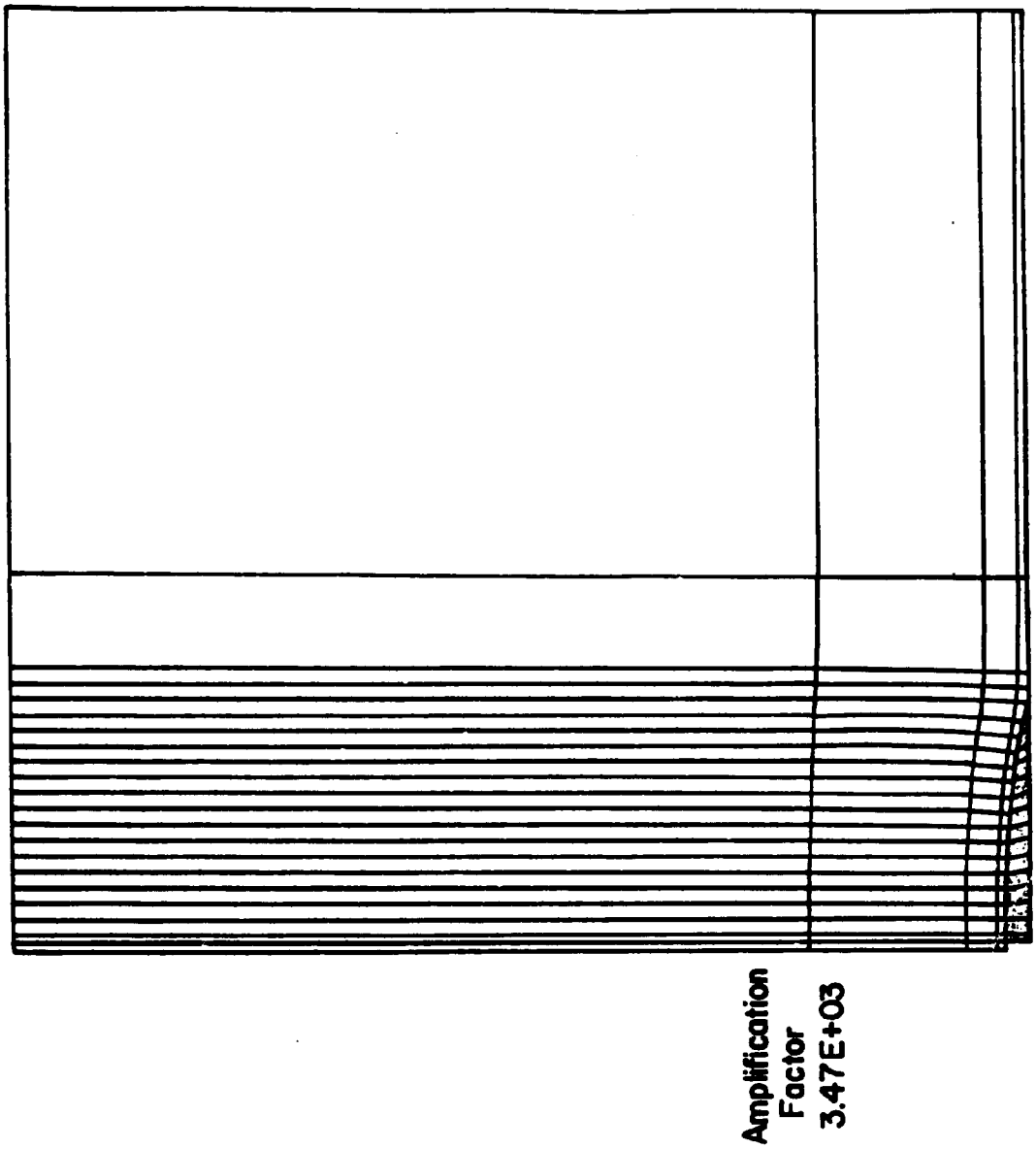

Figure 7. Displaced Shape for $\sigma_\infty = 54$

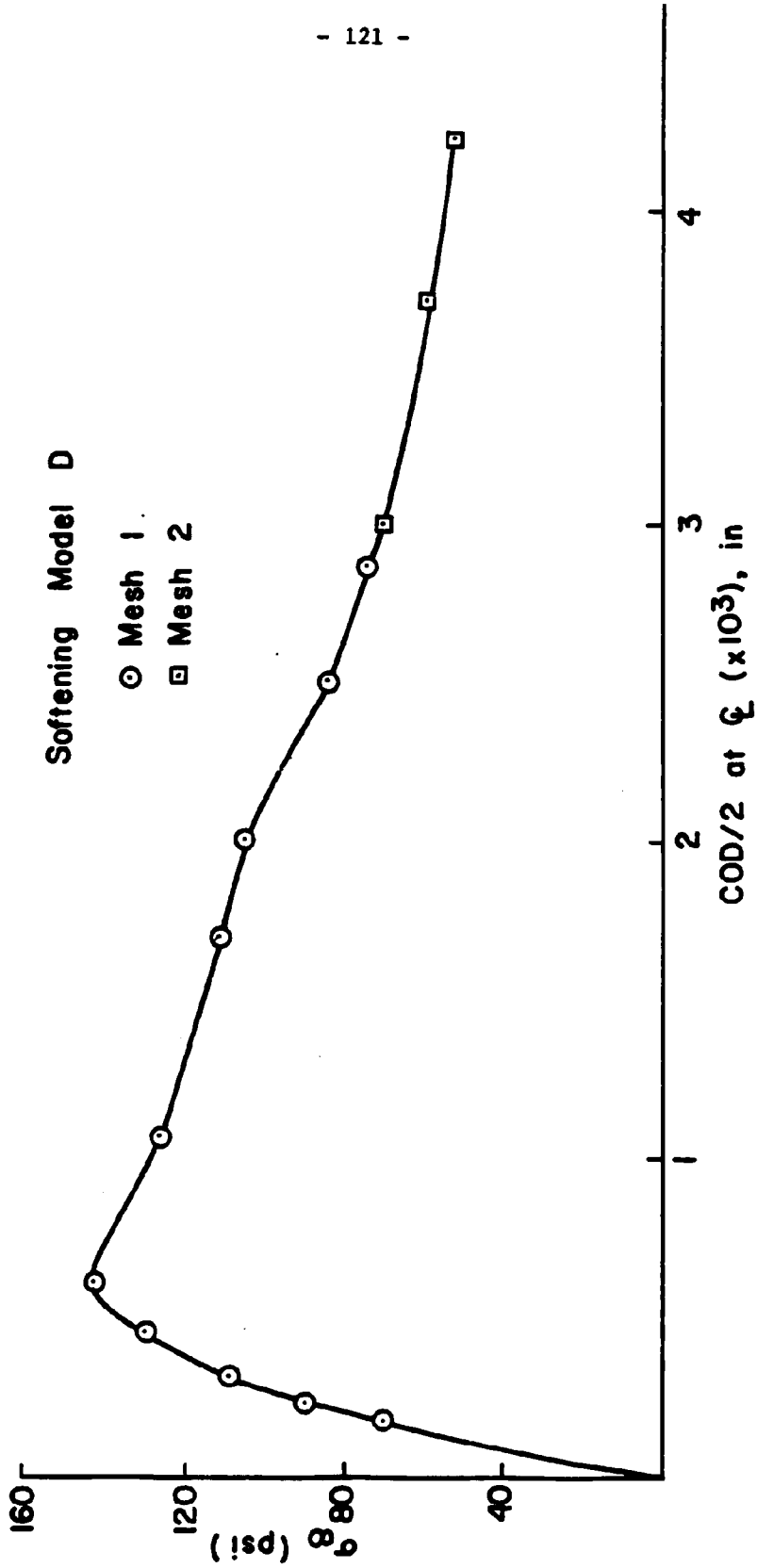

Figure 8. Load-Displacement Response

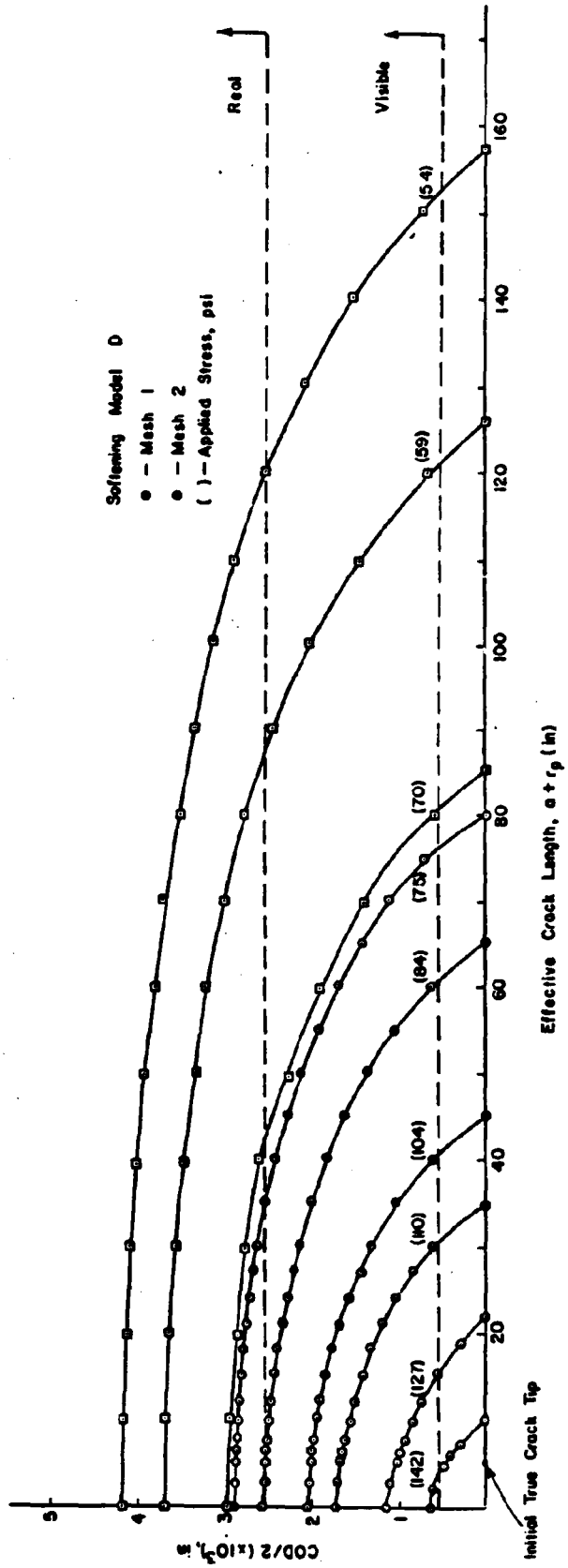

Figure 9. Post-Peak Crack-Opening-Displacement Profiles

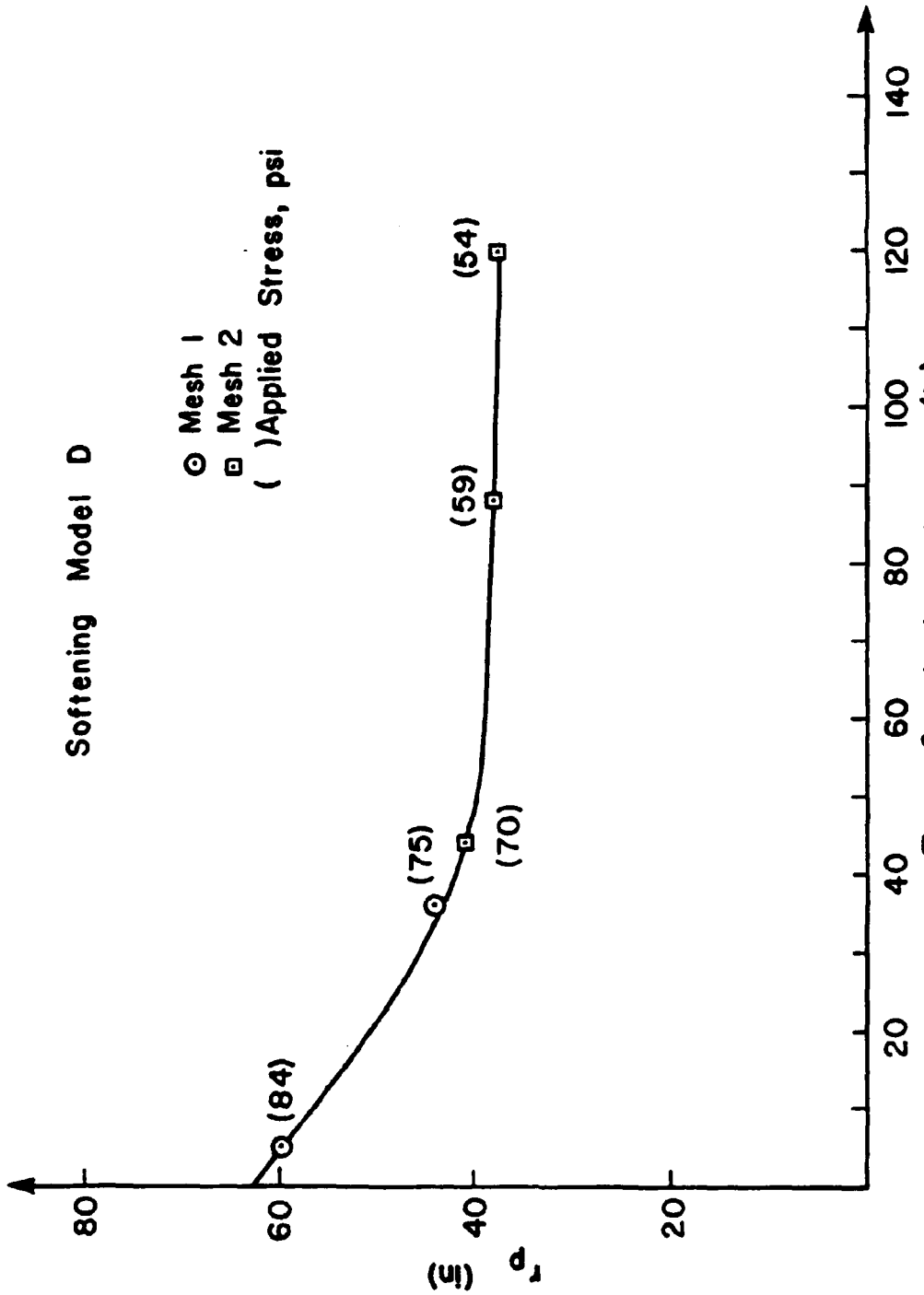

Figure 10. Process Zone Length Versus True Crack Length

Bond-Slip Relationships for Reinforced Concrete

Peter Gergely
Cornell University

The refined analysis of reinforced concrete, notably by the finite element method, requires detailed knowledge of the constitutive relationships of this composite material (1). Perhaps the most difficult parameter is the bond-slip law, especially for high-level reversed cyclic loading. Several experimental and analytical investigations have addressed this problem but agreement can be found only on some qualitiative conclusions.

The difficulties are manifold. It is well known (2, 3, 4, 5) that the properties of the bar (diameter, lug geometry) are important, particularly for cyclic loading. The properties of in-place concrete, especially the casting position of the bar, also affect the slip and bond strength. The greatest problem in arriving at general bond-slip relationships is the large variety of confinement conditions and radial stresses that may be caused by the cover, stirrups, and external loading. The failure mode, force level, extent of cracking, and slip all depend on the confinement.

Another complication is the effect of differences in loading conditions. In a beam large bond stresses exist at each crack and the concrete is in tension near the bar between cracks. On the other hand, anchorage bond is normally characterized by compression in the concrete.

The requirements of micro-modeling of reinforced concrete are much more exacting than those of design. It is necessary to know the variation of bond-slip relationships along a bar but it is impossible to measure the slip accurately right at the bar because of the complex stress and displacement conditions. The pioneering work and measurements by Nilson (6) are still used by most analysts. To avoid complications, one may ignore the local cracking

and crushing at bar lugs and define slip as relative displacements between the bar surface and a point (cylinder) chosen away from the bond zone around the bar (7). That idealization is simple for overall member analysis but it does not consider the details of local behavior.

Several researchers have proposed bond-slip relationships; for example at the University of Washington, in Japan, at Cornell University, Greece, Stuttgart, and TNO. When the bond stress gradient is large, it is insufficient to use average bond stress. Attempts have been made to generate bond-slip relationships by examining short bonded lengths with 1, 2, and more lugs (4). External pressure could be applied to simulate confinement.

Typical repeated and monotonic force-slip curves are shown in Fig. 1 for a specimen with 200 psi external pressure on a common concrete cylinder. Hysteresis curves in Fig. 2 illustrate the highly nonlinear behavior at low stress levels. The effect of confinement is evident in Fig. 3 and the number of ribs in Fig. 4. Not much change in behavior is expected for more than 3 ribs.

Idealized bond-slip hysteretic curves are shown in Fig. 5, based on 1, 2, and 3-rib tests. Such curves may be used in analysis, though the actual loading conditions must be similar to those used in the tests.

For anchorage problems in situations where high confinement is present, for example in a well-reinforced joint, quite accurate analytical models have been developed (8, 9) that can predict the cyclic bond behavior even at high loads. The confinement and joint geometry preclude cover cracking and associated uncertainties.

It is not likely that general bond-slip relationships can be developed that are equally applicable to tension situations, anchorage, varying confinement, external pressure, and loading history. However, research during the

past three years has resulted in several models that are applicable in specific situations.

References

1. deGroot, A.K., G.M.A. Kusters, and Th. Monnier, "Numerical modelling of bond-slip behavior," Concrete Mechanics, Part B, Heron, V. 26, 1981.

2. Tassios, T.P. and P.J. Yannapoloulos, "Analytical Studies on R/C Members under Cyclic Loading Based on Bond Stress-Slip Relationships," ACI Journal, V. 78, May-June 1981.

3. Tassios, T.P., "Properties of Bond Between Concrete and Steel under Load Cycles Idealizing Seismic Actions," CEB Bull. No. 131, April 1979.

4. Loizias, M.P., "Local Bond Between a Reinforcing Bar and Concrete under High Intensity Reversed Cyclic Load," M.S. Thesis, Department of Structural Engineering, Cornell University, January 1983.

5. Hassan, F.M. and N.M. Hawkins, "Anchorage of Reinforcing Bars for Seismic Forces," SP-53, ACI, Detroit, 1977.

6. Nilson, A.H., "Internal Measurement of Bond Slip," ACI Journal, Vol. 63, No. 7, July 1972.

7. Groeneveld, H. and M. Dragosavic, "Bond between concrete and reinforcement," TNO-IBBC, summary in this report.

8. Filippou, F.C., E.P. Popov, and V.V. Bertero, "Modeling of R/C Joints under Cyclic Excitations," Journal of Structural Engineering, ASCE, V. 109, No. 11, November 1983.

9. Eligehausen, R., E.P. Popov, and V.V. Bertero, "Local Bond Stress-Slip Relationships of Deformed Bars under Generalized Excitations," EERC-83/23, University of California, Berkeley, October 1983.

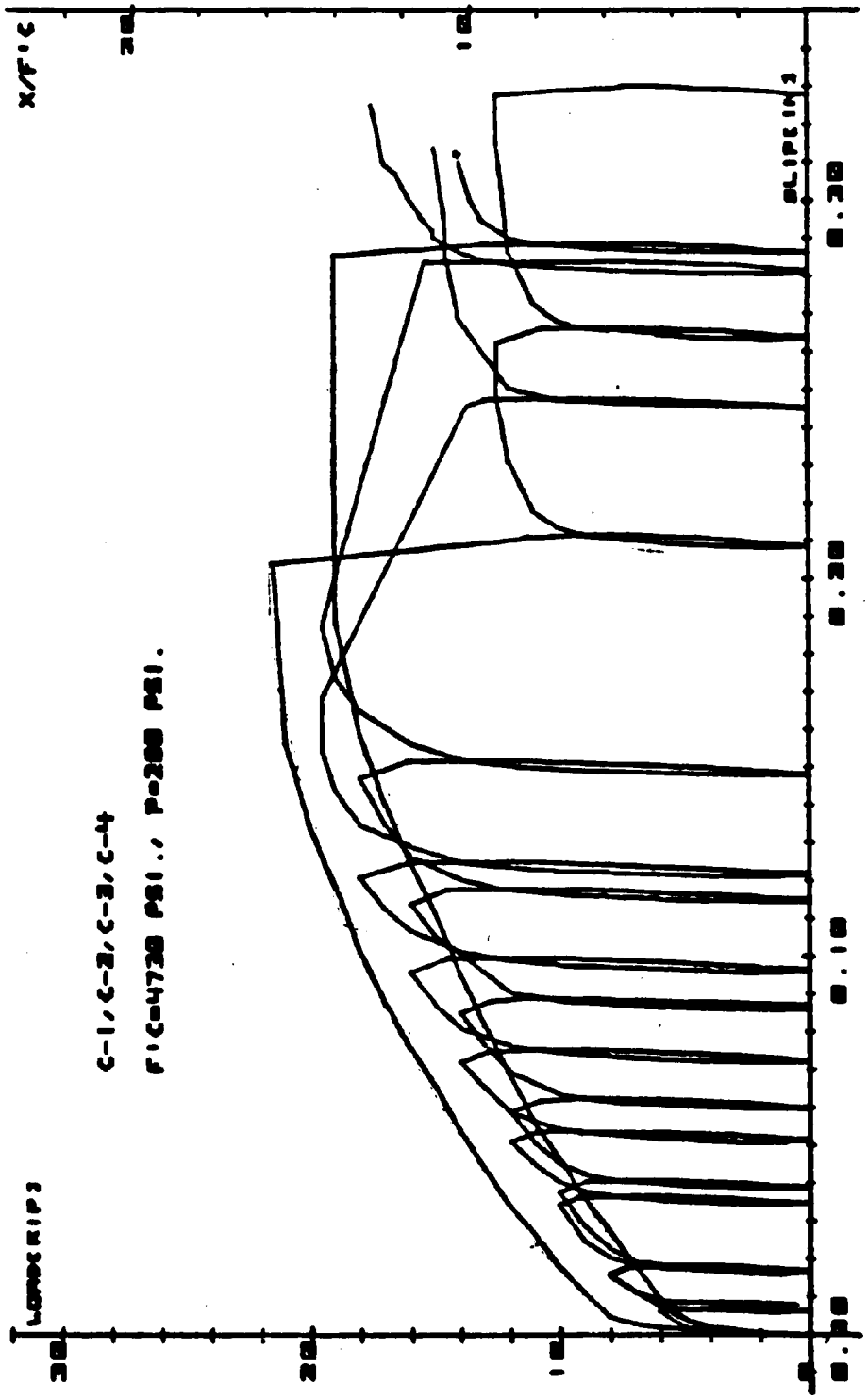

Fig. 1. Repeated vs. monotonic bond-slip curves

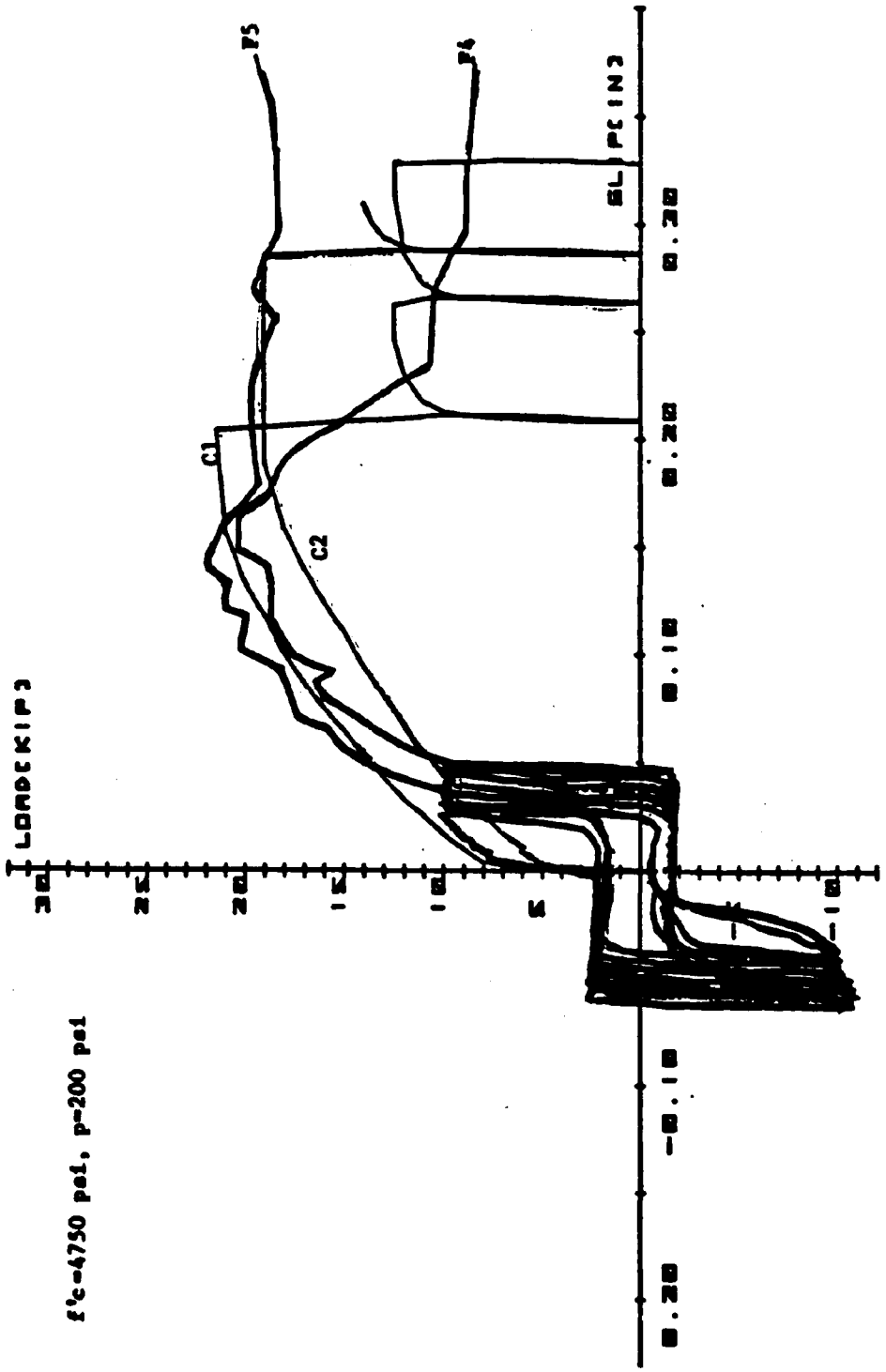

Fig. 2. Comparison of the monotonic loading bond-slip curves (C1 & C2) with the reversed cyclic loading bond-slip curves (F4 & F5)

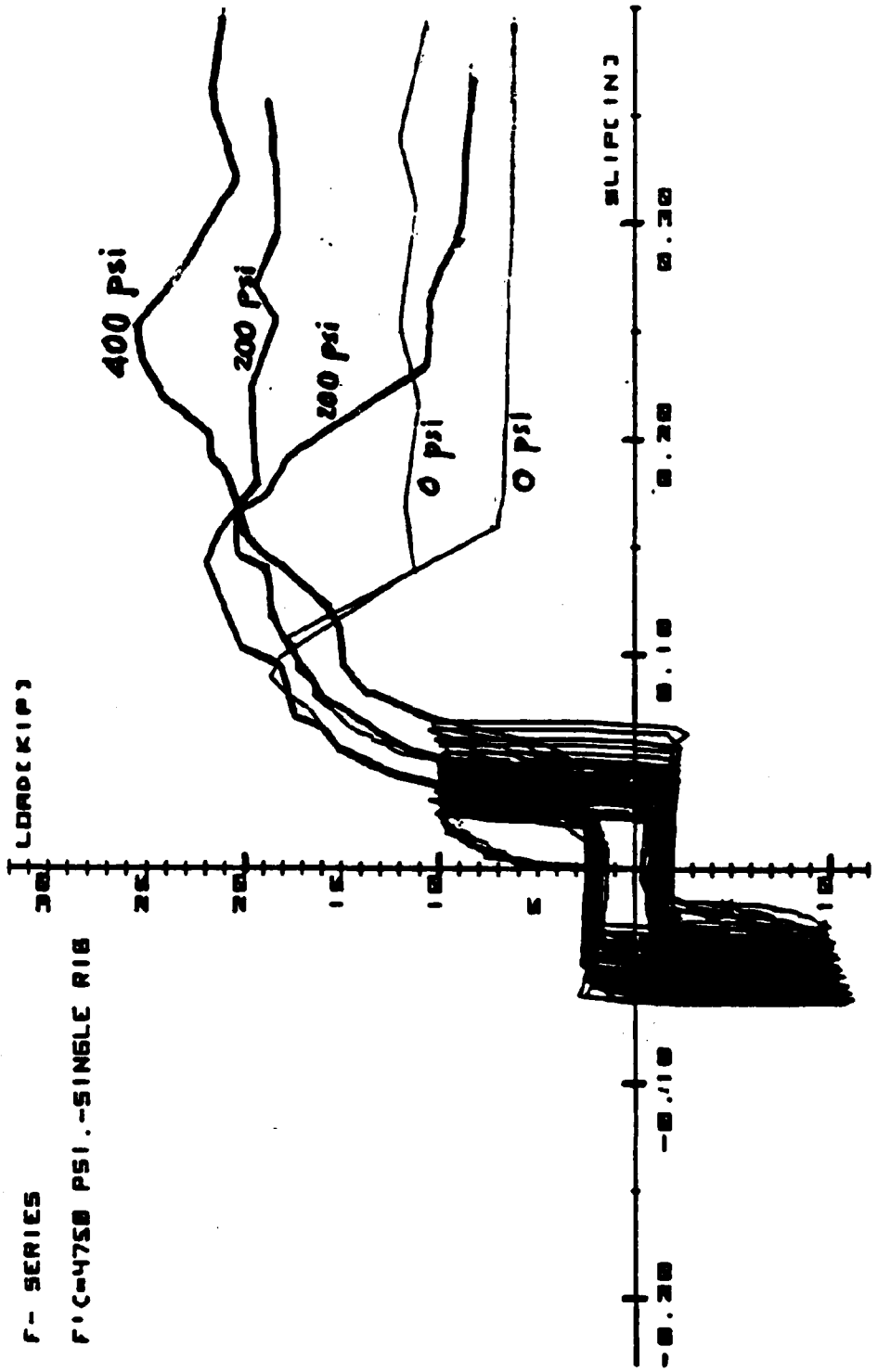

Fig. 3. Effect of confining pressure on bond under reversed-cyclic load

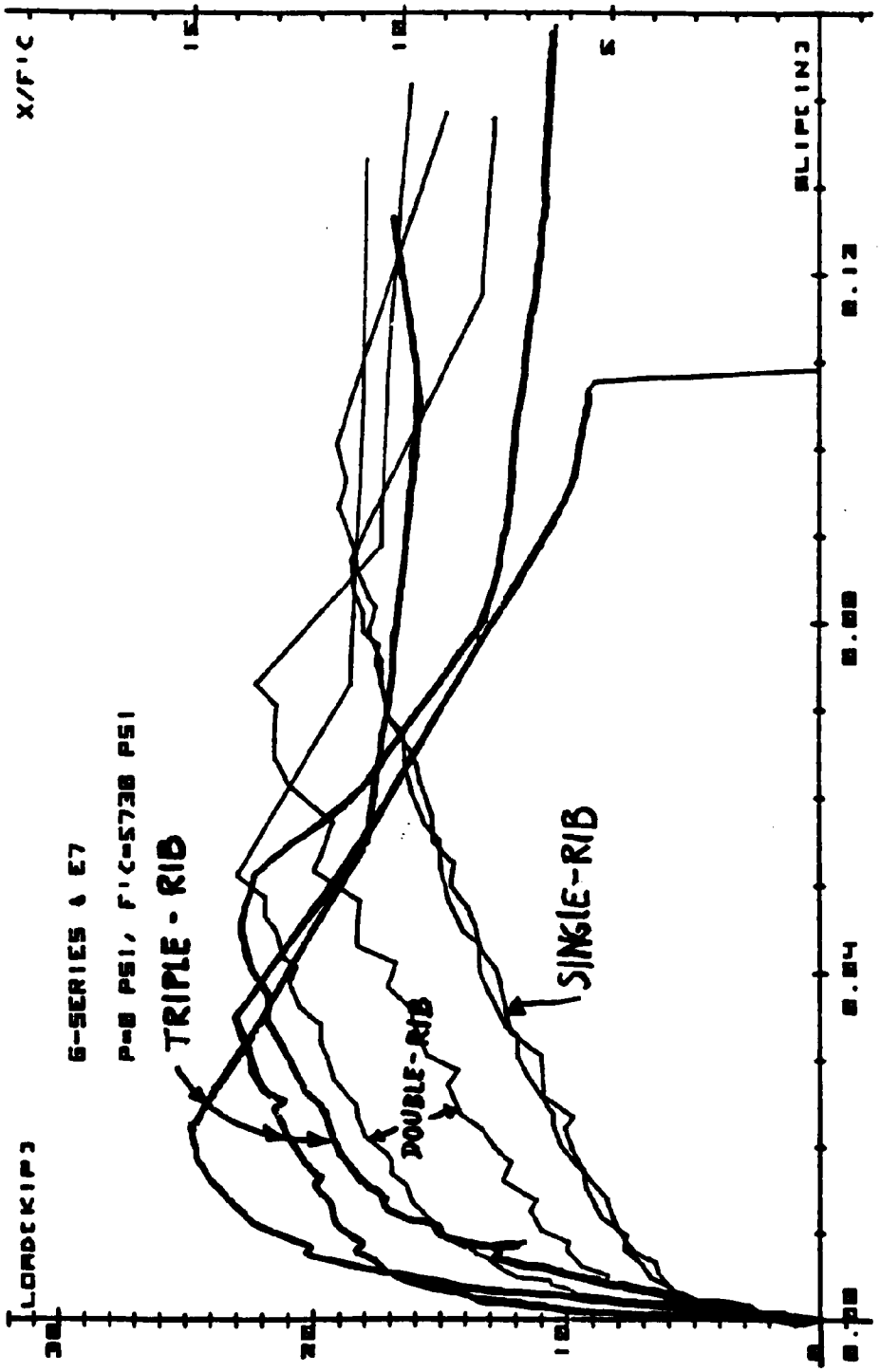

Fig. 4. Effect of number of ribs

Models for Analysis of Concrete

Oral Buyukozturk
MIT

Hybrid Model for Discrete Cracks

A method is proposed for the analysis of mode I and mixed mode crack propagation in concrete. It is based on a hybrid technique which uses finite elements to represent the uncracked specimen, and distributed dislocations to represent the crack. Consequently, no remeshing of the finite elements is required after crack propagation. This method is improved and further developed to make it applicable to concrete by incorporating the nonlinear traction transfer characteristics in a crack in concrete. By incorporating expressions obtained from previous studies to represent the aggregate interlock and imperfect debonding (i.e., tensile softening) in the crack, the propagation in a single edge notched beam, subjected to four point bending, is modeled correctly, while the predicted reduction in load corresponds satisfactorily with the experimentally obtained results.

A hybrid method, which combines the advantages of the finite element and boundary integral methods, was recently proposed for the analysis of cracks in finite bodies. This new approach utilizes finite elements to represent the features (particularly the finite geometry) of the body in which the crack occurs, while a continuous distribution of dislocations are used to model the crack. The effects of the dislocations are evaluated with a surface integral method. The crack can be treated as a pseudo substructure in the body by assuming that superposition holds for the specimen. A generalized stiffness matrix is assembled, and the displacements and dislocation densities can be obtained explicitly. A brief discussion of the derivation of the generalized stiffness matrix is outlined here.

Assume that a linear elastic body, in which a crack exists, is subjected to boundary tractions R. Tractions of magnitude T act on the crack. The actual stress and displacement fields in the body can then be treated as the superposition of two problems, by using the general method of substructuring. First, consider a crack with the same configuration as the actual problem, but in an infinite domain. Represent this crack by the superposition of mode I and mode II dislocations, distributed along the crack. Assume that tractions T^{si} act along this crack, which create certain stress and displacement fields in the infinite body. When the boundaries of the actual body are mapped onto the infinite body, the normal and shear tractions along this path can be calculated from the stress influence functions for dislocations. The corresponding equivalent nodal forces, R^{si}, (which act on the finite body) can be calculated from these tractions as

$$R^{si} = GF, \tag{1}$$

where G is the traction influence matrix, and

F are the dislocation density amplitudes (derivatives of the dislocations with respect to the distance along the crack). The surface tractions along the crack can also be written in terms of the dislocation density amplitudes as

$$T^{si} = CF, \tag{2}$$

where C is the matrix representing the stress influence functions along the crack.

The displacements (at the finite element nodes) due to the dislocations are given by the displacement influence functions. Special care has to be taken to represent the line of discontinuity of the crack correctly. These influence functions are used to compile the matrix L, which expresses the

displacements at the nodes in terms of the dislocation density amplitudes,

$$U^{si} = LF. \tag{3}$$

Consider also a finite body without a crack which is represented by finite elements and subjected to applied boundary tractions R^{fe}. The displacements can be found from the well-known expression

$$KU^{fe} = R^{fe},$$

where K is the stiffness matrix of the specimen. These displacements will in turn create stresses along the line of the crack that can be written as

$$SU^{fe} = T^{fe} \tag{4}$$

where S is traction influence matrix. The total displacements (U) are the sum of the displacements due to the dislocations and the load vector R^{fe}. Thus,

$$U = U^{fe} + U^{si} = U^{fe} + LF. \tag{5}$$

The total applied load vector, R, is

$$R = R^{fe} + R^{si} = KU^{fe} + GF, \tag{6}$$

and from equation (5),

$$R = K(U - LF) + GF = KU + (G - KL)F. \tag{7}$$

Similarly, the tractions along the crack will be

$$\begin{aligned} T &= T^{fe} + T^{si} \\ &= SU^{fe} + CF \\ &= SU + (C - SL)F. \end{aligned} \tag{8}$$

The global generalized stiffness matrix can be written as

$$\begin{bmatrix} K & (G-KL) \\ S & (C-SL) \end{bmatrix} \begin{bmatrix} U \\ F \end{bmatrix} = \begin{bmatrix} R \\ T \end{bmatrix} \tag{9}$$

or

$$\begin{bmatrix} K & C^* \\ S & C^* \end{bmatrix} \begin{bmatrix} U \\ F \end{bmatrix} = \begin{bmatrix} R \\ T \end{bmatrix} \tag{9a}$$

The stress intensity factors at the crack tips can be calculated from the dislocation density amplitudes. If the critical stress intensity factor of the material (K_{IC}) is known, and it is assumed that crack extension will take place in a direction normal to the direction of maximum tensile stress, the load level required to propagate the crack can be calculated. The general approach to this problem is to extend the crack by a certain increment, and then calculate the loads corresponding to this extension. Since this is an incremental method, two different approaches can be followed to calculate the direction of crack extension. In the first method it is assumed that the stress field around the current crack tip can be modeled with the normal expression for stresses at a crack tip. The new direction of a short crack increment will be in the direction where K_{II} is zero. Erdogen and Sih pointed out that the relation between K_I and K_{II} is given by

$$K_I \sin\theta + K_{II} (3\cos\theta - 1) = 0$$

where θ is the direction with respect to the previous crack direction in which K_{II} will be zero. The value of θ can be calculated from this expression when K_I and K_{II} are known.

Although the constitutive relations of the two phenomena of aggregate interlock and tension softening are vastly different, it will be assumed that the influence functions for tractions along the crack will be independent of the source of these tractions. The particular constitutive relations, which express the stresses along the crack in terms of the relative crack displacements, are discussed in another section. In this section a procedure is proposed for the solution of the general set of nonlinear equations. Generally, these crack face tractions are load path dependent. Due to the lack of sufficient experimental data to formulate the overly complex model that will be needed to incorporate all the significant features, it will be assumed that the stresses are path independent. In that case, the stresses across the crack (T_{cr}) are functions of the relative displacement of the crack faces (U_{cr}) or

$$T_{cr} = T_{cr}(U_{cr}). \tag{10}$$

The relative crack displacements (U_{cr}) are in turn linear functions of the dislocation densities along the crack, or

$$U_{cr} = DF \tag{11}$$

where D represents the displacement influence functions along the crack.

Constitutive Model for Concrete

A rational analysis and, hence, design of complex concrete structures through computer based methods is often limited by the lack of adequate material models for concrete. This is particularly true for structural situations where concrete is subjected to multi-dimensional loading conditions. In the past, numerous attempts have been made, with limited success, to establish constitutive equations of concrete for a variety of load conditions including cyclic load effects. Several clearly outlined approaches

used for defining the stress-strain behaviour of concrete may be categorized into the following main groups:

(1) linear- and nonlinear-elasticity theories

(2) elastic perfectly plastic models

(3) elastic strain-hardening plasticity models

(4) plastic-damage (fracturing) type models

(5) endochronic theory of inelasticity

A recent summary of finite element analyses of a variety of reinforced concrete structures shows that, in spite of the general recognition of the nonlinear material behaviour of concrete, most of these analyses use a linear-elasticity approach for modeling material response in pre- and post-peak stress range. This may be attributed to the difficulties encountered in assessing various parameters involved with complex material models and in their computer implementation. Significant realism in predictions can be achieved by assuming a nonlinear elastic stress-strain relationship. In general, two different approaches are employed in the formulation of nonlinear elasticity-based stress-strain laws. There are: (1) finite (or total) material behaviour characterization in variable secant-modulus form, known as hyperelastic type of formulation; (2) incremental or differential material descriptions of the hypoelastic type using variable tangent-modulus. Hyperelastic formulations approximate a load-path independent reversible process with no memory. That is, the material response at any instant is a function only of the current state of stress and not of the load history. These models simulate the response of concrete sustaining proportional loading with reasonable accuracy, but they fail to predict inelastic deformations when the material experiences unloading. The hypoelastic formulation approximates a path-dependent, irreversible process with limited memory. That is, the material response

at any instant is a function of the current state of strain, and of the stress path followed to reach that strain.

In the finite element Program ARC, four nonlinear constitutive models, three based on the theory of elasticity and one based on the incremental theory of work-hardening plasticity have been implemented. These formulations are described herein and critically evaluated. A material model developed for refractory concretes is also described. Thermal expansion-contraction and creep modeling capabilities in the program are discussed with regard to normal and refractory concrete.

An overview is presented of the approaches generally used in defining constitutive relations for concrete. Capabilities of the finite element computer program ARC, developed for the three dimensional analysis of complex reinforced, prestressed and refractory concrete systems is described. In that program the material models based on isotropic elastic, orthotropic elastic, and plasticity formulations have been implemented. This analysis capability is used to analyze some selected structural concrete problems; through these analyses, the verification of the implemented constitutive models is shown, and the applicability of the developed computer analysis capability to concrete structures is demonstrated. In the process of this verification an automatic check on the stability and effectiveness of the numerical procedures was also achieved.

Most elasticity-based models are computationally simple and particularly well suited for application in finite element codes. They provide a reasonably good representation of the deformational behaviour of concrete for practical applications. However, some of these formulations do not model the behaviour of concrete at high stress levels accurately. Moreover, these formulations are limited to proportional loading cases which may result in prediction errors

in certain structural situations. The development of plasticity-based models reaches greater generality. These models accurately predict inelastic dilatancy and hydrostatic pressure sensitivity observed in concrete.

The developed computer analysis capability incorporates special structural effects inherent to complex concrete systems. These include temperature dependent nonlinear material properties, cracking in concrete, shear transfer in cracked reinforced concrete sections, and time dependent effects such as transient temperature distributions and creep and shrinkage.

From the wide range of structural problems analyzed using the developed computer program, it is concluded that cracking, load-displacement response and ultimate strength predictions are achieved with adequate accuracy. The developed computer analysis capability may be used as a powerful tool for three dimensional structural analysis of complex concrete sytems. It can be used as a tool for gaining better insight into the behaviour of concrete structures, and as a valuable aid for improving existing design codes. The usefulness of the program can be enhanced by incorporating finite elements to analyze planar type of structures such as beams, panels and shells.

Damage Model for Concrete

A rate-independent damage-type constitutive model is proposed for the multiaxial cyclic behaviour of concrete. The material composite is assumed to experience a continuous damage process under load histories. The model adopts a damage-dependent bounding surface in stress space, which predicts the strength and deformation characteristics of the gross material under general loading path. Reduction in size of the bounding surface as damage accumulates and the adopted functional dependence of material moduli on stress and damage permit a realistic modeling of the complex behaviour of concrete

under multiaxial load cycles. Satisfactory prediction is obtained of the generally nonlinear stress-strain response, degradation in stiffness during load cycles, shear compaction-dilatancy phenomena, aggregate interlocking and post-failure strain softening behaviour. Finite element implementation of the proposed model is feasible and computationally efficient.

REFERENCES

Wium, Daniel J.W., Buyukozturk, Oral, and Li, Victor C., "Hybrid Model for Discrete Cracks in Concrete," Department of Civil Engineering, MIT, Cambridge, Massachusetts, September 1983, 35 pp.

Buyukozturk, Oral and Shareef, Syed Sarwar, "Constitutive Modeling of Concrete in Finite Element Analysis," Department of Civil Engineering, MIT, Cambridge, Massachusetts, December 1983, 100 pp.

Chen, En-Sheng and Buyukozturk, Oral, "Damage Model for Concrete in Multiaxial Cyclic Stress," Department of Civil Engineering, MIT, Cambridge, Massachusetts, 35 pp.

Delft Meeting on Mechanics of Concrete, June 22-24, 1983

CRACK SHEAR IN CONCRETE : ROUGH CRACK MODEL AND MICROPLANE MODEL

Pietro G.Gambarova[1]
Professor of Structural Engineering
Politecnico di Milano, Milan, Italy

Introduction

Concrete members are subject to cracking, which reduces the mechanical properties of the material compared to solid concrete. However, cracked concrete properties (strength and stiffness) may still be important on condition that the confinement action across the cracks is significant.

Both shear strength and stiffness of cracked concrete are mostly ensured by the roughness of crack surfaces (Aggregate Interlock Mechanism). Consequently, a first approach to the description of the behaviour of cracked concrete subject to shear should be based on Aggregate Interlock properties. Nevertheless, a more general approach is needed to describe not only the shear transmission capabilities of existing cracks, but also the process of formation of the cracks themselves.

Within these different approaches, two constitutive models are here presented: the first (Rough Crack Model) refers to a system of existing parallel cracks, and is based on finite stress-strain relations between the stresses at the crack interface and the equivalent strains produced by cracking itself.

The second (Model of Weak Planes or Microplane Model) assumes that the non linear behaviour in tension (up to cracking, which is introduced by means of equivalent strains) is the result of concrete behaviour along randomly distributed weak planes or microplanes. A one-to-one functional dependence is assumed between the normal stress and the normal strain in each microplane; cracking is represented in each plane by the tail of the $\sigma_n(\epsilon_n)$ function, characterized by large strain values and by zero stress values.

Rough Crack Model

The Rough Crack Model describes the Aggregate Interlock Mechanism, Fig.1 /1/, starting from some simple micromechanical models (Fig.2) and from the available test data (Paulay and Loeber, Daschner and Kupfer). Total stress-total displacement relations are worked out at the crack interface /1,3/. These relations can be regarded as constitutive laws of the material (cracked concrete) if the following assumptions are introduced: the cracks are linear, parallel and densely spaced; solid concrete deformations between two contiguous cracks are negligible; crack displacements can be replaced with equivalent strains obtained by smearing the displacements over a length equal to crack spacing s. The stress-strain relations are formulated as follows:

---

[1] Theory and results shown in this compact have been coauthored by Prof.Z.P.Bazant of Northwestern University (Evanston, Illinois) and by C.Karakoc of Istanbul Tech. University (Istanbul, Turkey).
This compact is a first version of the short paper published in the Transactions of W.Prager Symposium, held in Evanston at Northwestern University, September 11--15, 1983.

$$\sigma^c_{nt} = \tau_o \left(1 - \sqrt{\frac{2\,s\,\epsilon_n}{d_a}}\right) r \frac{a_3 + a_4 |r|^3}{1 + a_4 r^4}\,, \quad \sigma^c_{nn} = -\frac{a_1 a_2 r \sqrt{s\,\epsilon_n}}{(1 + r^2)^{0.25}}\,\sigma^c_{nt} \qquad (1,2)$$

where a_1, a_2, a_3, a_4 are constants, $\tau_o = 0.25\text{-}0.30\, f'_c$, $r = \gamma_{nt}/\epsilon_n$, with $\gamma_{nt} = \delta_t/s$, $\epsilon_n = \delta_n/s$. At constant crack dilatancy (δ_n linearly proportional to σ^c_{nt})-Fig.3-, the shear modulus $E_{33} = \partial\sigma^c_{nt}/\partial\gamma_{nt}$ has large values (comparable to elastic concrete), and so also the stiffness coefficient $E_{31} = \partial\sigma^c_{nt}/\partial\epsilon_n$, which represents the shear-opening coupling (crack opening of course).

Microplane Model

Because of the nature of concrete, which has hard inclusions and a weak matrix, (Fig.4), the stresses are far from uniform at the local level, having sharp extremes in the thin cement-paste layers between two contiguous aggregate particles (weak planes or microplanes). Assume now that in each microplane the static behaviour is characterized by an uniaxial law $\sigma_n = C_n(\epsilon_n)\cdot\epsilon_n$, where n is the normal to the microplane (Figs.5,6); the shear stiffness is negligible; the normal strain ϵ_n is equal to the resolved macroscopic tensor ϵ_{km} for the same plane ($\epsilon_n = n_k n_m \epsilon_{km}$, with k,m= 1,2 in two dimensions); the law $\sigma_n(\epsilon_n)$ has a softening branch (Fig.6); the microplanes have a random distribution at the macroscopic level (Fig.5). For the loading in tension of the microplanes, the following intrinsic law has been adopted: $\sigma_n = E_n \epsilon_n e^{-\epsilon_n/\epsilon_o}$. Superimposing the responses of all microplanes, the stresses σ_{ij} and the coefficients E_{ijkm} of the stiffness matrix of the material can be obtained as follows:

$$\sigma_{ij} = (1/\pi)\int_o^\pi C_n\, n_k n_m n_i n_j\, \epsilon_{km}\, d\varphi\,, \quad E_{ijkm} = (1/\pi)\int_o^\pi (C_n + dC_n/d\epsilon_n)\, n_i n_j n_k n_m\, d\varphi \qquad (3,4)$$

With a suitable formulation for C_n, the elastic behaviour can also be described, with ν=0.33 (plane stresses), which can easily be corrected to 0.18-0.20 /2/. The formulation of the laws $\sigma_n(\epsilon_n)$ for loading in tension and in compression, and for unloading, can be based on the results of Aggregate Interlock Tests ,see Fig.7, where δ_t and δ_n have been smeared over a "crack band width" w equal to a multiple of the maximum aggregate size d_a ($w = d_a$ has been so far adopted). Although the constitutive law of the microplanes is path-independent, the superposition of the responses is path-dependent.

Comparison with test results, and concluding remarks

Both models give shear-slip curves (under imposed strain histories) which are in good agreement with the experimental results, Figs.8-10 (here reference is made only to Aggregate Interlock Tests, namely those tests performed on concrete specimens having one single preformed crack and external confinement devices).

The fitting obtained with the Rough Crack Model is even better, but the Microplane Model is much more general and efficient (for instance, the orientation of cracking within the crack band is intrinsically linked to the imposed strain history, and it is not supposed to be constant as in the Rough Crack Model).The Microplane Model can describe also the overall behaviour of concrete in tension and shear.

Both models can usefully be introduced into FEM programs, for updating the stiffness matrix of cracked concrete.

References

1. Bazant,Z.P., Gambarova,P.G., "Rough Cracks in Reinforced Concrete", Journal of the Structural Division, ASCE, Vol.106, No.ST4, Proc.Paper 15330, April 1980, pp.819-842.

2. Bazant,Z.P., Gambarova,P.G., "Crack Shear in Concrete: Crack Band Microplane

Model", Report, Center for Concrete and Geomaterials, Northwestern University, Evanston, Illinois, May 1983.

3. Gambarova,P.G., Karakoc,C, "A new approach to the analysis of the confinement role in regularly cracked concrete elements", 7th Int.Conf. on Structural Mechanics in Reactor Technology (SMiRT 7), Paper H5/7, Chicago, August 1983.

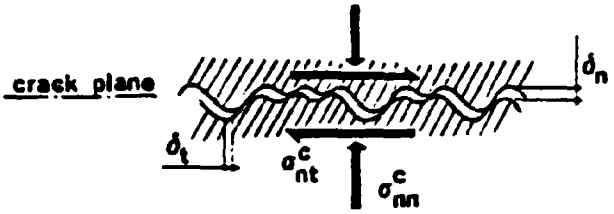

Fig.1 - Crack morphology (plane stresses).

Fig.2a - Wedge effect : crack response depends on the ratio $r = \delta_t/\delta_n$.

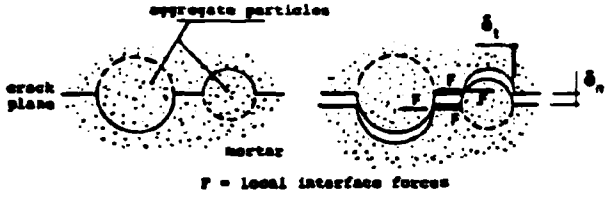

Fig.2b - At small crack openings, a limited confinement action is required.

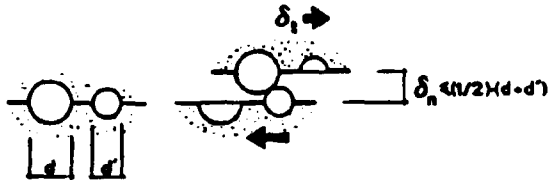

Fig.2c - The local contact is lost when $\delta_n > (1/2)(d+d')$.

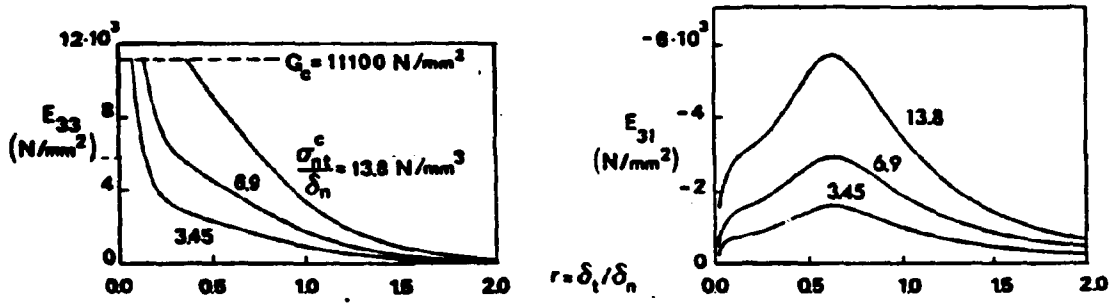

Fig.3 - Curves of the stiffness coefficients E_{33} and E_{31} (from Eqs.1 and 2), for different values of the crack dilatancy. $f'_c = 31$ N/mm², $d_a = 19$ mm, $s = 190$ mm.

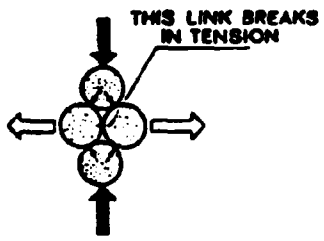

Fig.4 - Simplified model for concrete, with weak planes in tension and in compression.

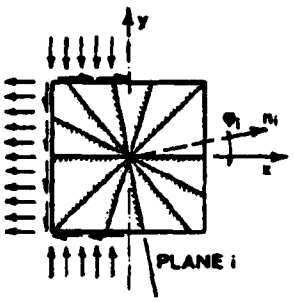

Fig.5 - Weak planes (microplanes) in the bidimensional case.

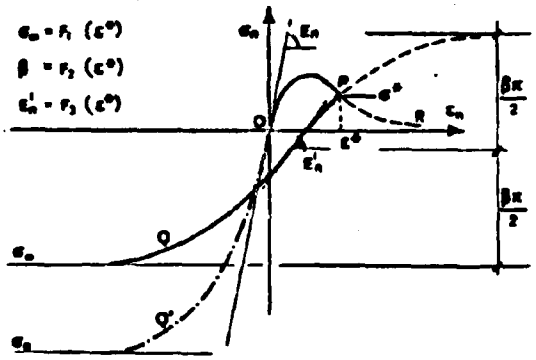

Fig.6 - Loading in tension (OPR), unloading in tension (PQ), loading in compression (OQ').

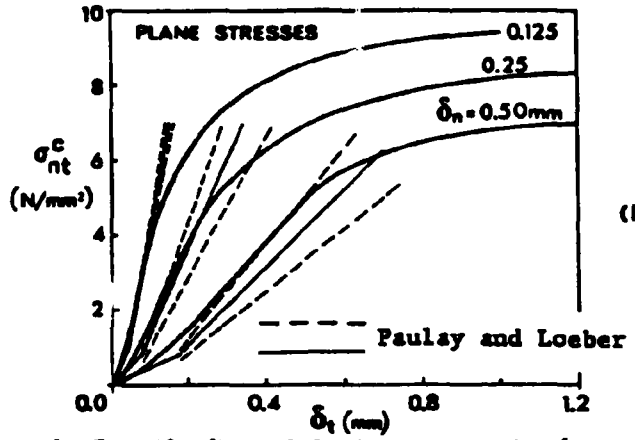

Fig.7 - Fitting of Paulay and Loeber' test results at constant crack opening by means of the Microplane Model. f'_c= 31 N/mm², d_a=19 mm.

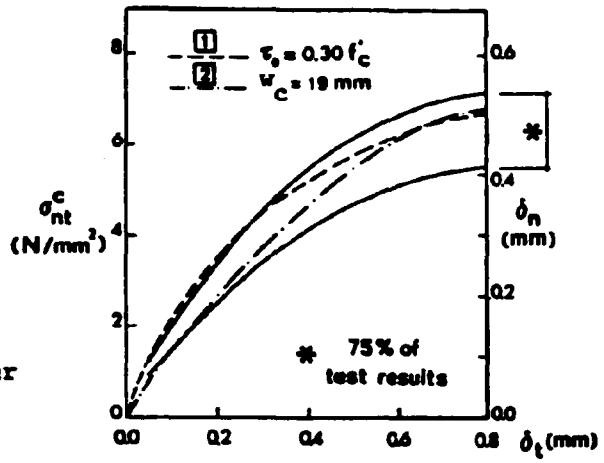

Fig.8 - Fitting of Paulay and Loeber' test results at constant crack dilatancy δ_n/σ^c_{nt}=0.0725 mm³/N : 1 = Rough Crack Model, 2 = Microplane Model.

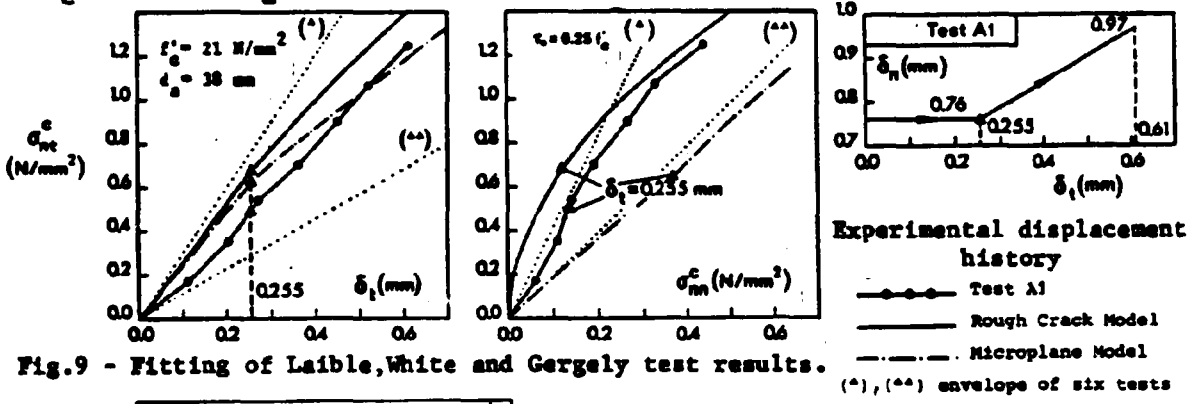

Fig.9 - Fitting of Laible, White and Gergely test results.

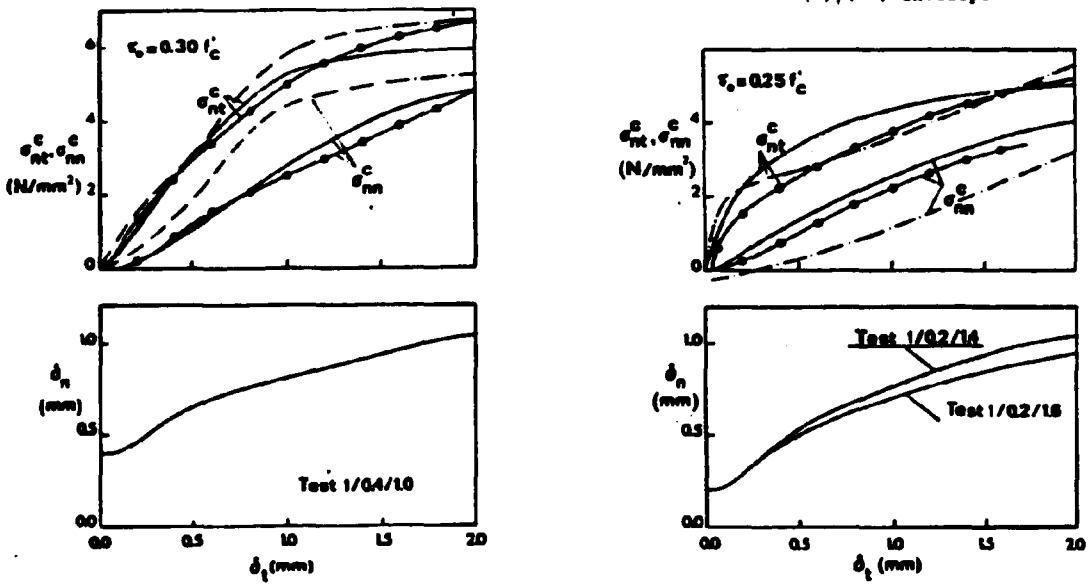

Fig.10 - Fitting of Reinhardt and Walraven' test results (curves with solid circles) : Rough Crack Model solid curves, Microplane Model dash-dotted curves. f'_c= 31.2 N/mm² (average value), d_a= 16 mm.

Meeting of THD/THE/TNO/RWS/TH Darmstadt/Milano University
US Universities
at Delft University of Technology
Department of Civil Engineering
Stevinlaboratory
NETHERLANDS

Program

Wednesday 22 June 1983	
9.00 a.m.	- departure from Delft
10.30 a.m. - 12.30 p.m.	- visit to lab at Eindhoven University - triaxially loaded concrete (Van Mier)
LUNCH	
1.30 p.m.	- departure from Eindhoven
3.00 p.m.- 5.00 p.m.	- visit to lab at TNO-IBBC in Delft

Meeting of THD/THE/TNO/RWS/TH Darmstadt/Milano University/
US Universities
at Delft University of Technology
Department of Civil Engineering
Stevinlaboratory
NETHERLANDS

Program

Thursday 23 June 1983	Friday 24 June 1983
9.00 a.m. - 1.00 p.m. - introduction (Reinhardt) - bench mark problems (US Universities, Blaauwendraad : MICRO Kusters : DIANA)	9.00 a.m. - 11.00 a.m. - shear transfer under sustained and cyclic loading(Frénay, Pruijssers, Walraven) 11.30 a.m. - 1.00 p.m. - bond under sustained and repeated loading (Dragosavić, Groeneveld, US Universities)
LUNCH	LUNCH
2.00 p.m. - 5.00 p.m. - bench mark problems, continued - current developments of numerical analysis (US Universities, De Borst : DIANA). 7.00 p.m. - informal meeting at The Hague	2.00 p.m. - 4.00 p.m. - tensile failure of concrete (Cornelissen : creep and fatigue, Reinhardt : deform. controlled slow cracking). 4.30 p.m. - 5.00 p.m. - creep under compressive loading (Mijnsbergen) 5.00 p.m. - closure.

List of Participants

1. Bouma, A.L. (THD)
2. Bruggeling, A.S.G.
3. Cornelissen, H.A.W.
4. Frênay, J.W.I.J.
5. Luijerink J.
6. Mijnsbergen, J.P.G.
7. Pruijssers, A.F.
8. Walraven, J.C.
9. Reinhardt, H.W.
10. Mier, J. van (THE)
11. Vlugt, B.W. van der
12. Borst, R, de
13. Dragosavić, M.
14. Groeneveld, H.
15. Monnier, Th.
16. Kusters, G.M.A.
17. Foeken, R. van
18. Rots, J.
19. Berg, F. van den (RWS)
20. Blaauwendraad, J.
21. Merks, P.J.G.
22. Zwol, B. van
23. Gambarova, J. (Milano University)
24. Cervenka, V. (TH Darmstadt)
25. Dinges, D.
26. Buyukozturk, O. (US Univ.)
27. Darwin, D.
28. Gergeley, P.
29. Ingraffia, A.
30. Schnobrich, W.C.
31. William, K.

Appendix A

Cooperative Research Between Cornell University, Other U.S. Research Laboratories, and Research Laboratories in The Netherlands

Summary of First Meeting
Held on June 9 and 10, 1981
Delft, The Netherlands

by
Richard N. White and Peter Gergely

September 1981

ATTENDANCE LIST

U.S.

1. Stephen Mahin
   779 Davis Hall
   Department of Civil Engineering
   University of California, Berkeley
   Berkeley, California 94720

2. James Jirsa
   Department of Civil Engineering
   University of Texas
   Austin, Texas 78712

3. Neil M. Hawkins
   Department of Civil Engineering
   201 More Hall
   University of Washington
   Seattle, Washington 98195

4. Peter Gergely
   Department of Structural Engineering
   Hollister Hall
   Cornell University
   Ithaca, New York 14853

5. Richard N. White
   Department of Structural Engineering
   Hollister Hall
   Cornell University
   Ithaca, New York 14853

6. Anthony R. Ingraffea
   Department of Structural Engineering
   Hollister Hall
   Cornell University
   Ithaca, New York 14853

THE NETHERLANDS:

1. Hans Reinhardt
   Delft University of Technology
   Stevin Laboratory
   Stevinweg 4, 2628 CN Delft
   The Netherlands

2. Joost C. Walraven
   Delft University of Technology
   Stevin Laboratory
   Stevinweg 4, 2628 CN Delft
   The Netherlands

3. Erik Vos
   Delft University of Technology
   Stevin Laboratory
   Stevinweg 4, 2628 CN Delft
   The Netherlands

4. Johan Blaauwendraad
   Rijkswaterstaat
   Bouwresearch
   P. O. Box 20,000
   3502 LA Utrecht
   The Netherlands

5. Theodore Monnier
   TNO-IBBC
   P. O. Box 49
   2600 AA Delft
   The Netherlands

6. M. Dragosavic
   TNO-IBBC
   P. O. Box 49
   2600 AA Delft
   The Netherlands

7. Ger. M.A. Kusters
   TNO-IBBC
   P. O. Box 49
   2600 AA Delft
   The Netherlands

8. Arie K. de Groot
   TNO-IBBC
   P. O. Box 49
   2600 AA Delft
   The Netherlands

9. Hans Groeneveld
   TNO-IBBC
   P. O. Box 49
   2600 AA Delft
   The Netherlands

1. Introduction

The National Science Foundation awarded Cornell University a grant for "Cooperative Research Between Cornell University, Other U.S. Research Laboratories, and Research Laboratories in the Netherlands" on April 23, 1981. The primary intent of this project is to facilitate research and development in the general area of reinforced concrete structures. The personnel involved are engaged in experimental and analytical studies of bond, cracking, splices, and shear transfer, plus development of several levels of computer analysis programs for reinforced concrete structures. Five U.S. universities and three groups in The Netherlands are represented.

Planned activities of the cooperative program include the following: (a) organized exchange of reports and papers, (b) annual meeting of researchers, (c) cooperative activities in both analytical and experimental research projects, (d) exchange of research personnel, and (e) issuing of joint proposals for new research.

This brief report summarizes the first meeting held at the Stevin Laboratory of the Delft University of Technology in Delft, The Netherlands, on June 9 and 10, 1981.

2. Participants

Seventeen individuals participated in the meeting -- 6 from the U.S. and 11 from The Netherlands. A listing of participants and their addresses is given at the front of this report.

3. Agenda

The agenda for the meeting, which was under the general chairmanship of Dr. Reinhardt, is given in Appendix A. Half day sessions were devoted to each of three topics -- analysis, shear transfer, and bond, and the final half day was devoted to general discussion and setting of plans for future activities.

4. Presentations

a. Introductory comments by Reinhardt. In addition to the Phase II of Betonmechanica (outlined below), there is strong interest in the shear capacity of frames, hollow core slabs, punching shear strength of circular slabs and cylinders, general aspects of shear transfer, and size effects in shear.

b. Blaauwendraad on Betonmechanica. The first phase focused on five main areas: plain concrete, steel rebars, crack zone, bond zone, and anchorage, all under monotonic loading. Fine scale advanced behavioral models were incorporated into computer programs STANIL and MICRO/1. The second phase is directed more toward offshore structures, with attention focused on cyclic loading, sustained loading, and environmental effects such as effect of saltwater, temperature changes, etc. Experimental investigations led to better basic physical models. Micromodels are

formulated from these, using the discrete crack approach. The micromodels are then blended into a macromodel global analysis approach using a smeared crack representation.

Delft University of Technology (DUT) has responsibility for the sustained load experiments; TNO for the cyclic load experiments and for derivation of the fine scale physical model for bond zone; DUT for the modeling of crack zone and plain concrete; and the constitutive laws are being based on material available in the literature.

Research on plain concrete is directed to tensile strength under sustained loads, interaction between shrinkage and tensile strength, and environmental effects.

Two analysis programs are being developed: DIANA and MICRO 1. DIANA is for design engineers. Program development for 2D and 3D is done at TNO; program verification is shared by TNO and Rijkswaterstaat (RWS); and implementation and documentation is done by TNO. MICRO/1 is for very special operations to be done in-house by TNO and RWS and possibly by a few other research groups in the Netherlands.

c. Kusters described the DIANA program. This DIsplacement method ANAlyzer general purpose finite element program has been under development since 1972. It now has about 200,000 program lines with some 40% devoted to comments. It is flexible, portable, and efficient. More than 40 types of elements are incorporated. Steel material models include plasticity by von Mises or Tresca, three types of hardening, creep with creep data supplied by user, and combinations of placticity and creep. Concrete material modeling includes several cracking criteria, tension stiffening, special yield criteria, and bond-slip relationships. Analysis capabilities include large displacements, dynamic response, eigenvalue determination and heat transfer.

   Some examples were presented, and considerable discussion ensued as to how bond and shear transfer effects will be put into practical use, which in turn raised the broader question of practicality of the program for design use. It was agreed that the end product of this type of development must be usable by the profession, and considerable effort has gone into making the program user-friendly and amenable to the design engineer who is not a computer specialist.

d. Ingraffea summarized Cornell research related to finite element analysis of reinforced concrete structures. Major efforts have been in the area of defining bond-slip relations, local effects at the ribs under cyclic loads, and cracking. The new fracture mechanics-based program FEFAP was described and examples given.

e. Mahin summarized many research programs at Berkeley. Current analysis developments are concentrated in the areas of dynamics, sustained loads, thermal shock, and a wide variety of inelastic nonlinear approaches to structural analysis. Macroscopic models are being developed for large structures, such as for R/C beams with a modified Takeda hysteretic model, beams with inelastic shearing action, and inelastic 3-D column action under biaxial bending. Other topics currently being studied include modeling

with layered elements at critical locations in beams, simplified FEM for sustained and thermal loads, connection area models with simplified M-θ relations, and special elements for large panel structures and nonstructural components. Local idealization is receiving considerable attention: concrete under multiaxial stresses, cracking analysis, creep and environmental effects, post-yield behavior of steel, and models for bond and shear at the local level.

f. Walraven presented his theory of shear transfer in cracked concrete (now available in the literature). The model, which is based on a combination of basic principles and data taken from experiments, predicts the shear transfer phenomena quite well. Experiments that have been done to provide input data and to check the theory were described. The role of concrete strength in the shear friction analogy and in shear transfer was discussed. Differences between results of pull-off and push-off specimens were discussed in terms of the difference in confinement stress afforded to the reinforcement. Conflicting evidence on the effect of high strength concrete on shear transfer was presented. Problems in idealization caused by cyclic loading were described, and the new experimental program for three concrete strengths, three initial crack widths, and different levels of restraining stiffness was outlined.

g. White summarized research on shear transfer conducted at Cornell University, the Portland Cement Association, and MIT. Experimental studies on interface shear transfer, dowel action, and on combined biaxial tension and cyclic in-plane shear have been supplemented by development of several analytical models of varying sophistication. Models for IST and DA at a single crack subjected to cyclic shear have been formulated. Experiments on membrane shear and biaxial tension have been done on 6 in. thick and 24 in. thick flat elements. Punching shear tests on flat elements subjected to simultaneous biaxial tension have revealed that the tension has relatively little influence on punching strength.

h. Hawkins presented research results on shear transfer at the University of Washington. Variables covered included shear plane characteristics, rebar size and percentage, type and strength of concrete, direct stress parallel and perpendicular to the plane of shear, moment across the plane of shear, angle of rebar to the plane, and type of loading (cyclic and repeated). Results indicated that more information is needed on the falling branch part of the shear-slip curves. In the Mattock equation for shear strength it was shown that the first term (400 psi) should be a function of the concrete strength, with $6.7\sqrt{f'_c}$ a reasonable value.

Discussion of these various topics led to several questions:

1. what do we want to put into computer codes?
2. how do we best contrast the applications ranges that go from pure monotonic response to severe seismic response?
3. how do box girders behave under torsional loading?
4. what needs to be done in the laboratory? Can we concentrate on cyclic shear and be content with current knowledge on monotonic response?
5. a combined failure envelope and damage rule formulation is needed urgently.

i. de Groot discussed models for bond, with extensions to beams under constant moment. A nonlinear shear-slip relation is used, with springs at an angle for producing radial pressure forces in addition to the regular spring element for bond forces parallel to the bar axis. The rebar and slip element are combined into a single element. Concrete is modeled with a Mohr-Coulomb criterion with a tensile cutoff. Round concentric specimens have been analyzed. New experiments on rectangular prisms and on beam ends were reported. Discussion focused on the need for more study of the interface layer and on the fact that the elasto-plastic formulation is difficult to extend to cyclic loading.

j Dragosavic discussed the behavior of the bond zone under monotonic loading, and the influence of cylcic and sustained loads. Emphasis was on the influence of primary cracks and the local damage at ribs near the cracks. The sequencing of primary cracks dominates the level and discontinuous reverses of the bond stresses. The local damage at ribs, with stresses and deformations far beyond the uniaxial collapse of concrete, allows large slip. The result is a highly nonlinear and discontinuous stress-slip curve. Cyclic or sustained loads cause additional damage, with redistribution of the bond stresses and a larger slip. Experiments by Mehlhorn, Rehm, and others were compared. It is recommended that experiments be done by long specimen to introduce a more adequate cracking. It was concluded that for bond stress and slip, the radial stresses and deformations must be included in any model for the bond zone, including the concrete out at least one half the diameter of the reinforcing bar.

Points made in discussion: We must look at imposed deformations and not only tensile loads. A micromodel of bond must be very basic if it is to include such important factors as direction of casting, top layer vs. bottom layer effects, and number of bars in a layer.

k. Gergely summarized Cornell research on local behavior at a rib. Experiments on 1, 2, and 3 rib bars, with and without external confining pressure on the concrete cylinder, have been conducted. Monotonic and repeated loads have been used. The presence of secondary internal cracks, both radial and longitudinal, has been verified at low steel stresses by injection techniques.

l. Ingraffea discussed the analysis of the bond specimens, with attention to high-intensity, low level cyclic loads. Fracture mechanics concepts applied to thick-walled cylinders were presented. There is an urgent need to have empirical data to properly define the properties of concrete immediately in front of the rib, where effective stresses of several times the uniaxial strength of concrete exist.

m. Hawkins described research on bond on multi-ribbed bars. Development of cracks were explained in detail as a function of load history, where displacements of up to 0.6 in. were measured. Push-pull tests on 1, 2, and 3 rib specimens were done to simulate the effect of reversed moment on beam-column joints. Steel modeling is done with a Ramberg-Osgood formulation. Excellent comparisons of model with experimental results for monotonic loading were given. Steel deformations and bond-slip displacements were superimposed to permit a definition of finite bond length.

n. Mahin reported on work on anchorage regions in R/C beam column joints, including interior joints with combined V, P, and M on the columns. Bond tests were conducted on bars run through a specimen reinforced like a typical column, with three bar sizes, normal and light-weight concrete, and both original and epoxy repaired specimens.

o. Jirsa pointed out some of the practical difficulties of dealing with bond in analysis, including the rather sobering fact that bond is more sensitive to construction practice than is any other parameter in R/C design.

5. Summary of Future Activities

a. Define overall goals and intended ranges of application in research and design practice.

b. Conduct an organized exchange of reports and papers. Direct mailing is satisfactory, but copies of all correspondence and reports should be sent to Drs. Reinhardt and Gergely.

c. Hold conference meetings annually, and have more informal discussions whenever a "critical mass" of participants is together at an international conference.

d. Cooperate on research projects:

1. General - exchange informal progress reports; correspondence.

2. Analytical - analyze the same benchmark cases.
- divide parametric studies and sensitivity studies.
- divide work on future developments on 3-D analysis, long-term loading, and fracture mechanics.

3. Experimental - Divide test programs, particularly on bond studies.
- duplicate selected critical experiments in different labs.

4. Exchange personnel for periods from several weeks up to one year.

5. Write joint proposals for new research in structural concrete.

e. Next meeting will be in Atlanta, Georgia in the general time period of 19-23 January, which is the scheduled time for the ACI Spring Convention.

6. Commentary on Future Work

a. Program MICRO: incorporate cyclic loading effects, improved interface layer, results of ongoing materials research, and update creep laws. Run benchmark problems and propose new parametric studies, with all studies completed by March 1982. Extend program with fracture mechanics options in 1983-84. This program now has 40,000 lines with 200 subroutines.

The possible role of the U. of Illinois in cooperative work on analysis needs clarification.

b. Experimental: Final decisions on test programs should be reached by correspondence. More work is needed to build up a better understanding of basic bond behavior, particularly under cyclic loads. Careful planning of experiments to get critical parameters for analytical formulation of bond-slip laws is needed. By January 1982, the Netherlands group wants to have plans for a new three year experimental program that includes cyclic loads, sustained load effects, confining pressure, and variable cover. A visitor to Cornell for about one month is proposed.

Walraven detailed the planned program on shear transfer on both plain and reinforced concrete. Initial crack widths of 0.05, 0.10, and 0.15 mm are planned. Other variables include degree of external restraint stiffness.

c. Future research at Cornell University:

1. Summer 1981 research at Cornell will include development of new design recommendations for membrane shear in combination with uniaxial and biaxial tension, and additional punching shear experiments with larger shear spans and larger loaded areas to better mobilize the membrane forces in the reinforcing steel.

2. Research proposed to the Electric Power Research Institute by a joint team from PCA, Cornell, and MIT include the following topics:

   a. Membrane shear experiments at two scales as required to verify design criteria for containment walls: (1) study of construction joint effects, (2) steel ratios and stress conditions simulating prestressed concrete containments, (3) influence of a steel liner plate on one side of the specimen, (4) heavily reinforced specimens to determine the limits of membrane shear strength. Concurrent development of simple analytical models.

   b. Punching shear experiments at two scales as needed to formulate realistic new design criteria, with variables to include ratio of loaded area to slab thickness, level of biaxial tension, slab depth/shear span ratio, ρ, f'_c, and pipe penetration loading.

   c. Radial shear studies on full cylindrical models at base mat-wall juntion regions and on two scales of specimens simulating a unit width strip of the base mat-wall junction.

   d. Analytical developments in four areas:

      1) Element modeling to represent initially cracked reinforced concrete limits subjected to monotonic and cyclic inplane shear forces.

      2) Equivalent linear models for containment dynamic response, using system identification techniques.

3) Nonlinear analysis models for discontinuity areas in containment structures.

4) Models to better predict strength, ductility, and failure modes in nuclear safety-related structures.

7. Laboratory Tours

Tours were conducted through the DUT and TNO laboratories to observe ongoing experiments.

APPENDIX A - MEETING AGENDA

Meeting CUR/TNO/THD - Cornell at Delft University of Technology

Tuesday, 9 June 1981	Wednesday, 10 June 1981
10:00 a.m. - 1:00 p.m. - Welcome (Reinhardt) - general introduction to "Betonmechanica 2e fase" (Blaauwendraad) - DIANA (Kusters) - US research in FEM	9:00 a.m. - 1:00 p.m. "Bond" - Research in the Netherlands (De Groot, Dragosavic) - Research in the US
Lunch	Lunch
2:00 p.m. - 5:00 p.m. "Shear Transfer" - Research in the Netherlands (Walraven) - Research in the US	2:00 p.m. - 4:00 p.m. - Further topics - Visit to the laboratories of TNO-IBBC and THD
7:00 p.m. Party	

Each session will contain a presentation of topics of Delft and US research and an extensive discussion. As far as the experimental program is not yet fixed, an attempt should be made to adjust the the parameters of Cornell and THD/TNO. At the end of each session the way of cooperation should be clearly formulated.

Appendix B

Cooperative Research Between Cornell University, other U.S. Research Laboratories, and Research Laboratories in The Netherlands

Summary of Second Meeting

January 18 and 19, 1982

Atlanta, Ga., USA

by

Peter Gergely

and

Richard N. White

April 1982

LIST OF PARTICIPANTS

U.S.

1. Peter Gergely
   Dept. of Structural Engrg.
   Hollister Hall
   Cornell University
   Ithaca, New York 14853

2. Anthony R. Ingraffea
   Dept. of Structural Engrg.
   Hollister Hall
   Cornell University
   Ithaca, New York 14853

3. Z.P. Bazant
   Dept. of Civil Engrg.
   Northwestern University
   Evanston, IL 60200

4. N.M. Hawkins
   201 More Hall - FX-10
   University of Washington
   Seattle, Washington 98195

5. K.J. Willam
   Dept. of Civil Engineering
   University of Colorado
   Boulder, Colorado 80302

6. O. Buyukozturk
   Dept. of Civil Engineering
   MIT
   Boston, Mass. 02100

The Netherlands

1. H. Reinhardt
   Dept. of Civil Engineering
   Delft University of Technology
   Stevinweg 1
   Delft 8
   The Netherlands

2. M. Dragosavic
   TNO
   Delft
   The Netherlands

3. J.C. Walraven
   Dept. of Civil Engineering
   Delft University of Technology
   Stevinweg 1
   Delft 8
   The Netherlands

4. J. Blaauwendraad
   Rijkswaterstaat
   Delft
   The Netherlands

5. G.M.A. Kusters
   TNO Delft
   The Netherlands

6. B. van Zwol
   Rijkswaterstaat
   Delft
   The Netherlands

I. Introduction

This report summarizes the second meeting held between researchers in the U.S. and the Netherlands. The first meeting took place in Delft on June 9 and 10, 1981 with the participation of 6 people from the U.S. and 9 from the Netherlands. In addition, several observers also attended. The first meeting was summarized in a brief report by R.N. White and P. Gergely, dated September 1981.

The coordination of research activities and the exchange of fresh research information continued during the seven months between the two meetings. The fruitfulness of the cooperation is reflected by the fact that it was generally felt by the participants that the second meeting should be held sooner than one year after the first one.

II. Agenda

Monday, January 18

9 a.m. - 12:30 p.m.

-Welcome (Gergely)
-Discussion of agenda
-Current status of analytical program

2 p.m. - 5 p.m.

-Bond,
experimental results and
analytical models

Tuesday, January 19

9 a.m. - 12:30 p.m.

-interface shear transfer experimental
work and analytical modelling

2 p.m. - 5 p.m.

-Future work
-Selection of benchmark problems
-Future meetings
-Summary

III. Presentations

1. The development and use of a finite element analysis program (FEFA) was described by Ingraffea, with special emphasis on the modelling of crack propagation. The transfer of forces along the crack and in the "process zone" was discussed. The formation of primary and secondary cracks in tension specimens was revealed by the analysis. Several comments were made on the width of the process zone.

   Bazant observed that the blunt crack model can also give good results, especially in macro-idealization.

2. Willam commented on tension stiffening especially on the difference between uniform tension and loading with a gradient. The work of Hillerborg and others was cited.

3. Bazant elaborated on the effects of crack spacing on fracturing and on problems with the use of plasticity, especially for triaxial tension. He discussed the changes in the flexibility matrix in the idealization which cannot be obtained from loading surfaces. Bazant stated that the element size should not be changed near a crack and the element size depends also on the size of the structure.

4. Willam summarized the three basic approaches under discussion: discrete, continuum, and classical.

5. Reinhardt presented the analysis of shear transfer across mortar joints in precast construction, with emphasis on the effect of the length of the joint for strong mortars as would be predicted by linear fracture mechanics. This is not true for low quality mortars.

6. The planning of an extensive investigation of local bond was described by Dragosavic. Several reports have already been issued on analytical

modelling and the state of the art. The model involves a bond layer next to the bar and the slip of the bar is considered relative to the concrete outside this bond layer. The experimental work will include monotonic, cyclic, and sustained loading. Other variables are: the type of deformed bar, its diameter, concrete strength, cover, specimen size, and load history.

7. A discussion followed on the ways of incorporating bond in finite element analysis programs. Ingraffea described four types of bond representation using springs and link elements. The use of these refined models is justified only in research or in special applications.
8. The analytical representation of interface shear transfer along crack and its effect on certain types of problems was discussed by Ingraffea. The transfer of normal forces across cracks and the Hillerborg model were found to improve analytical results.
9. Walraven commented on the role of IST in beams without shear reinforcement, especially relative to the bending of concrete teeth between diagonal tension cracks. The effect of cycling is that the crack width does not keep increasing but the slip does. The effects of cycling and load duration on IST need further work. Hawkins observed that small aggregates are more important than large ones in IST.
10. Buyukozturk described a model of IST that involves normal and sliding stiffnesses. The effects of cycling are included. The dependence of the idealization on the crack width and on external reinforcing was questioned.

11. Hawkins summarized work done for the U.S. Navy on dynamic shear resistance involving IST. The main application is blast loading of slab in which case shear builds up much faster than moment. One of the main questions is what displacement (sliding) represents failure. Little-known tests by Karagozian and Case were cited. More information is needed on the unloading portion beyond the peak of the load-slip curve. Hawkins handed out copies of a paper in which local bond was studied for various bar lug geometries.
12. Kusters described in detail the DIANA program, especially its idealization of bond, IST, cracking, cycling, and plasticity. The 3-D plastic fracture and the 2-D Darwin-Pecknold models are incorporated and a comparison was presented with test results on pressurized concrete reactor vessels. The nonlinearities can be handled either with the regular or, more often, with the modified Newton-Raphson procedure.
13. Bazant commented that the results are element-size dependent, which creates problems for large structures. Convergence may not be to the correct solution; the limiting element size should be about three times the maximum aggregate size.
14. Buyukozturk outlined current and planned analysis work at MIT, which includes 3-D curved shell elements, cyclic loading, smeared or discrete reinforcing, and thermal problems. The analysis of refractory concrete was summarized.
15. van Zwol presented a short description of the treatment of creep in DIANA and SMART, together with alternative creep models. These were discussed by Willam and Bazant.

16. A detailed presentation of current and planned work at TNO was given by Blaawendraad. The IST idealization includes the effect of crack opening and will also include the relationship between normal stresses and crack width. Similar factors are to be included in bond modelling. Elements at crack tips are assigned a lower tensile strength. Comparisons with beam tests at TNO are being made. The analysis does not use fracture mechanics concepts. The question of the effects of scale was raised.

17. An extended discussion of future work followed the informal presentations. The concensus was that the principal task of the cooperative effort should be the selection of benchmark problems which should be analyzed by all concerned. The following suggestions were made:

    a) unreinforced specimen with shear crack (Ingraffea)

    b) reinforced beam with high shear (Delft)

    c) punching shear in a circular slab

    d) shear panels of Toronto (shear and also tension-compression)

    The comment was made that at least two sizes of specimens should be analyzed wherever tests are available, say 10 to 20 times and over 200 times the aggregate size.

    Gergely was asked to collect and distribute benchmark problems before the end of the year.

18. The view was expressed by the participants that this cooperative effort is highly beneficial and should be continued. As part of the present NSF project, at least two researchers will spend at least a week each at Delft.